Biochemical and physiological exploration of the nutrient sensing pathway upstream of mTORC1

by

Xin Gu

B.S., School of Life Sciences
Peking University

Submitted to the Department of Biology in Partial Fulfillment of the Requirements for the Degree of

DOCTOR OF PHILOSOPHY
AT THE
MASSACHUSETTS INSTITUTE OF TECHNOLOGY

February 2022

Signature of Author:

Xin Gu
Department of Biology

Certified by:

Pulin Li
Professor of Biology
Member, Whitehead Institute

Accepted by:

Amy Keating
Professor of Biology
Co-chair, Committee for Graduate Student

Biochemical and physiological exploration of the nutrient sensing pathway upstream of mTORC1

by

Xin Gu

Submitted to the Department of Biology
On Oct 15th, 2021 in Partial Fulfillment of the
Requirements for the degree of Doctor of Philosophy

Abstract

The mTORC1 (mechanistic target of rapamycin complex 1) protein kinase controls growth in response to environmental cues. Aberrant mTORC1 activity is linked to numerous diseases including cancer. Understanding the regulation of mTORC1 will facilitate therapeutic developments. Amino acids promote the translocation of mTORC1 to the lysosomal surface, a process dependent on the Rag GTPases nucleotide state, which is regulated by several multi-component complexes. Leucine and arginine are known activators of mTORC1 with reported corresponding sensors.

Despite years of research, two essential questions still remain: 1. What and how other inputs impact mTORC1 activity? 2. What are the physiological functions of the nutrient sensing pathway?

We identified SAMTOR as a previously uncharacterized protein that inhibits mTORC1 signaling by interacting with GATOR1, the GTPase activating protein (GAP) for RagA/B. The methyl donor S-adenosylmethionine (SAM) disrupts the SAMTOR-GATOR1 complex by binding directly to SAMTOR with a dissociation constant of approximately 7 μM. In cells, methionine starvation reduces SAM levels below this dissociation constant and promotes the association of SAMTOR with GATOR1, thereby inhibiting mTORC1 signaling. Methionine-induced activation of mTORC1 requires the SAM binding capacity of SAMTOR. Thus, SAMTOR is a SAM sensor that links methionine and one carbon metabolism to mTORC1.

In parallel, I explored the physiological roles of the nutrient sensing pathway in *Drosophila melanogaster*. Recent work in cultured cells established Sestrin as a conserved cytosolic leucine sensor, but its role in the organismal response to dietary leucine remains elusive. I found that *Sestrin* null flies ($Sesn^{-/-}$) fail to inhibit mTORC1 or activate autophagy upon leucine deprivation and survive worse on a low leucine diet. Knock-in flies expressing a leucine-binding deficient Sestrin mutant ($Sesn^{L431E}$) show decreased and leucine-insensitive mTORC1 activity. Interestingly, we found that flies can discriminate between food with or without leucine in a Sestrin-dependent manner. Leucine regulates mTORC1 activity in glial cells and a knockdown of *Sesn* in these cells reduces the ability of flies to detect leucine-free food. Thus, nutrient sensing by mTORC1 is not only necessary for flies to adapt to, but also to detect, a diet deficient in an essential nutrient.

Thesis supervisor: David M. Sabatini
Title: Professor of Biology

Acknowledgements

First and foremost, I would like to thank my thesis advisor David Sabatini, who has been incredibly supportive over the years. He has taught me how to pick important and interesting scientific questions and how to solve them rigorously. I would love to thank my thesis committee members Richard Young and Tyler Jacks, who have been listening to my progress and giving me a ton of helpful feedback.

I am also grateful to all the lab members in the Sabatini lab, who have been helping tremendously with the scientific discussions. Particularly, Max Valenstein, Raghu Chivukula, Pranav Lalgudi, Robert Saxton, Tim Wang, and Liron Bar-Peled all have become my close friends who also talk about science and everything happened in life with me constantly. They have carried me through hard time as well as celebrated progress and success along the way. I could not have gone through graduate school without their company and support.

I am deeply grateful to my collaborators, Jose Orozco, Patrick Jouandin and Norbert Perrimon. Doing science with them has been a wonderful experience that has taught me so much. Jose has helped me with the SAMTOR project. Patrick taught me how to do fly genetics and contributed to the fly Sestrin project. Norbert has almost been like a co-mentor to me, who has provided huge amount of support and guidance.

I would also like to thank Nav Chandel and Anjali Chandel. Talking with Nav has been very fun and inspiring, and mentoring Anjali for a summer has definitely made me a better teacher and mentor. I have learned so much from them both. I particularly want to thank Nav for believing in me and giving me opportunities to interview for an independent fellow position, which definitely has been an experience I cherish a lot.

I thank my parents who have taken my education so seriously. I want to especially thank my mom who has provided me with deep love and encouragement throughout the years. Being literally the opposite side of the world, I can barely visit my family but still can constantly feel their support.

Finally, I would like to thank Mike Greenberg and Steve Elledge, who I interviewed my postdoc with. Those two interviews both turned out to be life-changing events. I will join Mike Greenberg's lab as a postdoc after finishing grad school and brainstorming exciting ideas with him has been so pleasant. I enjoyed talking with Steve too, and through interviewing in his lab, I and Chris met and fell in love with each other. I am very grateful to Chris showing up in my life. His kindness, humor and positive energy light me up every day.

Table of Contents

Title page	1
Abstract	3
Acknowledgements	5
CHAPTER 1: Introduction	7
CHAPTER 2: SAMTOR is an S-adenosylmethionine sensor for the mTORC1 pathway	77
CHAPTER 3: Sestrin-mediated leucine sensing by mTORC1 is essential for detecting and adapting to a low leucine diet in *Drosophila*	110
CHAPTER 4: Summary and future directions	159

Chapter 1

Introduction

SECTION 1. Introduction

All organisms live in fluctuating environments and thus require mechanisms to appropriately sense factors in their environments, including the availability of nutrients, so that they can adapt their behavior and metabolism for optimal survival, growth, and reproduction. From unicellular to multicellular organisms, numerous examples of active nutrient sensing, integration, and adaptation have been reported, suggesting it is a universal attribute of most organisms. However, the nutrient sensing and integration process varies due to differences in the environmental conditions of distinct organisms. For multicellular organisms like humans, each cell senses its own environment in the body, then communicates and acts together with other cells to adapt as a whole. One of the challenges related to nutrition in humans is maintaining a healthy balance among food intake, nutrient storage, and energy expenditure. Imbalanced nutritional status leads to severe consequences including eating disorders, obesity, type-II diabetes, cardiovascular disease, and accelerated aging. The current trend in the human population of increasing obesity and diabetes emphasizes the importance of understanding the regulation of nutritional balance at the organismal level. Therefore, mechanistically elucidating how organisms sense and integrate nutrient availability to regulate growth is necessary for understanding physiology and its pathology.

At the cellular level, several signaling pathways are regulated by nutrient availability and impact downstream effectors in a nutrient-sensitive manner. Other than previously reported nutrients sensed via specific mechanisms, it remains elusive whether there are novel nutritional inputs that fluctuate in a diet-dependent fashion and affect major signaling pathways. Genetic manipulations of some of these signaling pathway, such as mTORC1, AMPK and GCN2, can lead to metabolic alterations and behavioral changes, such as the preference towards a certain nutrient. However, how these numerous signaling

pathways coordinate the sensing of various dietary factors to impact the behavior is poorly understood, mainly due to the lack of molecular mechanisms or efficient tools.

In this thesis, I first describe the identification and biochemical validation of a novel sensor that conveys the availability of S-adenosylmethionine to regulate a major nutrient regulated signaling pathway, the mTORC1 pathway; I then describe our effort to elucidate the physiological functions of a molecularly well-characterized cytosolic leucine sensor, Sestrin, in regulating the adaptation and detection of a low leucine diet. In this chapter, to provide context for these findings, I also review our current understanding of the nutrient sensing pathway at both the cellular and organismal level, focusing mainly on the detect of dietary protein, which is the main source of amino acids.

SECTION 2. Nutrient sensing at the cellular level

Nutrients refer to compounds obtained by ingesting food and that are essential to life. Five major types of nutrients are important for the function of the human body: proteins, carbohydrates (sugar and dietary fiber), fats, minerals, and vitamins. In sections 2 and 3 of chapter 1, I focus on summarizing current studies related to how protein availability is sensed at the cellular and organismal level due to the relevance to my studies described in chapters 2 and 3. Moreover, the crosstalk between carbohydrate sensing and protein sensing will be briefly mentioned in both sections.

As a primary macronutrient, protein is composed of amino acids, which are defined as organic substances that contain both an amine group (-NH2) and carboxyl group (-COOH). Most amino acids are stable in solution at physiological pH, while glutamine gradually cyclizes to pyroglutamate and cysteine is oxidized rapidly to cystine (Wu, 2009). All amino acids other than glycine contain an asymmetric carbon and display optical activity thus have L- and D- isoforms (Baker, 2009). The conversion from D-amino acids to L-amino acids is dependent on D-amino acid oxidases and transaminases, and this conversion can only happen to D-amino acids that are not D-cystine, D-histidine, D-arginine, D-threonine

and D-lysine due to the enzyme specificity (Baker, 2009). Interestingly, nature picked L-amino acids as the most efficiently utilized ones for biological processes compared to D-amino acids, likely by stochastic chance (Schmidt, 2006), and a similar bias exists towards higher efficiency of D-glucose usage compared to L-glucose.

A. The importance of amino acids

1. Proteogenic

Among more than 500 naturally existed amino acids, only 20 are proteogenic, meaning that they are building blocks of one of the most important macronutrients, protein (Flissi et al., 2020). Based on whether organisms need to obtain a certain amino acid via their diet or they can synthesize it, the 20 proteogenic amino acids are further categorized as nutritionally essential, conditionally essential, or non-essential (Sakami and Harrington, 1963). **Essential amino acids (EAA)** are indispensable. They cannot be synthesized or are synthesized *de novo* but fail to meet the needs of usage; thus they must be provided by the diet to fulfill requirements for organismal survival, development, growth, and reproduction (Furst and Stehle, 2004). **Conditionally essential amino acids (cEAA)** refer to those that normally can be synthesized in adequate quantity by the organism, but in a particular developmental stage, the needs dramatically change; thus they have to be provided from the diet to support the optimal continuation of developmental needs (Reeds, 2000). **Non-essential amino acids (NEAA)** can be synthesized de novo in more than enough quantities to meet organismal requirements (Reeds, 2000).

2. Metabolic roles

Numerous amino acids, independently of their roles in proteins, also play critical roles as metabolic intermediates. The biosynthesis of neurotransmitters like gamma-aminobutyric acid (GABA) requires glutamate in a reaction catalyzed by glutamic acid decarboxylase (GAD) (Hertz, 2013).

Tryptophan serves as a precursor for another key neurotransmitter serotonin (Savelieva et al., 2008). Phenylalanine can be metabolized to tyrosine, which is the precursor of the catecholamine neurotransmitters, including dopamine, epinephrine, norepinephrine, and various other trace amines (Fernstrom and Fernstrom, 2007). Another key trace amine derived from phenylalanine is phenethylamine, which acts on trace amine transporter to regulate monoamine mediated neurotransmission (Mazumder et al., 2013). Glycine is vital for porphyrins synthesis that includes the important oxygen-carrying molecule heme (di Salvo et al., 2013). Arginine is a precursor of nitric oxide, which is essential for brain metabolic regulation (Tejero et al., 2008). Polyamines are made from ornithine and S-adenosylmethionine (Rodriguez-Caso et al., 2006). Aspartate, glycine, serine, and glutamine are all necessary for nucleotide synthesis (Nilsson et al., 2020).

Beyond their proteogenic and metabolic roles, amino acids serve as essential signaling molecules to regulate multiple important signaling pathways as summarized in Part B below.

B. Amino acid sensing mechanisms

1. The mTORC1 (mechanistic target of rapamycin complex 1) signaling pathway

The mTORC1 protein kinase is the central component of a pathway that regulates anabolic and catabolic processes in response to environmental signals, including growth factors and nutrients like amino acids (Liu and Sabatini, 2020). Amino acids activate mTORC1 by promoting the translocation of mTORC1 to the lysosomal surface, where its activator Rheb resides (Buerger et al., 2006; Kim et al., 2008; Sancak et al., 2008). This localization depends on the nucleotide states of the heterodimeric Rag GTPases, which consist of RagA or RagB bound to RagC or RagD (Kim et al., 2008; Sancak et al., 2008).

The amino acid sensing pathway upstream of mTORC1 is complex (**Figure 1**), with several multi-component complexes regulating the nucleotide state of the heterodimeric Rag GTPases, each likely conveying a distinct amino acid input. Ragulator tethers the Rags to the lysosomal surface and presents

the Rags to be regulated by GATOR1 and FLCN-FNIP, which are known GAPs (GTPase activating protein) for RagA/B and RagC/D, respectively (Bar-Peled et al., 2013; Bar-Peled et al., 2012; Sancak et al., 2010; Tsun et al., 2013). The KICSTOR complex binds GATOR1 and is key to its lysosomal localization, and, like GATOR1, is necessary for amino acid starvation to inhibit mTORC1 signaling (Peng et al., 2017; Wolfson et al., 2017). The molecular function of GATOR2 remains elusive. It is required for amino acids to activate mTORC1 and interacts directly with several discovered amino acid sensors, indicating that it acts as a nutrient-sensing hub that might function upstream of GATOR1 (Bar-Peled et al., 2013).

Figure 1: The amino acid sensing pathway upstream of mTORC1

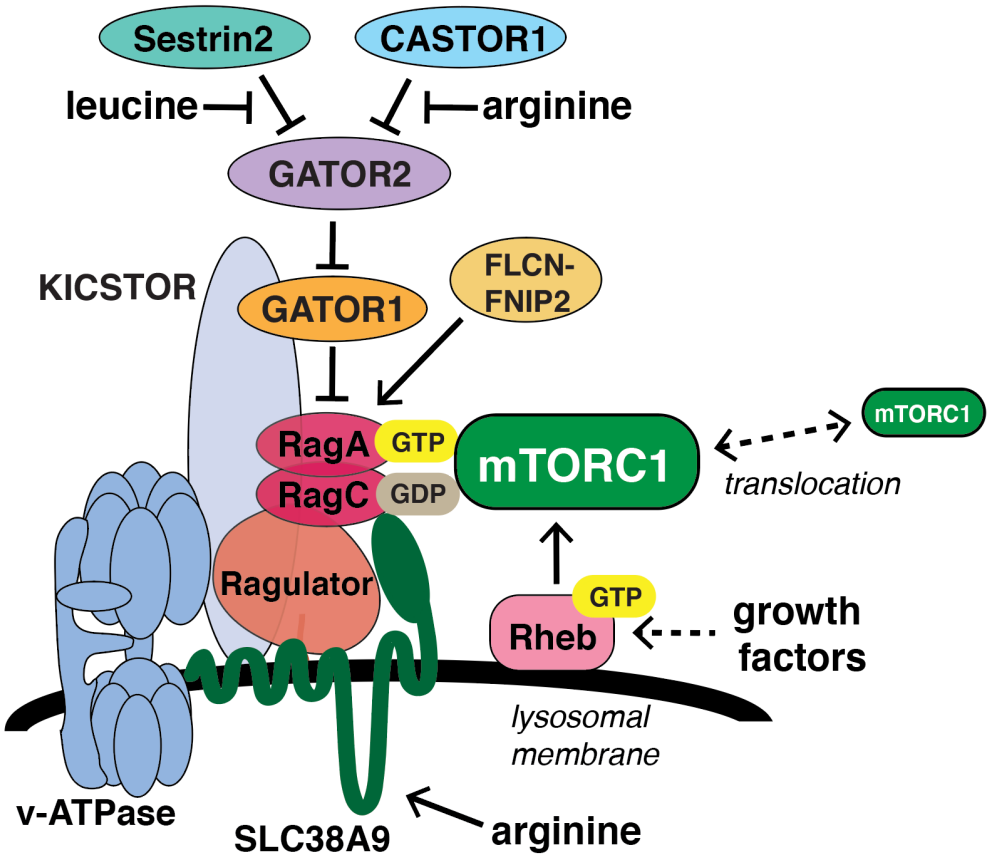

Figure 1: The amino acid sensing pathway upstream of mTORC1
The model depicting the key regulators involved in amino acid sensing upstream of mTORC1 in mammals (Modified from Gu et al., 2017).

Among all proteogenic amino acids, leucine and arginine are well-established activators of mTORC1, and recent work has revealed the involved molecular mechanisms (Gu et al., 2017). The lysosomal transmembrane protein SLC38A9 serves as a lysosomal arginine sensor and interacts with Ragulator to convey the lysosomal arginine availability using an inside-out sensing mechanism (Jung et al., 2015; Rebsamen et al., 2015; Wang et al., 2015; Wyant et al., 2017), while Sestrin1/2 and CASTOR1 are cytosolic leucine and arginine sensors, respectively, that bind to and inhibit the function of GATOR2 in the absence of their cognate amino acids (Chantranupong et al., 2016; Chantranupong et al., 2014; Saxton et al., 2016a; Saxton et al., 2016b; Wolfson et al., 2016). Work in cultured human cells has established that leucine activates mTORC1 by regulating the interaction of GATOR2 with the Sestrin family proteins, which function as repressors of mTORC1 (Wolfson et al., 2016). Human Sestrin1 and Sestrin2 bind leucine at affinities consistent with the concentration of leucine required to activate mTORC1 and are necessary for leucine starvation in cultured cells to inhibit mTORC1(Wolfson et al., 2016). Furthermore, a leucine-binding deficient mutant of Sestrin2 fails to dissociate from GATOR2 even when leucine is supplied (Wolfson et al., 2016). In cells expressing this mutant, the mTORC1 signaling activity remains low even in the presence of leucine (Saxton et al., 2016b; Wolfson et al., 2016). These results support that Sestrin1/2 are bona fide leucine sensors that functions upstream of mTORC1. In parallel, CASTOR1 functions as a cytosolic arginine sensor upstream of mTORC1 (Chantranupong et al., 2016). Arginine dissociates the interaction between CASTOR1 and GATOR2 to activate mTORC1 (Chantranupong et al., 2016; Saxton et al., 2016a). Whether there are other amino acid sensors in the mTORC1 pathway remains unclear and how important this amino acid sensing pathway is *in vivo* needs further exploration.

2. The GCN2 (General control nonderepressible 2) -ATF4 pathway for nutritional stress sensing

Eukaryotic cells also take advantage of accumulated uncharged cognate tRNAs to sense the scarcity of a specific amino acid or amino acids in bulk. Either limitation in an essential amino acid or inhibition of a non-essential amino acid synthesis is sufficient to activate this process (Masson, 2019). Uncharged tRNAs interact with the histidyl tRNA synthetase-like domain of GCN2, which is defective in specific histidine binding and synthetase activity. Thus, GCN2 can respond to various uncharged tRNAs (Wek et al., 1989; Wek et al., 1995). Upon binding, GCN2 homodimerizes and auto-phosphorylates, allowing GCN2 to phosphorylate eukaryotic initiation factor 2α (eIF2α), its only known substrate (Dever et al., 1992; Diallinas and Thireos, 1994; Narasimhan et al., 2004). However, how mammalian GCN2 is activated by nutritional stress mechanistically has remained elusive until recently. One study leads to the hypothesis that factors other than the levels of uncharged tRNAs exist to activate GCN2 upon amino acid deprivation was performed in neurons from mice lacking a specific neuronal tRNA as well as GTPBP2, the ribosome recycling factor. These neurons display elevated phosphorylation of eIF2α along with a high incidence of stalled translation elongation complexes without accumulation of uncharged tRNAs (Ishimura et al., 2016). Taken further, a recent study utilized in vitro reconstituted system to dissect the activation of mammalian GCN2 biochemically. They showed that human GCN2 binds directly to ribosomes via domain II of the ribosomal P-stalk protein uL10. Although deacylated tRNAs can activate GCN2 in vitro, purified ribosomes are much more potent activators of GCN2 (Inglis et al., 2019). Another study took advantage of CRISPR-Cas9 system and performed a genetic screen on GCN2 activation that led them to the same mechanism of GCN2 activation via the ribosomal P-stalk (Harding et al., 2019).

Phosphorylation of eIF2α by GCN2 attenuates the translation of most mRNAs by limiting the ternary complex composed of eIF2, GTP, and methionyl initiator tRNA so that the initiator tRNA delivery process to the small ribosomal subunit is inhibited (Abastado et al., 1991b; Dever et al., 1992; Rolfes and

Hinnebusch, 1993). However, several mRNAs can escape this global down-regulation upon nutritional stress, and one of them encodes for ATF4, a basic leucine zipper transcription factor, which induces a cascade of transcriptional regulators that are involved in modulating autophagy, amino acid metabolism and transport, apoptosis, and expression regulation of tRNA synthetases (Abastado et al., 1991b; B'Chir et al., 2013; Bunpo et al., 2009; Dever et al., 1992; Rolfes and Hinnebusch, 1993).

The activation of ATF4 is achieved via a cluster of four upstream open reading frames (uORFs) in the 5' untranslated region of its mRNA (Hinnebusch, 2005). A translation ternary complex forms at the first uORF, a positive element that promotes ribosome scanning and reinitiation (Renz et al., 2020). When nutrients are present, ribosomes that scan through the downstream of uORF1 reinitiate at the second uORF, which is an inhibitory element that prevents the main ATF4 ORF from being translated. However, when nutrients are deprived, GCN2 activation by uncharged tRNA leads to eIF2 phosphorylation and decreased ternary complex, causing increased time for the scanning ribosomes to become capable of reinitiating translation. This delayed reinitiation helps ribosomes scan through the inhibitory uORF and instead presents a higher chance of reinitiating at the ATF4 coding region (Abastado et al., 1991a; Hinnebusch, 1984; Mueller and Hinnebusch, 1986).

One factor worth mentioning about this pathway is that it usually takes hours to kick in due to its transcriptional nature, which strongly contrasts with the mTORC1 nutrient sensing pathway that responds within minutes to hours.

3. The AMPK pathway for energy sensing

Eukaryotes engulfed oxidative bacteria, which became mitochondria along evolutionary time. This acquisition has been suggested to permit a larger genome and thousands-fold more genes because multiple mitochondria inside of cells are the energy powerhouse that provides a large amount of ATP (Lane and Martin, 2010). Maintaining energy balance is key for survival; therefore, a dedicated sensing

system is required. An important and conserved energy sensor is the serine/threonine-directed AMP-activated protein kinase (AMPK). It regulates numerous catabolic and anabolic processes in response to the availability of energy inside of cells (Gowans and Hardie, 2014).

In response to decreasing energy levels, AMPK phosphorylates substrates that promote ATP generation and inhibit processes that consume ATP. The generation of ATP requires fuel, and glucose is one of the major sources. Thus, it makes sense for AMPK, when activated by low energy levels, to stimulate glucose uptake and glycolysis as well as inhibit glycogen synthesis (Yuan et al., 2013). Another key effector downstream of AMPK is the mTORC1 pathway mentioned above. AMPK inhibits mTORC1 in two ways: 1. AMPK phosphorylates TSC2, a major inhibitor of the mTORC1 pathway via acting as a GAP (GTPase activating protein) to Rheb GTPase, to activate TSC2 GAP activity, leading to decreased mTORC1 activity (Inoki et al., 2003); 2. AMPK also phosphorylates Raptor, a component of mTORC1. This phosphorylation event recruits 14-3-3, and inhibits mTORC1 kinase activity (Gwinn et al., 2008; Inoki et al., 2003). Other than what is mentioned here, hundreds of additional substrates have been found for AMPK, which indicates the broad spectrum of its regulation and impact (Hardie et al., 2012).

Circling back to the upstream of AMPK, how do changes in energy levels modulate AMPK kinase activity? AMPK senses the ratio of ATP to ADP/AMP by binding adenine nucleotides. When nutrients are available, this ratio is high. However, when nutrients are low, cells struggle to make enough energy currents, ATP, and this ratio decreases due to a drop of ATP levels and a rise of ADP, which turns to AMP quickly due to cytosolic adenylate kinase (Hardie and Hawley, 2001). AMPK is a trimeric complex that contains an alpha kinase domain, a beta carbohydrate-binding domain, and a gamma regulatory subunit (Fraser et al., 2005). Four nucleotide-binding sites exist in the gamma subunit. But for the mammalian gamma subunit, one is empty and another is constantly AMP bound (Xiao et al., 2007). When the other two regulatory subunits of AMPK bind AMP, the whole kinase goes through a conformational change that increases the capacity of the upstream regulatory kinase LKB1 and CaMKKKB to phosphorylate and

activate AMPK. This binding of AMP also prevents dephosphorylation of AMPK. Based on in vitro kinase activity data, AMP can further allosterically activate AMPK kinase activity up to 13 folds. All these processes are antagonized by ATP binding (Carling et al., 1989; Carling and Hardie, 1989; Corton et al., 1995; Gowans and Hardie, 2014). Therefore, with the competitive binding nature of AMP, ADP, and ATP, AMPK can regulate downstream proteins in a graded manner rather than on and off switch.

AMPK is a highly conserved energy sensor. Yeast and even plants contain AMPK orthologs, which suggest the importance of energy sensing across almost all living organisms (Crozet et al., 2014; Hong et al., 2003).

SECTION 3. nutrient sensing at the organismal level

Feeding is a fundamental behavior that exists for all animals. It is regulated by various external sensory circuits including olfactory and gustatory circuits, together with systemic internal hunger cues modulated by feeding status and metabolic needs. Different animals display different levels of feeding nature precision, which usually varies in terms of the amount of food eaten per meal, frequency of meals, preference of distinct food types, and foraging strategies. However, the basic principle among all animals is the same: the amount of food and each essential macronutrient needs to be sufficient to satisfy the requirements of the organism to grow, survive, and reproduce (Gahagan, 2012).

The unity of the fundamental principle of feeding across the whole animal kingdom suggests a fascinating question: how do animals sense the availability of food and essential macronutrients and integrate this information with internal hunger cues and innate metabolic needs to regulate physiology and behaviors?

A. Examples of active nutrient sensing in the animal kingdom and their mechanisms

1. Unicellular organisms

In most animals, nutrient regulation inside the body requires components specialized in regulating both the nutritional supply and demand. For example, for animals with a brain, the central nervous system controls the supply while listening to all parts of the body (including the nervous system itself) for demand. However, for many organisms, such as bacteria, yeasts, fungi, and protozoa animals, they do not contain a specialized component or a coordination center for the nutritional information integration. How do they maintain an optimal nutrient supply for their survival and reproduction?

Numerous examples exist for unicellular organisms being capable of sensing complex nutritional fluctuations in the environment and coordinate their 'behaviors' to adapt to the change for optimal growth.

1.1 Bacteria

For prokaryotes, bacteria have been intensely studied to elucidate their mechanisms to sense diverse nutrients, clearly depicting an adaptation to environments with highly variable and unpredictable changes in nutrient types and concentrations.

a. Chemoreceptors

Many procaryotes elicit conserved chemotaxis behaviors in a nutrient-regulated manner (Szurmant and Ordal, 2004). Here we only focus on *E. coli* due to the enormously detailed documentations. For *E. coli* to move, they rotate their flagella, bundles of filaments located at the pole. A bidirectional rotary motor powers this rotational movement: counter-clockwise rotation is the default direction that facilitates smooth swimming, whereas clock-wise rotation causes random tumbling (Berg, 2008; Turner et al., 2000). Abundant nutrients from extracellular environments promote the counter-clockwise rotations via signaling through transmembrane chemoreceptors. In contrast, the absence of nutrients leads to an activation of a signaling pathway that allows flagella to alternate rotational directions so *E. coli* can forage their environments (Sourjik and Wingreen, 2012).

Five dimeric single-pass transmembrane chemoreceptors function for *E. coli* as nutrient sensors that allow the detection and response to numerous extracellular molecules, which are summarized in Table 1 below. These chemoreceptors bind their cognate ligands with a wide range of concentrations, as low as 3 nM, which permits high detection sensitivity even when *E. coli* are in highly dilute nutrient environments (Mesibov et al., 1973).

Table 1. Bacterial chemoreceptors and their cognate ligands

CHEMORECEPTORS	MOLECULES THAT BIND AND SENSE
Tar (Reader et al., 1979; Wang and Koshland, 1980)	Aspartate, Maltose, Cobalt, Nickel
Tsr (Hedblom and Adler, 1980)	Ribose, Galactose
Tap (Manson et al., 1986)	Flavin adenine dinucleotide
Trg (Kondoh et al., 1979)	Serine
Aer (Szurmant and Ordal, 2004)	Dipeptides

The events downstream of the chemoreceptors is complex. It contains a series of signaling cascades that involve phosphorylation and methylation. Here we only briefly summarize these processes as they are not the direct sensing mechanisms that are the major focus of this introduction. When nutrients are sparse, a homodimeric histidine kinase, CheA, phosphorylates CheY, which then moves to the flagellar motor to facilitate clockwise rotation that triggers tumbling movements. After nutrients flow in, they contact with and alter the conformation of the cognate chemoreceptors, thus inhibiting CheA and CheY, and then flagella will move in the counter-clockwise direction. This phosphorylation cascade provides a binary regulation coupling the high or low levels of nutrients with the counter-clockwise or clockwise movements of flagella (Borkovich et al., 1989; Dyer et al., 2009; Sarkar et al., 2010a; Sarkar et al., 2010b; Wylie et al., 1988). To add in another layer of negative feedback regulation to facilitate adaptation, methylation and demethylation of chemoreceptors by CheR and CheB

respectively are also controlled by CheA. Methylation of the chemoreceptors increases the capacity to activate CheA despite persistently high ligand concentrations, whereas demethylation of the chemoreceptors does the opposite (Anand and Stock, 2002; Borkovich and Simon, 1990; Bren and Eisenbach, 2000). Thus, methylation resets the signaling state of the receptors for adaptation.

b. PII proteins

Chemoreceptors allow motile prokaryotes to forage for nutritionally richer environments. However, a more prevalent sensing pathway in almost all prokaryotes, motile or not, involves the PII superfamily of proteins that are major regulators of nitrogen assimilation (Forchhammer, 2010). When nitrogen sources are limited, many prokaryotes activate nitrogen assimilation via synthesizing organic molecules that contain nitrogen, like amino acids, from inorganic nitrogen molecules. Using a well-studied PII protein, GlnB, as an example, when nitrogen level is low, the precursor of nitrogen assimilation reactions, 2-oxoglutarate (2-OG), accumulates, binds to and inhibits the unmodified PII protein GlnB (Jiang et al., 1998). Thus, the downstream adenylyltransferase (ATase, glnE) cannot be stimulated via adenylylation reaction, and unmodified and active form of glutamine synthetase (GS) accumulates, leading to nitrogen assimilation. When the nitrogen level becomes high, glutamine levels are typically high, which inhibits the uridylyltransferase (UTase, GlnD), allowing unmodified GlnB to accumulate, thus promoting GS inhibition via activating the adenylylation of GS by ATase (Adler et al., 1975; Jiang et al., 1998; Mangum et al., 1973).

PII proteins not only bind with 2-OG, but also interact with key molecules like ATP. Although controversial, previous reports hypothesize that PII proteins may also serve as energy sensors by reacting to ADP to ATP ratio (Huergo et al., 2013; Jiang and Ninfa, 2007).

c. Riboswitches

Another fascinating bacterial-specific nutrient responder is a class of RNA molecules named riboswitches. These mRNA elements bind metabolites or metal ions as ligands and regulate mRNA

expression by forming alternative structures in response to the cognate ligand binding (Jackson and Yanofsky, 1973). Because these elements are encoded within the transcript they regulate, they act in cis to control the expression of specific genes. The broad spectrum of riboswitches enables a wide range of regulation by many types of molecules, including amino acids, nucleotides, metal ions, and other cofactors like vitamin b12 (Hammann and Westhof, 2007; Yanofsky et al., 1996).

Most riboswitch RNAs are located in the 5' region of sets of bacterial genes that are known or predicted to respond to specific physiological signals (Winkler, 2005; Winkler and Breaker, 2005). Riboswitches typically contain two domains: the aptamer domain (functions as a receptor for ligand binding), and the expression platform (acts on gene expression via interchanging between two conformational states in response to ligand interaction of the aptamer domain) (Winkler and Breaker, 2005). These elements are remarkably fine-tuned to the physiological concentration of the effector molecule. For example, riboswitches for S-adenosylmethionine molecule respond to low micromolar concentrations. In contrast, the lysine bound riboswitches produce a similar gene expression effect in response to low millimolar concentrations of lysine, 1000 folds difference between the two. This sensitivity is also partially dependent on the gene identity, temperature and pH (Garst et al., 2011). Another fascinating aspect is that recently riboswitch-like RNA molecules are also found in some plants (Wachter et al., 2007), illustrating the conservation of this metabolite-regulated RNA-based gene expression regulatory mechanism.

1.2 Amoeba

One of the most well-known protozoa, social amoeba (*Physarum polycephalum*), is a vast single cell containing thousands of nuclei, naturally found in decaying bottom of bodies of warm water like lakes or ponds. When offered various different food sources that have distinct ratios and concentrations of nutrients, amoebae (plural form of amoeba) strongly prefer a diet composed of twice the amount of

protein compared to sugar, and fail to survive on a sugar-rich diet. Interestingly, when given two suboptimal dietary choices, amoebae can reconstitute the ideal nutritional ratio and content by feeding on both options with a precise balance. Remarkably, on diluted nutrient sources, these amoebae change their morphology to extend farther to enhance the contact surface area as a compensation mechanism for low nutritional concentration in the environment. These results clearly indicate that amoebae are capable of sensing the nutritional content outside and integrating it with their own need, then executing a feeding protocol so they can make the supply and demand as equal as possible (Dussutour et al., 2010). The mechanism of these unicellular behaviors is under active exploration.

1.3 Yeast

Like bacteria, eukaryotic unicellular organism yeast also utilizes a variety of transmembrane proteins to sense an array of nutrients from the extracellular environment, including amino acids, glucose, and ammonium. Because these transmembrane proteins are also homologous to nutrient transporters, they are known by another name: transceptors. Here we only focus on the nutrient sensors specific to yeast. The shared sensing mechanisms of yeast with multicellular organisms will be discussed in the next section.

a. The Ssy1-Ptr3-Ssy5 (SPS) pathway for sensing extracellular amino acids

The Ssy1-Ptr3-Ssy5 pathway is found in S. cerevisiae, and it is conserved in most species of yeast but not in higher organisms. Initially, researchers found that S. cerevisiae that contains mutations in Ssy1 and Ptr3 show increased concentration of vacuolar basic amino acids (Klasson et al., 1999). Moreover, Ssy1 mutants display different sensitivity to extracellular amino acids (Klasson et al., 1999). These observations indicate that these proteins might be involved in sensing amino acids and maintaining intracellular pools of amino acids.

Ssy1 localizes in the plasma membrane of S. cerevisiae as a transporter-like protein. It shares sequence homology with amino acid permeases but does not contain active transport activity. A unique mechanism for Ssy1 is that it includes a very long N-terminal extended sequence that is key for conveying the amino acid availability to downstream signaling pathways. By forming a complex with Ptr3 and Ssy5, under the amino acid replete state, Ssy1 controls and activates a pathway that promotes the transcription of various metabolism-related genes and amino acid transporters. When amino acids are present in the environment, they bind with Ssy1 on the extracellular side of the plasma membrane and induce a conformational alteration in Ssy5 that binds with Ssy1 in a Ptr3-dependent manner, causing the phosphorylation and ubiquitin-mediated degradation of the auto-inhibitory pro-domain of Ssy5. This event leads to the release of the Ssy5 catalytic domain, which cleaves and activates two transcription factors, Stp1 and Stp2, which translocate to yeast nucleus and activate downstream genes upon activation (Abdel-Sater et al., 2004; Abdel-Sater et al., 2011; Didion et al., 1998; Omnus and Ljungdahl, 2013).

b. Snf3 and Rgt2 for sensing extracellular glucose

Both Snf3 and Rgt2 are plasma membrane localized transceptors but display different affinities for glucose (Bisson et al., 1987; Ozcan et al., 1996). Snf3 senses and responds to low glucose concentrations and promotes the transcription of high-affinity hexose transporter genes, whereas Rgt2 senses and responds to high glucose concentrations and activates the transcription of low-affinity hexose transporter genes (Bisson et al., 1987; Ozcan et al., 1996). Upon extracellular glucose binding, Snf3 and Rgt2 utilize an undiscovered mechanism to recruit two co-repressors Mth1 and Std1 to the plasma membrane for sequential phosphorylation, ubiquitination and degradation (Conrad et al., 2014). Without Mth1 and Std1, their binding partners Ssn6-Tub1 dissociates with Rgt1, a transcription factor necessary for glucose utilization (Roy et al., 2013). Unbound Rgt1 is phosphorylated and serves as an

active transcriptional activator of the HXT genes, such as hexose transporter genes (Jouandot et al., 2011).

c. MEP2 for sensing extracellular ammonium

Unlike most other eukaryotes, yeast can use ammonium as the sole source of nitrogen because it can assimilate ammonium using biochemical reactions in a similar way as bacteria. Yeast glutamate dehydrogenase performs a transamination reaction of 2-OG to produce glutamate, then glutamine synthase uses produced glutamate with ammonium to produce glutamine (Marini et al., 1994).

When nitrogen sources in the environment are limited, S. cerevisiae displays a dramatic morphological change to form a filament-like structure named pseudohyphae, which grows out from the main yeast colony to the surrounding media to forage for nutrients at a distance (Gimeno et al., 1992). This amazing nitrogen starvation induced morphological change indicates that there must be an active sensing mechanism for nitrogen sources. Adding ammonium alone is sufficient to reduce this shape change, suggesting that the sensor(s) are likely to contain the capacity to sense ammonium (Gimeno et al., 1992; Lorenz and Heitman, 1998a, b).

MEP2 (methylamine permease 2) has been proposed to be an ammonium sensor for yeast. MEP2 belongs to a conserved family of ammonium channels that contain three members, MEP1, 2, 3, where MEP2 binds ammonium with the highest affinity among all three (Marini et al., 1997). MEP2, especially the first intracellular loop of MEP2, is the only one required for pseudohyphal filamentous growth in ammonium-lacking environments. The ammonium transporter activity of MEP2 is necessary for pseudohyphal growth but not sufficient for ammonium sensing, as research has shown that transport-proficient but signaling-defective MEP2 mutants exist (Rutherford et al., 2008). The exact mechanism of how downstream signaling of MEP2 functions to transduce the availability of ammonium remains elusive, despite factors like GPA2 (a G protein alpha subunit), RAS2, and protein kinase A (PKA) might be involved (Lorenz and Heitman, 1998b).

Mammalian orthologs of MEP2 are named erythroid specific Rh (rhesus)-type proteins. They are expressed in various organs and show essential functions in physiology, especially in excreting ammonium out from cells to urine, as high ammonium concentration intracellularly is toxic (Biver et al., 2008; Chantranupong et al., 2015). It is a fascinating question to explore whether these Rh proteins serve as ammonium sensors for specific cells.

d. Pho85-Pho80 for sensing phosphate

Independent of carbon and nitrogen sources, yeast growth also requires a vital nutrient, phosphate. Studies in S. cerevisiae have shown that phosphate starvation leads to yeast cell cycle arrest. The mechanism of the stop of growth phenotype is proposed to be Pho85-Pho80 dependent (Valk and Loog, 2013).

An interesting paradox is that a low phosphate environment leads to an increased intracellular level of a phosphate-rich molecule, myo-D-inositol-heptakiphosphate (IP7), in yeast (Auesukaree et al., 2005; York and Lew, 2008). Nevertheless, this molecule binds with Pho81 to activate it, so Pho81 will serve as an active inhibitor to Pho85-Pho80 kinase complex, causing downstream dephosphorylation of a key transcription factor, Pho4, and its retention in the nucleus that allows increased expression of phosphate acquisition genes, like high-affinity phosphate transporters Pho84 and Pho89 as well as secretory phosphatase (Pho5) to help in phosphate scavenging. Interestingly, Pho4 also controls vacuolar degradation of a low-affinity phosphate transporter Pho87. Another low-affinity phosphate transporter, Pho90, also goes through degradation but in a Pho4-independent manner (Lee et al., 2008; Lee et al., 2007).

On the contrary, when yeast grow in a high or normal phosphate environment, phosphate is taken into cells by low-affinity transporters and utilized for various cellular processes. Vacuoles store the excess of phosphate in polyp form. The lack of IP7 accumulation prevents the activation of Pho81; thus,

the Pho85-Pho80 kinase complex remains active to phosphorylate Pho4 to maintain cytoplasmic (Tsang and Lin, 2015; Valk and Loog, 2013).

Many other ascomycetes universally share the importance of sensing phosphate and responding to phosphate level changes. However, the exact mechanisms seem to differ significantly. Like for S. pombe, IP7 accumulation is conserved upon phosphate deprivation. But for the central sensing elements, researchers have failed to find homologs of Pho81-Pho80-Pho85 in S. pombe, while Pho7 is the S. pombe homolog of S. cerevisiae Pho4 (Tomar and Sinha, 2014). Compared to the amino acid, glucose, and ammonium sensing in yeast which sensing elements are displayed in the plasma membrane, phosphate sensing seems to rely on an indirect mechanism that requires an accumulation of the metabolite IP7, which triggers signaling cascade changes downstream.

2. Multicellular organisms

With the onset of multicellularity, more complex mechanisms for nutrient sensing evolved. Hormones and cytokines greatly facilitate efficient cell-cell communication within an organism, thus once one cell senses the nutritional state in the environment, it can talk to and regulate cells even in other organs using these molecules. The essential hormones that are responsive to nutritional states include insulin, leptin, and ghrelin (Warchol et al., 2014).

When animals consume food, their blood glucose levels increase, which leads to insulin release from pancreatic beta cells. Insulin is a powerful hormone that promotes anabolic and inhibits catabolic processes in numerous tissues through at least partially the PI3K-Akt pathway. Surface receptors of insulin once in the bound form promote the downstream signaling pathway that leads to Akt activation, a kinase that phosphorylates and inhibits AMPK. This phosphorylation also antagonizes LKB1-mediated phosphorylation (Petersen and Shulman, 2018).

Leptin and ghrelin are two well-known feeding regulating hormones produced in periphery tissues, and then travel through blood stream and act on the brain. Upon fasting, stomach enteroendocrine cells produce and release ghrelin that signals hunger. During feeding, adipocytes release leptin that signals satiety. These two hormones act on the hypothalamus, the nutrient sensing and feeding control center of an organism (Klok et al., 2007).

The major nutrient-sensing signaling pathways mentioned in Section II have all been reported to regulate feeding. For AMPK, ghrelin activates AMPK in the hypothalamic neurons, which causes an increase in food intake. The mechanism for this activation is likely that ghrelin binds a G-protein-coupled receptor, GHSR1, in the presynaptic neuron, leading to the calcium release, which stimulates CaMKKK to promote AMPK kinase activity (Yang et al., 2011). There is also evidence showing that overexpression of AMPK dominant-negative mutation in the hypothalamus can decrease feeding, while injecting AMPK activator small molecules causes extreme hunger (termed hyperphagia) (Andersson et al., 2004; Minokoshi et al., 2004). On the other hand, leptin is also shown to regulate AMPK phosphorylation states via the PI3K-Akt pathway (Dagon et al., 2012).

GCN2 also plays key roles in regulating feeding behaviors, although the evidence appears to be controversial (Hao et al., 2005; Koehnle et al., 2003; Leib and Knight, 2015, 2016). mTORC1 and its downstream effector protein S6K1 are both indicated as nutrient sensors that modulate feeding behaviors in multiple organisms (Ribeiro and Dickson, 2010; Vargas et al., 2010; Wiczer and Thomas, 2010). Since both GCN2 and mTORC1 are predominantly regulated by the availability of amino acids and both regulate food choice in multicellular organisms, I summarize the relevant studies in Part C of this section along with other molecules, signaling, and systems that are indicated to be essential for protein appetite regulation.

B. The path of nutrients in animal bodies: anatomy, function and regulations of the digestive tract

Before considering potential nutrient sensing mechanisms at the organismal level, it is crucial to understand how consumed food gets digested and travels through the body. Demonstrating the anatomy of the digestive system helps elucidate the physiology. Here, I summarize the anatomy, functions, and regulations related to the digestive tract in both invertebrates and vertebrates, emphasizing the invertebrate system due to my research mentioned in Chapter 3.

1. Invertebrates

We use the digestive system of fruit flies, *Drosophila melanogaster*, as an example for invertebrates to summarize the path of nutrient flow *in vivo*. The natural food source for flies is decaying fruits, which contain water and carbohydrates from the fruits and protein and fat from the microorganisms, including yeast, bacteria, and mold from the rotted parts. Vitamins and minerals could be from both fruits and microorganisms. Therefore, the nutrients, especially carbohydrates, protein, and fat, exist in complex forms that need to be broken down and digested to be absorbed and sensed.

1.1 The anatomy of the fruit fly digestive tract

a. Proboscis: taste and potential regurgitation for extraoral pre-digestion

First of all, when a fly searches for a potential food source, the olfactory cues spreading out from the food helps to attract the fly. Unlike mammals who can only taste food with the mouth, flies have sensory neurons located on their legs, wings and proboscis, which serve as the essential feeding organ for taste detection and food ingestion (Miguel-Aliaga et al., 2018). These sensory neurons all contribute to evaluating various factors, including the food texture, temperature, and initial taste to make the first decision to eat or not to eat. Flies express several classes of taste receptors in these sensory neurons, including those activated by sugar and amino acids. However, if the vast majority of

nutrients are locked in the complex form in the original natural food, how are flies able to 'taste' anything because these receptors are reported to only be activated efficiently by amino acids, di-peptides, or glucose or fructose?

One possibility is that flies predigest the food in an extraoral manner. One interesting supporting evidence of this hypothesis is illuminated by generating a mutant fly strain of amylase, the enzyme for breaking down complex sugars (Hickey et al., 1988). Unlike wild-type flies, these amylase mutant flies fail to feed on a starch-only diet (Haj-Ahmad and Hickey, 1982). Their lethality can be rescued by either providing them simple sugar like glucose that does not require being broken down to be absorbed or surprisingly, housing the mutant flies together with wild-type flies (Haj-Ahmad and Hickey, 1982). These results suggest that flies either regurgitate amylase to predigest the food or excrete amylase, which lacks evidence so far. Whether other enzymes are regurgitated together with amylase to predigest food remains elusive, mainly due to the technical challenge of collecting enough samples for mass spectrometry studies to elucidate the identity of the potential enzymes.

b. Esophagus passes through the central brain

Secondly, due to the unique anatomy of the fly esophagus and central nervous system, the ingested food travels through the esophagus, which goes through the middle of the central brain. Mammals do not share this particular anatomy. Another class of animals that contains this esophagus-through-the-brain anatomy is the Cephalopod, including squids and octopuses. It is unclear why this anatomy is beneficial evolutionarily for insects and cephalopods, but some researchers hypothesize that it helps with limiting food size. From my work described in Chapter 3, I hypothesize that the brain area close to the esophagus in flies might serve as a potential nutrient sensing location that quickly transduces signals obtained from the diet to impact neuronal activity relatively acutely when food passes through the esophagus.

Esophageal peristalsis significantly contributes to facilitating food ingestion. Studies show that clusters of serotonergic neurons located in the central brain suboesophageal zone (SEZ), which serves as the central pattern generator for feeding rhythms (Huckesfeld et al., 2015), extend their processes along the esophagus to the anterior portions of the digestive tract, such as the stomatogastric ganglia, for food ingestion frequency regulation. After the initiation from the SEZ in the brain, peristaltic waves propagate via myogenic transmission down to the lower digestive system due to the lack of innervation for some of the areas in the digestive tract, which is very different from the mammalian system (Schoofs et al., 2018; Schoofs et al., 2014). The detailed regulation of Drosophila peristalsis will be summarized at the end of this session after introducing the lower digestive tract.

c. Crop, the equivalent organ to the stomach

Thirdly, food that passes the esophagus goes down to the crop, a stomach-equivalent organ containing enzymes for further digestion. The crop includes a diverticulated structure unique to Diptera and may play roles in early digestion, detoxification, microbial control, and food storage (Stoffolano and Haselton, 2013), although detailed functional studies are awaited. The crop is heavily innervated, and the stretch caused by the food ingestion is rapidly fed back to the central nervous system through these neurons via both acute mechanical sensing and chronic neuropeptide-mediated remodeling to regulate food intake that promotes the organismal fitness under different developmental stages.

Figure 2: The anatomy of the fly digestive tract (*Drosophila melanogaster)*

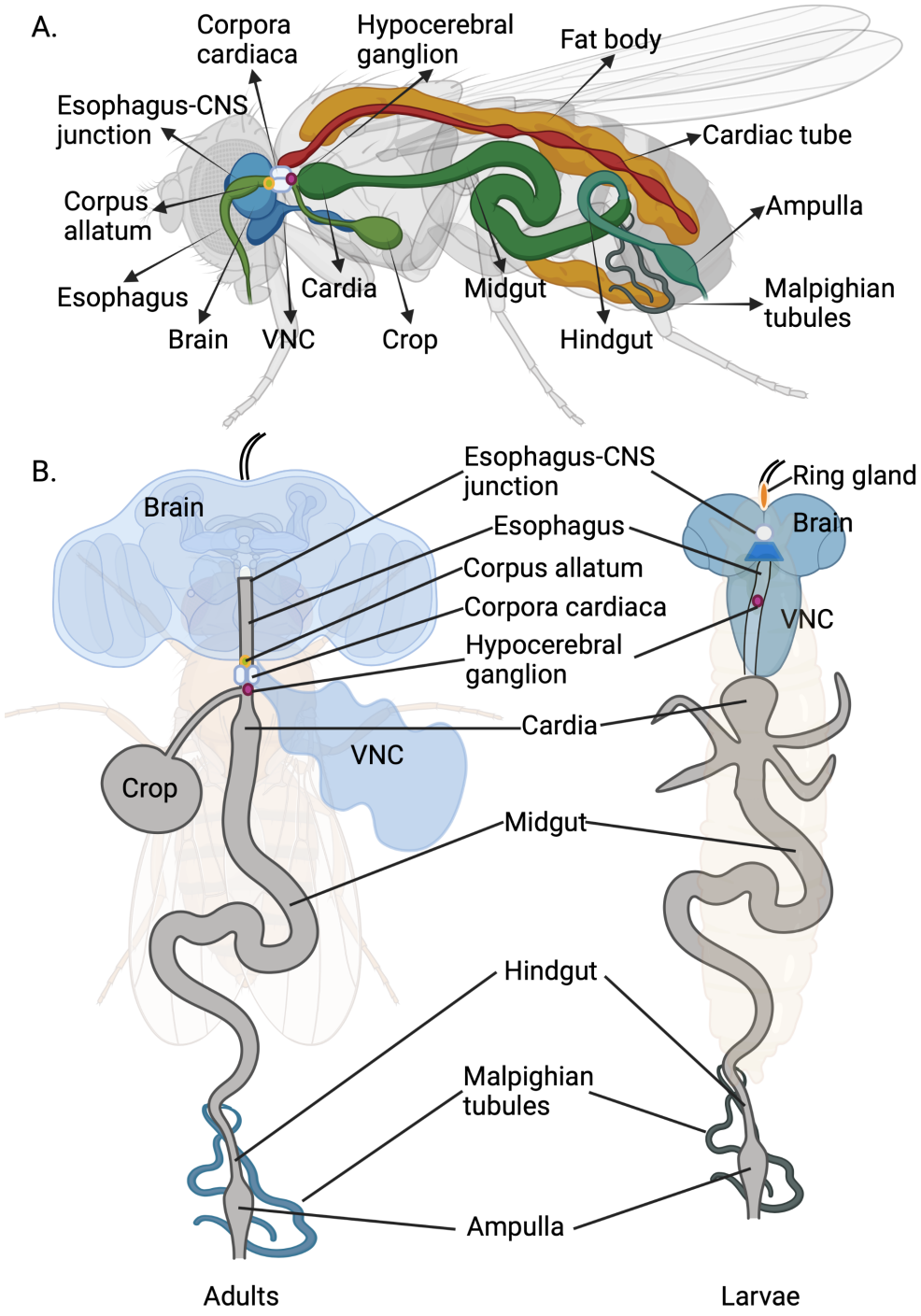

Figure 2. The anatomy of the fly digestive tract (*Drosophila melanogaster*)
(A) The side view of an adult *Drosophila melanogaster.* Key organs are shown in color and labeled. (B) The digestive tract of the adult (left) and larvae (right) flies. Key organs are shown in color and labeled. (Made using BioRender).

Two independent studies showed that a group of piezo-expressing neurons innervate the crop and monitor the crop volume acutely to avoid food overconsumption (Min et al., 2021; Wang et al., 2020). The soma of some of these neurons locates in the pars intercerebralis (PI), a neuro-secretory center that is important for regulating metabolic homeostasis (Wang et al., 2020), while some of these neurons are also reported to locate in the hypocerebral ganglion (HCG) (Min et al., 2021). This dual location observation of piezo neurons suggests the existence of multiple gut-innervating piezo positive neuronal subtypes. Piezo+ neurons are activated directly by crop distension and flies lack of piezo expression in these neurons fail to stop food consumption thus display higher amount of food intake, bigger crop size, and bigger body weight compared to their wild-type counterparts (Min et al., 2021; Wang et al., 2020). These results suggest that disrupting the mechano-sensation of the crop alters the feeding patterns of the flies.

For many animals, pre- and post-mating eating behaviors dramatically differ. It has been reported that female flies significantly increase their appetite and consume more food after mating, suggesting interesting crosstalk between feeding and reproduction. Research has shown that steroids and enteroendocrine hormones produced correlating with sex and reproduction act on gut-innervating neurons, leading to the release of neuropeptides from these neurons onto the muscles surrounding the crop (Hadjieconomou et al., 2020). This neuroendocrine regulation alters the crop enlargement dynamics and leads to increased food intake. Prevention of this dynamic regulation reduces reproductive hyperphagia and fitness, indicating that the plasticity of enteric neurons controlling crop enlargement plays vital role in reproductive success (Hadjieconomou et al., 2020).

d. Back to esophagus then cardia (also known as proventriculus)

Food from the crop travels back to the esophagus then down to the cardia, a complex bulb-shaped organ that produces peritrophic matrix, a major site for antimicrobial peptide production (King,

1988; Tzou et al., 2000). The cardia contains three layers of epithelium and might also serve as a valve to regulate the entry of ingested food to the midgut. The maintenance of the cardia may rely on a subpopulation of self-renewing stem cells located in the foregut-midgut junction (Singh et al., 2011).

A group of peripheral neurons on the cardia expresses a gustatory receptor Gr43a, a putative fructose receptor. Intriguingly, these neurons extend their axons to either the midgut muscles or the suboesophageal ganglion and their dendrites to the foregut lumen. This anatomy suggests that these neurons may transduce the nutrient availability information to both the central nervous system and the local gut area (Miyamoto et al., 2012).

Most metazoans separate their intestinal epithelium from the external environment via multiple layers of carbohydrate-rich barriers. For fruit flies, different areas of the gut contain various barriers. The foregut and hindgut are covered by a layer of hardly permeable cuticle, and the midgut is lined by the peritrophic matrix (PM) (Hegedus et al., 2009; Lehane, 1997). Due to the little amount one can collect, the exact composition and role of these barriers are poorly understood in flies. Studies have shown that the PM contains chitin fibrils that are held together by chitin-binding proteins like peritrophins. Cardia is the organ where PM gets synthesized and secreted because the transcripts encoding PM proteins like peritrophins are highly enriched in the cardia (Buchon et al., 2013).

Cardia synthesizes another vital enzyme, the lipase Magro (Horne et al., 2009). The expression of Magro is controlled by a transcriptional factor DHR96 (Sieber and Thummel, 2012). Magro or DHR96 knockdown prevents larvae from breaking down dietary triglycerides (Horne et al., 2009; Sieber and Thummel, 2012).

e. Midgut: the digestion and absorption center

(1) Regionization and composition

One key feature of the fly midgut is its heterogeneity. Its origin is from both endoderm and ectoderm. The midgut can be grossly subdivided into the anterior, middle, and posterior sections, and researchers have morphologically and molecularly further divided the midgut into 10-14 regions based on unique histological, cellular, and gene expression features. For example, a group of copper cells that produce gastric acid is categorized to the R3 area (R3ab). Extensive studies are still needed to further our genetic understanding of the midgut compartmentation.

The midgut is composed of a tube lined by a monolayer epithelium consisting of four major cell types: intestinal stem cells (ISCs), absorptive enterocytes (ECs), enteroendocrine cells (EEs), and enteroblasts (EBs). The EBs are postmitotic cells that can differentiate to ECs or EEs. This layer of the epithelium is tightly surrounded by muscle cells that facilitate the peristalsis.

(2) Organ plasticity

A shared feature of all regions of the midgut is that the local ISCs population can regenerate all cell types within the region (Buchon and Osman, 2015), which contribute primarily to organ plasticity. The ISCs from the different regions contain distinct gene expression patterns, suggesting the heterogeneity of these stem cells (Marianes and Spradling, 2013). Consistently, studies involving lineage tracing have shown that ISCs tend to maintain the progeny from their own region and rarely contribute to the differentiated cells even in the adjacent regions (Tian and Jiang, 2014). The existence of an ISC population in fly gut was initially elucidated in the posterior midgut (Micchelli and Perrimon, 2006; Ohlstein and Spradling, 2006), followed by numerous studies that have characterized the lineages and regulation of ISCs in the fly gut.

Long-term nutrient deprivation significantly but reversibly reduces the rate of ISC proliferation (Choi et al., 2011; McLeod et al., 2010). Interestingly, genetic downregulation or mutation of the intestinal insulin receptor or its downstream pathway components cause the same reduction of ISC proliferation rate (Biteau et al., 2010). Insulin signaling is important for the ISCs proliferation, the EBs

differentiation, and the maintenance of the EB/ISC cell-cell junction (Choi et al., 2011). Drosophila insulin signaling is regulated in a complex fashion and is summarized below in the next session.

(3) Digestive enzymes

The midgut serves as the main digestion site for fruit flies, although the ingested food is pre-digested extra-orally and by the enzymes in the foregut. Drosophila eats decaying fruits or vegetables and the microorganisms growing on them, which are very complex. The genetically encoded digestive enzymes of flies also reach an impressive number: ~350 by bioinformative prediction, with most contributions from endopeptidases or exopeptidases, lipases, and enzymes for complex sugar break-down (Miguel-Aliaga et al., 2018). The presence of numerous lysozymes ensures flies digest key bacterial wall components, peptidoglycan, whereas chitinases and glucosidases help with the digestion of yeasts.

Interestingly, related digestive enzymes often locate as gene clusters in the genome, which indicates that these gene clusters might exist due to gene duplication to both maximize the digestive capacity and facilitate the regional regulation of the expression of the clusters (Buchon et al., 2013; Zhang and Kishino, 2004). For example, enzymes for breaking down sugars are more enriched in the anterior midgut, while peptidases genes are more expressed in the posterior midgut.

Other than the genomic location, the digestive enzyme activity and expression are tightly regulated by numerous factors, including food intake (that determines nutritional excess or scarcity), the abundance of the end product of the enzymes, luminal bacteria, etc. (Miguel-Aliaga et al., 2018).

(4) Absorption of nutrients

For carbohydrates, after the breakdown of complex sugars by digestive enzymes discussed above, a series of transporters uptake simple sugars into the enterocytes (ECs) for further digestion and usage, including a GLUT/SLC2-like transporter (Escher and Rasmuson-Lestander, 1999), a disaccharide transporter (SLC45 family) that might function together with trehalose transporters (Kanamori et al., 2010; Meyer et al., 2011), and several other orthologs of the glucose transporters from other species.

How these transporters coordinate together for the carbohydrate absorption and whether there is bona fide sexual dimorphism are still under investigation. Meanwhile, recently it has been identified that ECs, enteric neurons, and EEs express putative sweet taste receptors and may serve roles to facilitate carbohydrate sensing and absorption in the gut.

After digestion by hundreds of peptidases, proteins are broken down to a mixture of amino acids and many di- and tri-peptides. The peptide/amino acid transporters in the gut are largely conserved from mammals to flies. These include amino acid transporters Minidiscs, Pathetic, NAT1, and other SLC6 family members, as well as oligopeptide transporters Yin and CG2930 (Goberdhan et al., 2005; Martin et al., 2000; Miller et al., 2008; Roman et al., 1998). Whether these transporters play roles in absorption of digested proteins and detection of available nutrients remains elusive. One study has shown that the oligopeptide transporters from the SLC15 family might play roles in detecting and internalizing bacterial derived peptidoglycan to trigger a putative immune response (Charriere et al., 2010).

Lipids are absorbed by intestinal cells along with sterols as the end products of digestion: free fatty acids, phospholipid derivatives, mono- and di-acylglycerols. The transport might include passive diffusion and active facilitation by some membrane proteins. The passive diffusion might be promoted by emulsification, a process achieved by forming complexes of fatty acid, amino acids and glycolipids together with fatty acids and lysophospholipid micelles (Miguel-Aliaga et al., 2018). In ECs, uptake lipid products are utilized to resynthesize TAG and diacylglycerols, which are combined with cholesterol and fat body-secreted carrier proteins to form lipoprotein particles (Palm et al., 2012). Sterols are essential for insects, because, unlike mammals that can synthesize sterols from acetate, insects can only rely on the dietary sources. Niemann-Pick C1 (Npc1) proteins are shown to play a crucial role in mammalian sterol intestinal absorption and intracellular trafficking (Jia et al., 2011). *Drosophila* contains 10

orthologs of mammalian Npc1. Npc1b is expressed highly in the midgut and is required for sterol absorption (Huang et al., 2007).

Water, osmolytes, and metal ions like iron, copper, and zinc are all essential for fly survival, and they all need to be adequately absorbed in the midgut. The regulations are very complex and can be found nicely summarized in this comprehensive review (Miguel-Aliaga et al., 2018)

f. Hindgut-ampulla

The hindgut contributes mainly to the excretion, intestinal fluid retention, pH adjustment, and ampulla for defecation. Hindgut also helps with excretion and defecation by using its strong surrounding muscle contractions to facilitate peristalsis. Meanwhile, some neurons innervating the hindgut area also play important roles in controlling fluid balance. The HGN1 neurons that originate from fly CNS project their long axons to the posterior segments of the abdominal ganglion, including the epithelium of the hindgut and the rectum. Ablating HGN1 neurons causes increased defecation, indicating its positive roles in intestinal fluid retention (Cognigni et al., 2011).

1.2 Innervation of the digestive system of flies

The regulation of the digestive system functions depends on the signaling internally and the communication among different organs systematically. Both enteric neurons and endocrine signals have been shown to play critical roles in regulating the digestive system functions, in turn impacting physiology and even behaviors.

Figure 3: The anatomy of the fly enteric innervation (*Drosophila melanogaster)*

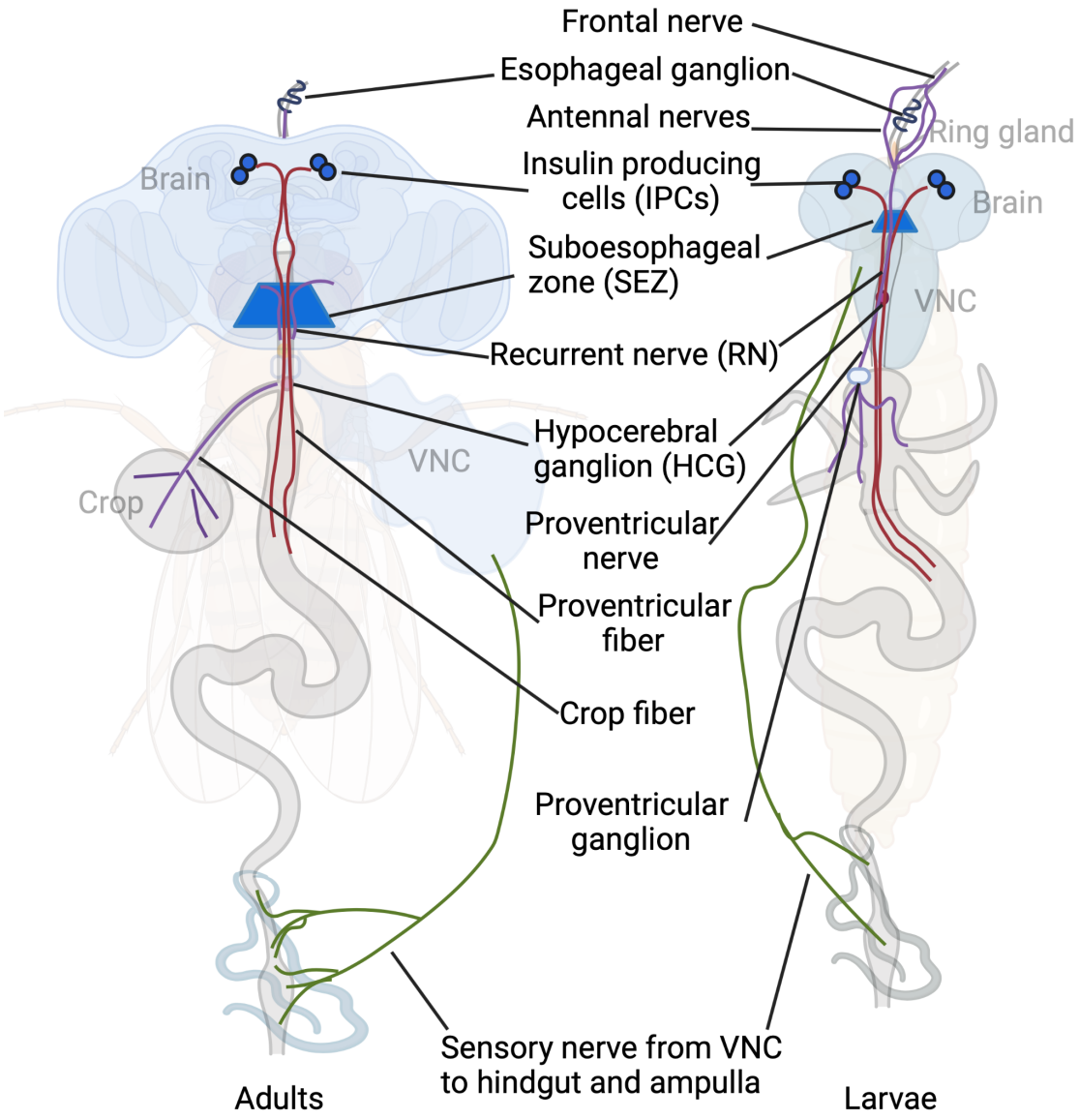

Figure 3. The anatomy of the fly enteric innervation (*Drosophila melanogaster*)
Based on the anatomy of the fly digestive tract shown in figure 2, the key innervation of the digestive system is drawn and labeled for both adults (left) and Larvae (right). (Made using BioRender).

a. The anatomy of Drosophila enteric innervation

Three distinct innervation groups project to the digestive tract of adult flies: (1) CNS neurons (Cognigni et al., 2011; Schoofs et al., 2014); (2) stomatogastric nervous system (Spiess et al., 2008); (3) corpora cardiaca (in adults, it fuses with hypocerebral ganglion) (Lee and Park, 2004). These innervations

are highly diverse in chemical regulations, including expressing a distinct array of neuropeptides and neurotransmitters. Meanwhile, different from the mammalian digestive tract that is innervated universally throughout the entire length, fly gut innervation is relatively limited to three significant portions: (1) the anterior part that includes the pharynx, esophagus, crop, and anterior midgut; (2) the junction of midgut and hindgut; (3) the posterior hindgut (Cognigni et al., 2011; Schoofs et al., 2014). Most neuronal projections terminate on the visceral muscles and regulate peristalsis and intestinal transit, whereas some neurites extend deeper and reach the underlying epithelium, which is shown to be predominantly in the fly esophagus, cardia, and ampulla (Kenmoku et al., 2016). These observations suggest the existence of neuronal regulation of epithelial functions like absorption and secretion. Interestingly, peripheral sensory neurons, such as the taste neurons from the pharynx, predominantly project their axons to the suboesophageal zone, and extend their dendrites to both anterior and posterior of the digestive system, particularly the esophagus and anterior midgut, indicating dual functions of these sensory neurons (Cognigni et al., 2011).

b. The functions of fly enteric neurons

Three primary functions of the enteric neurons in flies are: (1) the regulation of peristalsis; (2) the modulation of the hormone secretion; (3) the control of distant organs, including the trachea and Malpighian tubules (Miguel-Aliaga et al., 2018).

As mentioned in the earlier section related to the esophagus, studies involving innervation in flies have revealed an important function: peristalsis. It is proposed that the suboesophageal zone initiates the peristaltic waves, modulated by a group of serotonergic neurons located in this area of the brain. These neurons innervate the anterior parts of the digestive tract. Then the further propagation of the peristaltic waves relies on the muscles via myogenic transmission. The regulation of peristalsis in flies is complex, and many neuropeptides are involved, including myotropins (Kaminski et al., 2002),

Allatostatins (Price et al., 2002), and Drosulfakinins (Palmer et al., 2007). A study has shown that the Pdf-expressing neurons innervate the hindgut and contribute to muscle peristalsis and promote Malpighian tubule contractions (Talsma et al., 2012). Several Dh44 (Drosophila ortholog of mammalian corticotropin-releasing hormone CRH) expressing neurosecretory cells from CNS also innervate crop as well as anterior midgut and contributes to peristalsis and excretion (Dus et al., 2015). These neurons are also vital for flies to detect dietary nutritive sugars, thus linking the nutrient sensing function with gut motility regulation. Several gut-innervating neurons also regulate trachea branching in response to nutrient availability, providing an example of regulating adjacent organs via utilizing the intestine as a docking site (Linneweber et al., 2014).

1.3 The complex regulation of Drosophila insulin signaling

Unlike mammals, fruit flies do not have a pancreas. They express a series of Drosophila insulin-like peptides (DILPs) from multiple organs. DILP2, 3, and 5 are produced from a group of insulin producing cells (IPCs) located in the *pars intercerebralis* of the central nervous system and released from axon terminations in the corpora cardiacum, corpora allatum, crop, and anterior midgut. DILP3 is also produced by the gut muscle cells, and DILP5 is also from the ovaries and Malpighian tubules (for fluid secretion). DILP6 is from adipocytes of the fat body. DILP7 is from 20 neurons in the abdominal neuromeres of the ventral nerve cord (VNC), and then gets released to the posterior midgut, ovaries, and CNS (Nassel and Vanden Broeck, 2016). Interestingly, the genetic knockout of DILP1-5 leads to smaller larvae, pupa, and adult flies, while knockout of DILP6 or DILP7 does not impact body size and weight (Zhang et al., 2009).

How do the insulin producing cells sense nutrient availability to regulate DILP production and release? The mechanisms of the glucose-induced DILP release are surprisingly and interestingly similar

to those in mammalian pancreatic beta cells, indicating the high conservation of the insulin release regulation process across the evolution.

a. Adult flies

For adult flies, the brain IPCs contain a cell-autonomous glucose-sensing capacity as studies have shown that sugar meals directly activate IPCs to trigger DILP release (Park et al., 2014). IPCs also contain cell-non-autonomous glucose-sensing mechanisms that involve numerous hormones and neurotransmitters that are summarized below.

(1). GABA and Upd2 (Unpaired 2): IPCs express metabotropic GABA receptors and are hyperpolarized by GABA. This GABA regulation is inhibited by a leptin-like cytokine peptide produced from the fat body, Upd2, whose release is activated by elevated lipid or carbohydrate levels in the hemolymph. Upd2 travels through the blood-brain barrier with an unknown mechanism, then acts on the cytokine receptor domeless that promotes the JAK/STAT signaling pathway in the GABAergic neurons to block the release of GABA, thus hyperpolarizing the IPCs (Rajan and Perrimon, 2012).

(2). Adiponectin: IPCs express the adiponectin receptor. Knockdown of this receptor leads to elevated trehalose, glucose and stored lipids levels. Although the Drosophila adiponectin itself has not been identified, it was suggested that the fat body produces it and adding human adiponectin to IPCs in larvae is sufficient to decrease DILP2 expression (Kwak et al., 2013).

(3). Neuropeptide F (sNPF) and corazonin: these two neuropeptides are synthesized and released by a bilateral set of neurons (dorsal lateral peptidergic neurons) located in the *pars lateralis*. The IPCs express the sNPF receptor (sNPFR1) and corazonin receptor (CrzR). The knockdown of these receptors leads to decreased insulin signaling in flies. Interestingly, in the dorsal lateral peptidergic neurons, sNPF knockdown, but not corazonin knockdown, reduces the expression of DILP2 and DILP5, suggesting different actions of these two neuropeptides on the IPCs (Kapan et al., 2012). These dorsal lateral peptidergic neurons are heterogeneous genetically. A subset of it expresses a gustatory receptor

Gr43a (Miyamoto et al., 2012), which is activated by circulating fructose, while another subset is reported to express receptors for diuretic hormones 31 and 44, that modulate the activity of these neurons via produced peptides from other neurons or the endocrine cells of the gut (Johnson et al., 2005; Veenstra et al., 2008).

(4). Tachykinin: A Drosophila neuropeptide is reported to modulate DILP release from the IPCs. The tachykinin receptor (DTKR) is expressed on IPCs membrane. The knockdown of DTKR leads to the elevated secretion of DILP2 and DILP3 in fed flies as well as increased DILP2 but decreased DILP3 in starved flies (Birse et al., 2011). The possible sources of tachykinin are under investigation, possibly from both some brain neurons and enteroendocrine cells in the midgut (Siviter et al., 2000).

(5). Allatostatin A (AstA): Another neuropeptide is shown to be produced by several AstA producing neurons that display dendritic branches that superimpose the IPC branches in both the pars intercerebralis and the tritocerebrum (Hentze et al., 2015). AstA is also produced by midgut enteroendocrine cells (Yoon and Stay, 1995). IPCs are known to express a galanin receptor-like GPCR (DAR2) that can be activated by AstA (Hentze et al., 2015). In addition to IPCs, the AKH-producing cells (APCs) in the corpora cardiaca express the AstA receptor DAR2. Studies have shown that both AKH and DILP signaling pathways are stimulated by AstA via DAR2 (Hentze et al., 2015): although knockdown of DAR2 in both APCs and IPCs increases starvation resistance, consistent with decreased systemic DILPs, DAR2 knockdown specifically in APCs causes reduced AKH release that leads to specific changes to the AKH signaling pathway genes, while DAR2 knockdown specifically in IPCs inhibits the insulin pathway by decreasing DILPs. The APCs and IPCs crosstalk with each other, potentially via the physical contacts in the corpora cardiaca and the gut (Kim and Rulifson, 2004). Interestingly, diet, protein-rich or carbohydrate-rich, regulates the transcript levels of both AstA and Dar2 (Buch et al., 2008; Hentze et al., 2015). Both transcript levels decrease after nutrient starvation and intensely increase after re-feeding only on a carbohydrate-rich diet, but not a protein-rich diet. When you give well-fed flies a choice

between sucrose-rich food and yeast (protein)-rich food, wild-type flies prefer sucrose-rich food, whereas flies, especially females, with activated AstA neurons show a preference towards the yeast-rich diet (Hentze et al., 2015). These results strongly suggest that the AstA signaling pathway is actively involved in nutrient-sensing and acts on both IPCs and APCs to regulate feeding decisions.

(6). Serotonin and octopamine: These monoamines have been implicated in IPCs regulation (Crocker et al., 2010; Kaplan et al., 2008; Luo et al., 2012; Luo et al., 2014). The IPCs express both the serotonin receptor (5-HT1A) and octopamine receptor (OAMB). The knockdown of the serotonin receptor in IPCs causes elevated DILP2 and DILP5 on transcript levels, decreased resistance to starvation, reduced food intake, increased sensitivity to temperature change, increased glucose levels in the hemolymph, as well as enhanced glycogen and trehalose storage. Octopamine receptor OAMB knockdown in IPCs increased DILP3 transcript levels, enhanced starvation resistance and food uptake in fed flies. The neuronal circuits that underlie these two-monoamine signaling to regulate IPCs remain elusive.

(7). Olfactory cues: Food odors, such as vinegar (Lushchak et al., 2015), also affect IPCs and the expression of DILPs. Studies have shown that even a brief exposure to vinegar odor, less than half an hour, is sufficient to elevate the transcript levels of numerous components in the insulin signaling, including Akh, DILP2, 3, 5, 6, Upd2, etc. Researchers speculate that attractive food odors induce an anticipatory endocrine response in starved flies to get ready for food digestion.

(8). CCHamide2: This peptide hormone is produced by enteroendocrine cells of the midgut (Veenstra and Ida, 2014) and brain neuroendocrine cells in adult flies(Ren et al., 2015). CCHa2 acts on IPCs to impact DILP secretion (Ren et al., 2015; Sano et al., 2015). Adult flies with CCHa2 mutations eat less and show strongly reduced locomotor activity. The functional studies of CCHa2 are much more intensive in fly larvae. CCHa2 is mainly produced in the larvae fat body and intestine, whereas the CCHamide-2 receptor is expressed in the IPCs of larval brains. CCHa2 or CCHa2 receptor knockdown in

larvae reduces the release of DILP2 and DILP5, thus leading to reduced feeding, growth, and developmental delay (Ren et al., 2015; Sano et al., 2015). The expression of CCHa2 is also sensitive to dietary nutrient availability in a mTOR signaling-dependent manner in the fat body.

Figure 4: Regulation of the insulin signaling in *Drosophila melanogaster*

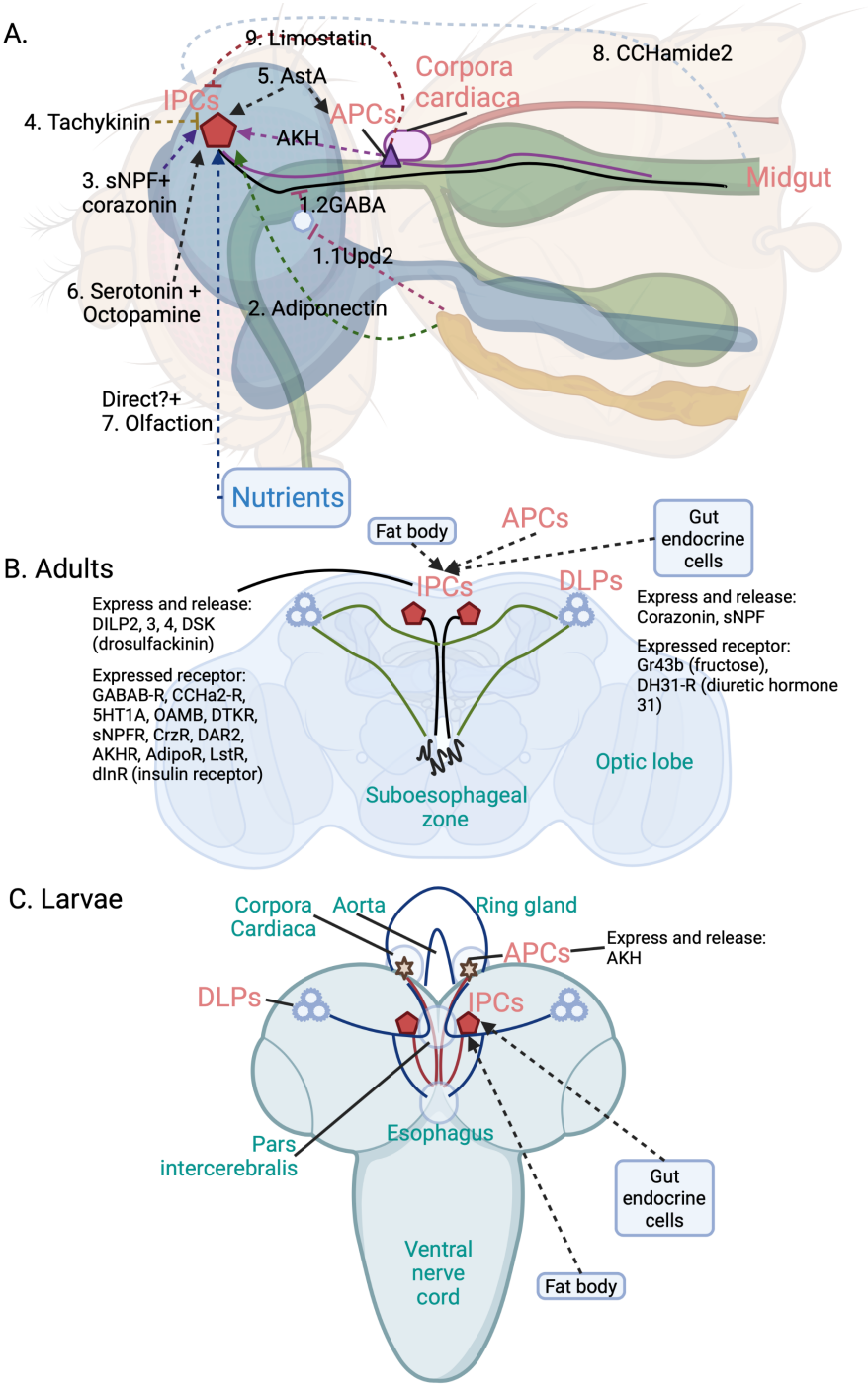

Figure 4. Regulation of the insulin signaling in Drosophila melanogaster
(A) Summarization of 9 signaling molecules that have been shown to regulate the activity of the insulin producing cells located in the central nervous system of Drosophila melanogaster. (B) A model depicting the regulatory relationship among insulin producing cells (IPCs), AKH producing cells (AKCs) and dorsal lateral peptidergic cells (DLPs) in adults. (C) A model depicting the regulatory relationship among insulin producing cells (IPCs), AKH producing cells (AKCs) and dorsal lateral peptidergic cells (DLPs) in larvae. (Made using BioRender).

(9). Limostatin: This polypeptide is identified to regulate insulin production and release negatively. Limostatin is expressed and released from both the fat body and APCs of the corpora cardiaca only during fasting. The expression of limostatin is elevated by a carbohydrate-rich diet but not a protein-rich diet, and this peptide blocks calcium release in the IPCs, thus reducing the DILP release (Alfa et al., 2015). Flies with limostatin mutations are hypoglycemic, show decreased DILP2, 3, and 5 mRNA levels, and live a short lifespan compared to wild-type flies. The receptor of limostatin is reported to be a GPCR named CG9918 (Cazzamali et al., 2005), which was shown previously as the receptor for pyrokinin-1, another peptide that is important to modulate muscle contraction (peripheral action) and coordinate feeding and energy homeostasis (central action) (Nusawardani et al., 2013).

b. Larval flies

Unlike adult flies, the IPCs of larval flies cannot sense nutrient availability directly via a cell autonomous manner. Instead, studies have shown that active nutrient sensing occurs in the AKH producing cells (APCs) in the ring gland (Kim and Rulifson, 2004), the adipocytes in the fat body (Geminard et al., 2009), and the gut endocrine cells (Ren et al., 2015).

Larval APCs express ATP-sensitive potassium channels (KATP), which serve as cellular sensors themselves of the ADP/ATP ratio dependent on the glucose levels in these cells (Kim and Rulifson, 2004). When glucose level is high, these channels depolarize APCs, thus increasing calcium currents to promote hormone release, especially AKH, a functional analog of mammalian glucagon. AKH acts on the AKH receptor to elevate glycogenolysis, lipolysis, and trehalose production in the fat body (Bednarova et al.,

2013). Interestingly, excess trehalose promotes AKH release from the APCs to act on the AKH receptor expressed on the surface of the IPCs, thus leading to DILP3 release, which activates the mTORC1 pathway in the larval fat body (Kim and Neufeld, 2015). These two opposing important hormones, DILPs and AKH, work together to control the metabolic homeostasis in both flies and mammals via conserved regulations.

The fat body adipocytes contain nutrient sensors that are mainly activated by dietary amino acids, such as the Slimfast-TOR pathway. This activation triggers the release of an unknown factor from the fat body that acts on IPCs for the DILP2 release (Geminard et al., 2009). Other than this unknown factor, the fat body also releases an adiponectin-like adipokine and a peptide hormone CCHamide-2, both mentioned above in adult flies. The alterations of adipokine signaling pathway do not impact larval growth, but it changes the carbohydrate and lipid homeostasis both during development and adult flies (Kwak et al., 2013).

2. Vertebrates – focus on human

There is great diversity among digestive systems from different vertebrates. The most obvious difference is the number of stomach chambers. They might contain a single stomach (monogastric), several stomach chambers, or accessory organs to facilitate food digestion. Monogastric animals like humans use their single stomach to release enzymes for food digestion. Other organs like the liver, salivary glands, and pancreas produce and secret additional gastric juices to assist digestion. Meanwhile, ruminants like sheep and cows contain four stomachs, and pseudo-ruminants, such as camels, have three stomachs, although only one out of three or four stomachs secrets digestive juice. These animals predominantly feed on plants and require larger space and extra microbial support to digest high-cellulose plants. Interestingly, the digestive system of birds functions quite differently. It contains two chambers: the proventriculus (similar to Drosophila cardia) that produces gastric juices, and the gizzard

stores and mechanically grounds food to facilitate further absorption in the intestine. Here we only focus on the human digestive tract (Hartenstein and Martinez, 2019).

2.1 The anatomy of the human digestive tract

The digestion begins in the mouth, then moves through the pharynx to the esophagus, stomach, and small intestine. (1). The mouth takes charge of mechanical and chemical digestion facilitated by teeth and saliva respectively. Saliva contains mucus to moisten the food and buffer the pH, immunoglobins and lysozymes to serve as antibacterial substances, salivary amylases to begin the digestion of starch, and lipases to breakdown fat. To prevent the food from reaching the trachea or lungs, the epiglottis is used to cover the trachea. (2) After the tongue positions the food in the mouth, the unidirectional peristalsis helps push the food down the esophagus to get into the stomach. (3) Acids and enzymes produced in the stomach break down food into smaller nutrient components. The stomach lumen is acidic, necessary for food breakdown and nutrient extraction. The stomach size is small when empty but can expand to 20 times bigger when food is ingested. The protein digestion happens majorly in the human stomach mediated by pepsin, an enzyme secreted by the chief cells then further processed to be active by hydrochloric acid in the stomach. Mechanical force is generated in the stomach via contraction and relaxation of surrounding smooth muscles. All these actions turn the food into chyme, the semifluid mass of partly digested food and gastric juice mixture. (4) chyme moves down to the small intestine that serves as the primary site for digestion completion and nutrient absorption. The length of the human small intestine is over 6 meters. It is divided to three parts: the duodenum (where the accessory organ juices flow in and where fatty acid absorption mainly happens), the jejunum (where most of the carbohydrate and amino acid absorption happens), and the ileum (where bile salts and vitamins are absorbed). (5) After the nutrients get absorbed in the small intestine, the undigested food is sent down to the large intestine, where reabsorption of water and generation of waste material occur.

It contains three major parts: the cecum, the colon (rich in bacteria), and the rectum. (6) The main function of the rectum is to store the feces temporarily until defecation. Peristaltic movements facilitate the elimination process that happens in the anus.

Parts (1)-(3) are components of the upper gastrointestinal tract, whereas parts (4)-(6) consist of the lower gastrointestinal tract (Grand et al., 1976; Montgomery et al., 1999).

2.2 The innervation of the human digestive tract

The central nervous system innervates the human digestive tract intensely via three primary sources: the vagal nerves, the sacral nerves, and the thoracolumbar nerves (Payne et al., 2019). These neurons further innervate the enteric nervous system and effector tissues to impact various functions, such as muscle movement-driven peristalsis, hormone release, and acid secretion. As a two-way communication, sensory information from the digestive tract feeds back to the central nervous system via these three sources of nerves about the status of the digestive system, including the physical state like stomach fullness and gastric acidity, nutritional contents like osmolarity and richness/scarcity, and pathological conditions like inflammation and infections. This feedback control is key to behavioral modulations, such as feeding or avoiding the food and active awareness of which diet fits the physiological needs better. These sensory neurons also convey sensations such as hunger and satiety.

a. Vagal nerves

Two types of nerve fibers consist of the vagal system: the afferent nerves (project from various internal organs to the lower brainstem) and the efferent nerves (project from the lower brainstem to internal organs). Vagal nerves innervate almost all organs forming the digestive tract.

For the afferent neurons, their cell bodies are located in the nodose and jugular ganglia. Their axons project to the nucleus tractus solitarius in the brain. Their dendrites that innervate the gastrointestinal tract are categorized into three types based on their shape and targets: the mucosal

endings (dense plexuses that locate close to the epithelium and receive hormonal signals from enteroendocrine cells like ghrelin, glucagon-like peptide 1, etc.), the intraganglionic laminar endings and the intramuscular endings (both are for detecting mechanosensitive purposes like gastric fullness) (Brookes et al., 2013; Prechtl and Powley, 1990). The mucosal endings play significant roles in nutrient detection and sensing, appetite regulation, and feeding behavior modulation (Berthoud, 2008; Dockray, 2013).

On the other hand, efferent axons in the vagal system come from two locations of the brainstem nuclei: the nucleus ambiguous (directly innervate the striated muscle of the esophagus to control its peristalsis) (Furness et al., 2014), and dorsal motor nucleus (innervate enteric ganglia in the pancreas, biliary tract, stomach, and intestine to control the release of pancreatic enzyme, motility of organs, and gastric acid secretion) (Furness, 2016).

b. Sacral nerves

The sacral nerves mainly control the functions of the colon and rectum via both autonomic and somatic nerve fibers. The autonomic nerve fibers innervate the pelvic nerves, which in turn affect the blood flow in the colon and rectum. In contrast, the somatic nerve fibers control the contraction of the anal sphincter. The afferent fibers convey the sensation and local status of the colon and rectum back to the brain (Brookes et al., 2013; Callaghan et al., 2018).

c. Thoracolumbar nerves

Some of the thoracolumbar nerves project back to the CNS to convey the pain sensation and nociceptive conditions from the gastrointestinal tract. The efferent nerves inhibit the movements of the digestive system and may even convey anti-inflammatory effects (Furness et al., 2014; Ness and Gebhart, 1990).

2.3 Insulin release regulation in human

The mechanisms of insulin secretion from the pancreatic beta cells in mammals have been studied intensely. Increased circulating glucose levels are sensed by beta cells via a glucose transporter (GLUT1), which triggers insulin secretion by inducing membrane depolarization and fusion and release of vesicles that contain insulin. The activated glycolysis pathway leads to an increased rate of ATP production in mitochondria, which inactivates the ATP-sensitive potassium channel (KATP), then depolarizes the beta cell. Sequentially, the voltage-sensitive calcium channels are activated by depolarization, which results in insulin secretion via exocytosis. This process highly resembles the neurotransmitter release process that happens in the synapses. They even require similar synapse and channel proteins. Other nutrients like amino acids and fatty acids also contribute via feeding into appropriate metabolic pathways leading to key molecules being produced to influence insulin secretion.

Numerous neurotransmitters and circulating hormones regulate the calcium-dependent exocytosis process through the interactions with plasma membrane receptors that either alter ion channel activity or recruit secondary messengers (Fu et al., 2013; Rorsman and Braun, 2013). The inhibitors include somatostatin released from pancreatic delta cells, adrenalin released from the adrenal glands, melatonin from the pineal glands, and galanin from the gut cells. These hormones and neurotransmitters hyperpolarize beta cells and inhibit insulin secretion via somatostatin, alpha2-adrenergic, melatonin, and galanin receptors, respectively (Gesmundo et al., 2017; Nassel and Vanden Broeck, 2016; Prentki et al., 2013). The stimulators of insulin release other than glucose include ATP (co-released with insulin) that acts on P2X3 receptors, acetylcholine that acts on M3 muscarinic receptors, GABA that acts on ionotropic GABAA receptors, glucagon and glucagon-like peptide-1 (GLP-1) that act on their respective G protein coupled receptors. GABA is produced by beta cells, similar to ATP, it gets released and works on the same cells in an autocrine manner. Two GABA receptors, ionotropic GABAA and metabotropic GABAB receptors, stimulate and inhibit the vesicle exocytosis respectively to regulate

insulin release, which indicates the existence of a locally fine-tuned mechanism (Rorsman and Renstrom, 2003).

C. A variety of protein (amino acid) sensing mechanisms impact food choice

All organisms have developed distinct sensing mechanisms to detect and adapt to the scarcity and abundance of diverse types of nutrients. As described above, unicellular organisms sense the nutrient availability in the environment directly like bacterial cells programming their transcriptional control to sense the availability of amino acids, while multicellular organisms contain a much more complex sensing system, which is composed of both cell autonomous and cell non-autonomous mechanisms to sense both extracellular and intracellular nutrient fluctuations. These mechanisms utilize transporters, receptors, or signaling proteins to fulfill the sensing mission. The goal is to demonstrate a causal relationship among genes (proteins), signaling pathways, neuronal processes, and behavior. Organisms alter their internal states, defined by the state of a series of molecular and cellular processes, to reflect the physiological needs based on the changing environment, then internal states change neuronal processes to impact the organismal behavior to meet the physiological needs. Here I summarize the studies on how internal states shape complex neuronal connections that lead to behavioral changes driven by nutrient-specific appetites.

Nutrient homeostasis is essential for health, and the balanced uptake of all kinds of nutrients is important for optimal growth and reproduction. The nutritional imbalance caused by lack of certain nutrients or overeating negatively influences organismal fitness. Therefore, all organisms require a tight regulation towards food intake for fitness gain.

For many nutrients, it has been established that deprivation of a given nutrient in an organism triggers a specific appetite toward that deprived nutrient. For example, female animals, after birth, crave calcium-rich food due to an increased need for milk production (Rabinowitch, 1938). Fruit flies

prefer protein-rich over carbohydrate-rich food more after a period of protein starvation. Thus, these classic behavioral experiments demonstrate that animals across evolution regulate their appetite for certain nutrients as compensation for the deprivation or in anticipation of particular physiological requirements.

Protein is one of the most important macronutrients and is strongly preferred by animals, and this preference is modulated by various factors including sex, baseline nutritional state, hunger cues, and olfactory cues. Due to numerous available genetic tools of the system, many studies utilize fruit flies to study protein appetite. The mechanisms that encode protein preference include amino acid transporters, taste receptors, GCN2, serotonin, octopamine and dopamine signaling, sex peptide receptor, microbiome, gut-produced neuropeptides, as well as mTOR and S6K1. A detailed summary of these mechanisms is as below:

(1) Amino acid transporters. A recent study has shown a putative amino acid transporter, CG13249, is highly expressed in the DH44 positive neurons, which are rapidly activated by amino acids like glutamate and aspartate. Knockdown of this transporter in DH44 neurons reduces the food consumption increase, which supports the hypothesis that CG13248 is key for food intake regulation in response to dietary amino acids in fruit flies (Yang et al., 2018).

(2) Taste receptors. For Drosophila larvae that constantly food on food to support rapid growth, a study has shown that a putative taste receptor for glutamate, IR76b, is broadly expressed in larval taste neurons and essential for feeding regulation of a group of amino acids, including arginine (Croset et al., 2016). Interestingly, IR76b positive sensory neurons are also involved in salt sensing via functioning together with IR20a, suggesting the crosstalk between two nutrients via the same receptor (Ganguly et al., 2017). Additionally, a recent systematic study aims to elucidate the physiology of amino acid taste. The researchers have found that one class of sensilla of Drosophila labellum, the S sensilla, conveys the

most potent responses to amino acids (Park and Carlson, 2018). Further work is needed to tease apart the response of these sensory neurons toward individual amino acids in a physiological setup. Although taste and smell might contribute to amino acid sensing, they are shown not to be the dominant factors, especially compared to the internal state of an animal, especially for mammals (Leung et al., 1972).

(3) GCN2. The studies of GCN2 function in feeding behavior regulation are controversial. In rodents, it has been reported that GCN2 activity in the anterior piriform cortex (APC) is sensitive to the food source that misses a single essential amino acid, and rodents must reduce the intake of this nutrient imbalanced food. Additionally, injecting amino acid alcohol derivatives to APC brain area leads to an increase of uncharged tRNA levels via a dominant-negative manner, and rodents with this injection appear to reject the diet low in the corresponding amino acid (Hao et al., 2005; Maurin et al., 2005).

However, more recent work argues against this GCN2-dependent mechanism. Intriguingly, rodents, within the first hour of eating, can rapidly sense a single essential amino acid deficiency in their food (Koehnle et al., 2003). This fast-speed sensing phenomenon allows animals to sense the nutritional content in their food and reject diets that fail to meet physiological needs quickly. But GCN2 pathway, even on the cellular levels, takes hours to create the downstream stress response upon amino acid deprivation, which fails to match the physiological timeline. Moreover, the indicated brain area where GCN2 plays an essential role is APC, a component of the olfactory cortex. APC in mammals is tightly protected by the blood-brain barrier, contrary to other organs that have been relatively exposed to ventricular liquid like arcuate nucleus from the hypothalamus. These factors make GCN2 in APC an unusual mechanism for amino acid sensing. Indeed, it has been shown that wild-type mice without pre-starvation cannot quickly distinguish food with or without essential amino acids like leucine or threonine. But pre-deprivation of a certain essential amino acid is sufficient to induce a quick rejection of the food that does not contain the missing amino acid. Surprisingly, none of these phenotypes

depend on GCN2, as the GCN2 knockout mice behave the same as the wild-type mice when facing these food choices, suggesting the existence of an undescribed mechanism for quick amino acid sensing (Leib and Knight, 2015).

In Drosophila larvae, GCN2 is key for repressing GABA signaling in the dopaminergic neurons, which is significant to regulating the rejection behavior of the imbalanced diet (Bjordal et al., 2014). Whether this mechanism remains true in adults is awaited to be tested.

(4) Serotonin, octopamine, and dopamine signaling. Monoamines have long been linked with food choice regulation in multiple organisms. Most of the evidence is shown on the neuronal circuitry level. In Drosophila larvae, rejecting imbalanced food relies on innate sensing of amino acids in the dopaminergic neurons of the fly brain. Starvation for certain essential amino acids induces rapid activation of several dopaminergic neurons that are key for food rejection (Bjordal et al., 2014). This finding is further confirmed in adult flies that contain a dopamine circuit, which encodes protein-specific hunger. This circuit activity is enhanced upon protein starvation. Interestingly, this circuit promotes protein intake and reduces carbohydrate consumption. These findings indicate the existence of a dedicated neuronal circuit in the fly brain to regulate protein intake (Liu et al., 2017). Several studies have demonstrated the involvement of serotonin and octopamine (Curzon, 1990; Mayack et al., 2019; Stallone and Nicolaidis, 1989; Tian and Wang, 2018; Vargas et al., 2010; Yadav et al., 2011; Zhang et al., 2013). All these studies together suggest the importance of monoamines in regulating food intake.

(5) Sex peptide receptor. For female flies, mated females prefer protein-rich food much more than virgin females, indicating a mating-induced appetite change. It has been shown that sex peptide/ sex peptide receptor plays essential roles in this appetite shift (Ribeiro and Dickson, 2010).

(6) Microbiome and gut-derived neuropeptides. More data has suggested that the gut microbiome is essential for homeostasis maintenance in health and disease, particularly the food intake and appetite. Early studies have shown that germ-free mice contain higher appetite but display lower body fat, mainly due to the difference in nutrient absorption. However, interestingly, colonization of germ-free mice with a gut microbiota from an obese human being leads to much higher body fat compared to a gut microbiota from a lean individual. Further studies show that gut microbiota diversity correlates the tightest with healthy appetite and weight regulation (Han et al., 2021; van de Wouw et al., 2017). This so-called microbiota-gut-brain axis has recently gained enormous attention due to the complexity and feasibility of manipulation to treat pathological conditions like eating disorders. As summarized in Part B of this section, several gut-derived neuropeptides also contribute to appetite regulation and systematic communication of nutritional states between organs.

(7) mTOR and S6K1. In flies, two studies independently elucidate the role of mTOR/S6K1 in nutrient balancing (Ribeiro and Dickson, 2010; Vargas et al., 2010). In rodents, mTOR/S6K1 signaling is also crucial for metabolism and food intake control, but the regulation is much more complex, potentially due to the dominant roles of hormonal controls. Several studies have shown that in the arcuate nucleus of the hypothalamus, mTOR/S6K1 signaling regulates the effects of insulin and leptin and leads to energy expenditure alteration and appetite change (Tavares et al., 2020; Wiczer and Thomas, 2010). But how to cleanly tease apart the effect of mTOR/S6K1 signaling in the CNS and PNS remains a technical challenge. Meanwhile, exploration of the function of this signaling pathway in animals specifically starved of a particular nutrient is still lacking, because most studies were performed for either total starved or fed animals.

In all, how these mechanisms coordinate together to impact organismal protein detection in the diets remains unclear. It will be interesting to investigate whether each of them conveys the availability

of distinct components of protein (i.e., individual amino acids) and whether different cell types predominantly utilize certain mechanisms for bulk protein detection.

D. Coordination between amino acid sensing with other macronutrient sensing

Macronutrients are typically divided to four main types: carbohydrate, protein, lipid, and low-abundant macromolecules like vitamins. Carbohydrate sensing has been documented to the greatest detail among all four types. The sweet taste of many classes of carbohydrates, such as glucose and fructose, typically initiates as a substantial reward for most animals. Thus, most animals automatically feed on high glucose/fructose-containing food. And this phenomenon is typically described as sugar addiction, which is commonly seen in children and a common cause for obesity.

Sugar triggers a strong response on taste buds containing the sweet receptor (TAS1R2/TAS1R3), which encodes neurological response to the reward circuits in the brain, indicating the preference for sugar. This taste receptor-mediated process happens acutely, within seconds of sweet food consumption (Ahmad and Dalziel, 2020). After digestion of carbohydrates, most of them break down to monosaccharides. The digested sugar flows into the intestine, where most of the absorption happens. In parallel, numerous reports suggest that sensing of the sugar also occurs in the gut, which takes a longer time scale than the first layer taste response. Rodent studies indicate that artificial sweeteners, even taste similarly sweet but cannot be absorbed by the body, are preferred less than monosaccharides like glucose or fructose. These results suggest that the absorption and further metabolism of the sugar impact the food choice independent of the taste (Zhang et al., 2018). The mechanism encoding this behavior is under active investigation.

To explore the crosstalk between protein sensing and carbohydrate sensing, researchers focus on the effects of typical dietary nutrient mixtures on specific neurons that might have metabolic regulation roles. A group of neurons in the mammalian hypothalamus is reported to serve as essential

regulators of energy balance. The Orexin expressing cells are directly activated by mixtures of dietary amino acids, especially non-essential amino acids, both *in vitro* and *in vivo*. The same group of cells was also reported to be inhibited by glucose. And with physiological concentrations with both amino acids, it is sufficient to overwrite the inhibitory impact by glucose, indicating a competition between these two macronutrients. One hypothesis for the reason of the existence of this competition is that this reduction of glucose response by amino acids could amplify the influence of amino acids on these neurons since the physiological fluctuations of amino acids in the brain only occur within a much smaller concentration range than those of glucose (Karnani et al., 2011).

SECTION 4. Contributions of this thesis

A. SAMTOR is an S-adenosylmethionine sensor for the mTORC1 pathway (CHAPTER 2) (Gu et al., 2017)

To identify novel regulators in the mTORC1 pathway, I mined a public protein-protein interaction dataset, Bioplex, and identified a poorly studied protein C7orf60 that pulls down all GATOR1-KICSTOR components. Then I validated that this novel sensor regulates mTORC1 activity in response to the availability of S-adenosylmethionine (SAM), a key metabolite generated directly from methionine and ATP and essential for key cellular processes including methylation reactions and one-carbon metabolism. We named this previously uncharacterized protein SAMTOR (SAM sensor upstream of mTORC1). It is the first sensor in nutrient sensing pathway that responds to the downstream metabolite of an amino acid. I found that SAMTOR inhibits mTORC1 signaling by interacting with GATOR1-KICSTOR complex and that SAM disrupts this interaction by binding directly to SAMTOR. In cells, I determined that methionine starvation strongly reduces SAM levels and promotes the association of SAMTOR with GATOR1-KICSTOR, thereby inhibiting mTORC1 signaling in a SAMTOR-dependent fashion. Methionine-induced activation of mTORC1 requires the SAM binding capacity of SAMTOR. Thus, SAMTOR is a SAM

sensor that links methionine and one-carbon metabolism to mTORC1 signaling. Importantly, it has been reported that diets low in methionine reduce tissue SAM levels and extend lifespan in mice and rats. It is intriguing to speculate that these benefits might be mediated in part via the SAMTOR-dependent inhibition of mTORC1, which is well appreciated to impact glucose metabolism and aging. Meanwhile, for decades, SAM itself is prescribed as an anti-depressant. Given that SAMTOR has a SAM-binding pocket, it may be possible to modulate SAMTOR functions pharmacologically.

B. Sestrin-mediated leucine sensing by mTORC1 is essential for detecting and adapting to a low leucine diet in *Drosophila* (CHAPTER 3)

I explored the physiological functions of the nutrient sensing pathway. Detecting nutritional quality of diets and balancing nutrient intake are key for optimal organismal growth. Protein is an essential macronutrient and its constituent building blocks, amino acids, are potent regulators of mTORC1. Thus, I hypothesized that on the organismal level, mTORC1 is able to detect imbalance of nutrients in diets and regulate downstream metabolic responses. Generating knockout and nutrient binding deficient mutants of nutrient sensors facilitates tracking physiological consequences upon acute corresponding dietary deprivation. *Drosophila melanogaster* is a powerful system with numerous genetic tools and amenable to biochemical validation and characterization of organismal phenotypes. I decided to manipulate Drosophila Sestrin, the single gene with sequence homology to mammalian Sestrins. I validated that Drosophila Sestrin protein binds leucine and that its interaction with GATOR2 is strongly enhanced specifically by leucine deprivation *in vivo*. Flies lacking Sestrin fail to inhibit mTORC1 activity upon leucine starvation, while flies with homozygous leucine binding deficient mutant show lower mTORC1 activity even on standard diet and are unable to further inhibit mTORC1 when deprived of leucine. Interestingly, flies lacking Sestrin are less capable of tolerating a low leucine diet compared to wild type flies, perhaps due to an inability to inhibit mTORC1 and activate autophagy as a compensatory

response. In addition, loss of Sestrin influences processes known to be regulated by mTORC1, such as ovarian size control. Surprisingly, I also found that given two food choices, one with leucine, the other without, wild type flies prefer to consume leucine containing food while Sestrin mutant flies fail to detect the difference and show little preference. Functional Sestrin in fly glial cells is essential for encoding this preference. This study sheds light on a novel *in vivo* function of this cytosolic leucine sensor Sestrin, and opens doors for future studies to further characterize the roles of mTORC1 in organismal amino acid sensing.

References

Abastado, J.P., Miller, P.F., and Hinnebusch, A.G. (1991a). A quantitative model for translational control of the GCN4 gene of Saccharomyces cerevisiae. New Biol *3*, 511-524.

Abastado, J.P., Miller, P.F., Jackson, B.M., and Hinnebusch, A.G. (1991b). Suppression of ribosomal reinitiation at upstream open reading frames in amino acid-starved cells forms the basis for GCN4 translational control. Mol Cell Biol *11*, 486-496.

Abdel-Sater, F., El Bakkoury, M., Urrestarazu, A., Vissers, S., and Andre, B. (2004). Amino acid signaling in yeast: casein kinase I and the Ssy5 endoprotease are key determinants of endoproteolytic activation of the membrane-bound Stp1 transcription factor. Mol Cell Biol *24*, 9771-9785.

Abdel-Sater, F., Jean, C., Merhi, A., Vissers, S., and Andre, B. (2011). Amino acid signaling in yeast: activation of Ssy5 protease is associated with its phosphorylation-induced ubiquitylation. J Biol Chem *286*, 12006-12015.

Adler, S.P., Purich, D., and Stadtman, E.R. (1975). Cascade control of Escherichia coli glutamine synthetase. Properties of the PII regulatory protein and the uridylyltransferase-uridylyl-removing enzyme. J Biol Chem *250*, 6264-6272.

Ahmad, R., and Dalziel, J.E. (2020). G Protein-Coupled Receptors in Taste Physiology and Pharmacology. Front Pharmacol *11*, 587664.

Alfa, R.W., Park, S., Skelly, K.R., Poffenberger, G., Jain, N., Gu, X., Kockel, L., Wang, J., Liu, Y., Powers, A.C*., et al.* (2015). Suppression of insulin production and secretion by a decretin hormone. Cell Metab *21*, 323-334.

Anand, G.S., and Stock, A.M. (2002). Kinetic basis for the stimulatory effect of phosphorylation on the methylesterase activity of CheB. Biochemistry *41*, 6752-6760.

Andersson, U., Filipsson, K., Abbott, C.R., Woods, A., Smith, K., Bloom, S.R., Carling, D., and Small, C.J. (2004). AMP-activated protein kinase plays a role in the control of food intake. J Biol Chem *279*, 12005-12008.

Auesukaree, C., Tochio, H., Shirakawa, M., Kaneko, Y., and Harashima, S. (2005). Plc1p, Arg82p, and Kcs1p, enzymes involved in inositol pyrophosphate synthesis, are essential for phosphate regulation and polyphosphate accumulation in Saccharomyces cerevisiae. J Biol Chem *280*, 25127-25133.

B'Chir, W., Maurin, A.C., Carraro, V., Averous, J., Jousse, C., Muranishi, Y., Parry, L., Stepien, G., Fafournoux, P., and Bruhat, A. (2013). The eIF2alpha/ATF4 pathway is essential for stress-induced autophagy gene expression. Nucleic Acids Res *41*, 7683-7699.

Baker, D.H. (2009). Advances in protein-amino acid nutrition of poultry. Amino Acids *37*, 29-41.

Bar-Peled, L., Chantranupong, L., Cherniack, A.D., Chen, W.W., Ottina, K.A., Grabiner, B.C., Spear, E.D., Carter, S.L., Meyerson, M., and Sabatini, D.M. (2013). A Tumor suppressor complex with GAP activity for the Rag GTPases that signal amino acid sufficiency to mTORC1. Science *340*, 1100-1106.

Bar-Peled, L., Schweitzer, L.D., Zoncu, R., and Sabatini, D.M. (2012). Ragulator is a GEF for the rag GTPases that signal amino acid levels to mTORC1. Cell *150*, 1196-1208.

Bednarova, A., Kodrik, D., and Krishnan, N. (2013). Unique roles of glucagon and glucagon-like peptides: Parallels in understanding the functions of adipokinetic hormones in stress responses in insects. Comp Biochem Physiol A Mol Integr Physiol *164*, 91-100.

Berg, H.C. (2008). Bacterial flagellar motor. Curr Biol *18*, R689-691.

Berthoud, H.R. (2008). The vagus nerve, food intake and obesity. Regul Pept *149*, 15-25.

Birse, R.T., Soderberg, J.A., Luo, J., Winther, A.M., and Nassel, D.R. (2011). Regulation of insulin-producing cells in the adult Drosophila brain via the tachykinin peptide receptor DTKR. J Exp Biol *214*, 4201-4208.

Bisson, L.F., Neigeborn, L., Carlson, M., and Fraenkel, D.G. (1987). The SNF3 gene is required for high-affinity glucose transport in Saccharomyces cerevisiae. J Bacteriol *169*, 1656-1662.

Biteau, B., Karpac, J., Supoyo, S., Degennaro, M., Lehmann, R., and Jasper, H. (2010). Lifespan extension by preserving proliferative homeostasis in Drosophila. PLoS Genet *6*, e1001159.

Biver, S., Belge, H., Bourgeois, S., Van Vooren, P., Nowik, M., Scohy, S., Houillier, P., Szpirer, J., Szpirer, C., Wagner, C.A*., et al.* (2008). A role for Rhesus factor Rhcg in renal ammonium excretion and male fertility. Nature *456*, 339-343.

Bjordal, M., Arquier, N., Kniazeff, J., Pin, J.P., and Leopold, P. (2014). Sensing of amino acids in a dopaminergic circuitry promotes rejection of an incomplete diet in Drosophila. Cell *156*, 510-521.

Borkovich, K.A., Kaplan, N., Hess, J.F., and Simon, M.I. (1989). Transmembrane signal transduction in bacterial chemotaxis involves ligand-dependent activation of phosphate group transfer. Proc Natl Acad Sci U S A *86*, 1208-1212.

Borkovich, K.A., and Simon, M.I. (1990). The dynamics of protein phosphorylation in bacterial chemotaxis. Cell *63*, 1339-1348.

Bren, A., and Eisenbach, M. (2000). How signals are heard during bacterial chemotaxis: protein-protein interactions in sensory signal propagation. J Bacteriol *182*, 6865-6873.

Brookes, S.J., Spencer, N.J., Costa, M., and Zagorodnyuk, V.P. (2013). Extrinsic primary afferent signalling in the gut. Nat Rev Gastroenterol Hepatol *10*, 286-296.

Buch, S., Melcher, C., Bauer, M., Katzenberger, J., and Pankratz, M.J. (2008). Opposing effects of dietary protein and sugar regulate a transcriptional target of Drosophila insulin-like peptide signaling. Cell Metab *7*, 321-332.

Buchon, N., and Osman, D. (2015). All for one and one for all: Regionalization of the Drosophila intestine. Insect Biochem Mol Biol *67*, 2-8.

Buchon, N., Osman, D., David, F.P., Fang, H.Y., Boquete, J.P., Deplancke, B., and Lemaitre, B. (2013). Morphological and molecular characterization of adult midgut compartmentalization in Drosophila. Cell Rep *3*, 1725-1738.

Buerger, C., DeVries, B., and Stambolic, V. (2006). Localization of Rheb to the endomembrane is critical for its signaling function. Biochem Biophys Res Commun *344*, 869-880.

Bunpo, P., Dudley, A., Cundiff, J.K., Cavener, D.R., Wek, R.C., and Anthony, T.G. (2009). GCN2 protein kinase is required to activate amino acid deprivation responses in mice treated with the anti-cancer agent L-asparaginase. J Biol Chem *284*, 32742-32749.

Callaghan, B., Furness, J.B., and Pustovit, R.V. (2018). Neural pathways for colorectal control, relevance to spinal cord injury and treatment: a narrative review. Spinal Cord *56*, 199-205.

Carling, D., Clarke, P.R., Zammit, V.A., and Hardie, D.G. (1989). Purification and characterization of the AMP-activated protein kinase. Copurification of acetyl-CoA carboxylase kinase and 3-hydroxy-3-methylglutaryl-CoA reductase kinase activities. Eur J Biochem *186*, 129-136.

Carling, D., and Hardie, D.G. (1989). The substrate and sequence specificity of the AMP-activated protein kinase. Phosphorylation of glycogen synthase and phosphorylase kinase. Biochim Biophys Acta *1012*, 81-86.

Cazzamali, G., Torp, M., Hauser, F., Williamson, M., and Grimmelikhuijzen, C.J. (2005). The Drosophila gene CG9918 codes for a pyrokinin-1 receptor. Biochem Biophys Res Commun *335*, 14-19.

Chantranupong, L., Scaria, S.M., Saxton, R.A., Gygi, M.P., Shen, K., Wyant, G.A., Wang, T., Harper, J.W., Gygi, S.P., and Sabatini, D.M. (2016). The CASTOR Proteins Are Arginine Sensors for the mTORC1 Pathway. Cell *165*, 153-164.

Chantranupong, L., Wolfson, R.L., Orozco, J.M., Saxton, R.A., Scaria, S.M., Bar-Peled, L., Spooner, E., Isasa, M., Gygi, S.P., and Sabatini, D.M. (2014). The Sestrins interact with GATOR2 to negatively regulate the amino-acid-sensing pathway upstream of mTORC1. Cell Rep *9*, 1-8.

Chantranupong, L., Wolfson, R.L., and Sabatini, D.M. (2015). Nutrient-sensing mechanisms across evolution. Cell *161*, 67-83.

Charriere, G.M., Ip, W.E., Dejardin, S., Boyer, L., Sokolovska, A., Cappillino, M.P., Cherayil, B.J., Podolsky, D.K., Kobayashi, K.S., Silverman, N.*, et al.* (2010). Identification of Drosophila Yin and PEPT2 as evolutionarily conserved phagosome-associated muramyl dipeptide transporters. J Biol Chem *285*, 20147-20154.

Choi, N.H., Lucchetta, E., and Ohlstein, B. (2011). Nonautonomous regulation of Drosophila midgut stem cell proliferation by the insulin-signaling pathway. Proc Natl Acad Sci U S A *108*, 18702-18707.

Cognigni, P., Bailey, A.P., and Miguel-Aliaga, I. (2011). Enteric neurons and systemic signals couple nutritional and reproductive status with intestinal homeostasis. Cell Metab *13*, 92-104.

Conrad, M., Schothorst, J., Kankipati, H.N., Van Zeebroeck, G., Rubio-Texeira, M., and Thevelein, J.M. (2014). Nutrient sensing and signaling in the yeast Saccharomyces cerevisiae. FEMS Microbiol Rev *38*, 254-299.

Corton, J.M., Gillespie, J.G., Hawley, S.A., and Hardie, D.G. (1995). 5-aminoimidazole-4-carboxamide ribonucleoside. A specific method for activating AMP-activated protein kinase in intact cells? Eur J Biochem *229*, 558-565.

Crocker, A., Shahidullah, M., Levitan, I.B., and Sehgal, A. (2010). Identification of a neural circuit that underlies the effects of octopamine on sleep:wake behavior. Neuron *65*, 670-681.

Croset, V., Schleyer, M., Arguello, J.R., Gerber, B., and Benton, R. (2016). A molecular and neuronal basis for amino acid sensing in the Drosophila larva. Sci Rep *6*, 34871.

Crozet, P., Margalha, L., Confraria, A., Rodrigues, A., Martinho, C., Adamo, M., Elias, C.A., and Baena-Gonzalez, E. (2014). Mechanisms of regulation of SNF1/AMPK/SnRK1 protein kinases. Front Plant Sci *5*, 190.

Curzon, G. (1990). Serotonin and appetite. Ann N Y Acad Sci *600*, 521-530; discussion 530-521.

Dagon, Y., Hur, E., Zheng, B., Wellenstein, K., Cantley, L.C., and Kahn, B.B. (2012). p70S6 kinase phosphorylates AMPK on serine 491 to mediate leptin's effect on food intake. Cell Metab *16*, 104-112.

Dever, T.E., Feng, L., Wek, R.C., Cigan, A.M., Donahue, T.F., and Hinnebusch, A.G. (1992). Phosphorylation of initiation factor 2 alpha by protein kinase GCN2 mediates gene-specific translational control of GCN4 in yeast. Cell *68*, 585-596.

di Salvo, M.L., Contestabile, R., Paiardini, A., and Maras, B. (2013). Glycine consumption and mitochondrial serine hydroxymethyltransferase in cancer cells: the heme connection. Med Hypotheses *80*, 633-636.

Diallinas, G., and Thireos, G. (1994). Genetic and biochemical evidence for yeast GCN2 protein kinase polymerization. Gene *143*, 21-27.

Didion, T., Regenberg, B., Jorgensen, M.U., Kielland-Brandt, M.C., and Andersen, H.A. (1998). The permease homologue Ssy1p controls the expression of amino acid and peptide transporter genes in Saccharomyces cerevisiae. Mol Microbiol *27*, 643-650.

Dockray, G.J. (2013). Enteroendocrine cell signalling via the vagus nerve. Curr Opin Pharmacol *13*, 954-958.

Dus, M., Lai, J.S., Gunapala, K.M., Min, S., Tayler, T.D., Hergarden, A.C., Geraud, E., Joseph, C.M., and Suh, G.S. (2015). Nutrient Sensor in the Brain Directs the Action of the Brain-Gut Axis in Drosophila. Neuron *87*, 139-151.

Dussutour, A., Latty, T., Beekman, M., and Simpson, S.J. (2010). Amoeboid organism solves complex nutritional challenges. Proc Natl Acad Sci U S A *107*, 4607-4611.

Dyer, C.M., Vartanian, A.S., Zhou, H., and Dahlquist, F.W. (2009). A molecular mechanism of bacterial flagellar motor switching. J Mol Biol *388*, 71-84.

Escher, S.A., and Rasmuson-Lestander, A. (1999). The Drosophila glucose transporter gene: cDNA sequence, phylogenetic comparisons, analysis of functional sites and secondary structures. Hereditas *130*, 95-103.

Fernstrom, J.D., and Fernstrom, M.H. (2007). Tyrosine, phenylalanine, and catecholamine synthesis and function in the brain. J Nutr *137*, 1539S-1547S; discussion 1548S.

Flissi, A., Ricart, E., Campart, C., Chevalier, M., Dufresne, Y., Michalik, J., Jacques, P., Flahaut, C., Lisacek, F., Leclere, V.*, et al.* (2020). Norine: update of the nonribosomal peptide resource. Nucleic Acids Res *48*, D465-D469.

Forchhammer, K. (2010). The network of P(II) signalling protein interactions in unicellular cyanobacteria. Adv Exp Med Biol *675*, 71-90.

Fraser, S., Mount, P., Hill, R., Levidiotis, V., Katsis, F., Stapleton, D., Kemp, B.E., and Power, D.A. (2005). Regulation of the energy sensor AMP-activated protein kinase in the kidney by dietary salt intake and osmolality. Am J Physiol Renal Physiol *288*, F578-586.

Fu, Z., Gilbert, E.R., and Liu, D. (2013). Regulation of insulin synthesis and secretion and pancreatic Beta-cell dysfunction in diabetes. Curr Diabetes Rev *9*, 25-53.

Furness, J.B. (2016). Integrated Neural and Endocrine Control of Gastrointestinal Function. Adv Exp Med Biol *891*, 159-173.

Furness, J.B., Callaghan, B.P., Rivera, L.R., and Cho, H.J. (2014). The enteric nervous system and gastrointestinal innervation: integrated local and central control. Adv Exp Med Biol *817*, 39-71.

Furst, P., and Stehle, P. (2004). What are the essential elements needed for the determination of amino acid requirements in humans? J Nutr *134*, 1558S-1565S.

Gahagan, S. (2012). Development of eating behavior: biology and context. J Dev Behav Pediatr *33*, 261-271.

Ganguly, A., Pang, L., Duong, V.K., Lee, A., Schoniger, H., Varady, E., and Dahanukar, A. (2017). A Molecular and Cellular Context-Dependent Role for Ir76b in Detection of Amino Acid Taste. Cell Rep *18*, 737-750.

Garst, A.D., Edwards, A.L., and Batey, R.T. (2011). Riboswitches: structures and mechanisms. Cold Spring Harb Perspect Biol *3*.

Geminard, C., Rulifson, E.J., and Leopold, P. (2009). Remote control of insulin secretion by fat cells in Drosophila. Cell Metab *10*, 199-207.

Gesmundo, I., Villanova, T., Banfi, D., Gamba, G., and Granata, R. (2017). Role of Melatonin, Galanin, and RFamide Neuropeptides QRFP26 and QRFP43 in the Neuroendocrine Control of Pancreatic beta-Cell Function. Front Endocrinol (Lausanne) *8*, 143.

Gimeno, C.J., Ljungdahl, P.O., Styles, C.A., and Fink, G.R. (1992). Unipolar cell divisions in the yeast S. cerevisiae lead to filamentous growth: regulation by starvation and RAS. Cell *68*, 1077-1090.

Goberdhan, D.C., Meredith, D., Boyd, C.A., and Wilson, C. (2005). PAT-related amino acid transporters regulate growth via a novel mechanism that does not require bulk transport of amino acids. Development *132*, 2365-2375.

Gowans, G.J., and Hardie, D.G. (2014). AMPK: a cellular energy sensor primarily regulated by AMP. Biochem Soc Trans *42*, 71-75.

Grand, R.J., Watkins, J.B., and Torti, F.M. (1976). Development of the human gastrointestinal tract. A review. Gastroenterology *70*, 790-810.

Gu, X., Orozco, J.M., Saxton, R.A., Condon, K.J., Liu, G.Y., Krawczyk, P.A., Scaria, S.M., Harper, J.W., Gygi, S.P., and Sabatini, D.M. (2017). SAMTOR is an S-adenosylmethionine sensor for the mTORC1 pathway. Science *358*, 813-818.

Gwinn, D.M., Shackelford, D.B., Egan, D.F., Mihaylova, M.M., Mery, A., Vasquez, D.S., Turk, B.E., and Shaw, R.J. (2008). AMPK phosphorylation of raptor mediates a metabolic checkpoint. Mol Cell *30*, 214-226.

Hadjieconomou, D., King, G., Gaspar, P., Mineo, A., Blackie, L., Ameku, T., Studd, C., de Mendoza, A., Diao, F., White, B.H.*, et al.* (2020). Enteric neurons increase maternal food intake during reproduction. Nature *587*, 455-459.

Haj-Ahmad, Y., and Hickey, D.A. (1982). A molecular explanation of frequency-dependent selection in Drosophila. Nature *299*, 350-352.

Hammann, C., and Westhof, E. (2007). Searching genomes for ribozymes and riboswitches. Genome Biol *8*, 210.

Han, H., Yi, B., Zhong, R., Wang, M., Zhang, S., Ma, J., Yin, Y., Yin, J., Chen, L., and Zhang, H. (2021). From gut microbiota to host appetite: gut microbiota-derived metabolites as key regulators. Microbiome *9*, 162.

Hao, S., Sharp, J.W., Ross-Inta, C.M., McDaniel, B.J., Anthony, T.G., Wek, R.C., Cavener, D.R., McGrath, B.C., Rudell, J.B., Koehnle, T.J.*, et al.* (2005). Uncharged tRNA and sensing of amino acid deficiency in mammalian piriform cortex. Science *307*, 1776-1778.

Hardie, D.G., and Hawley, S.A. (2001). AMP-activated protein kinase: the energy charge hypothesis revisited. Bioessays *23*, 1112-1119.

Hardie, D.G., Ross, F.A., and Hawley, S.A. (2012). AMPK: a nutrient and energy sensor that maintains energy homeostasis. Nat Rev Mol Cell Biol *13*, 251-262.

Harding, H.P., Ordonez, A., Allen, F., Parts, L., Inglis, A.J., Williams, R.L., and Ron, D. (2019). The ribosomal P-stalk couples amino acid starvation to GCN2 activation in mammalian cells. Elife *8*.

Hartenstein, V., and Martinez, P. (2019). Structure, development and evolution of the digestive system. Cell Tissue Res *377*, 289-292.

Hedblom, M.L., and Adler, J. (1980). Genetic and biochemical properties of Escherichia coli mutants with defects in serine chemotaxis. J Bacteriol *144*, 1048-1060.

Hegedus, D., Erlandson, M., Gillott, C., and Toprak, U. (2009). New insights into peritrophic matrix synthesis, architecture, and function. Annu Rev Entomol *54*, 285-302.

Hentze, J.L., Carlsson, M.A., Kondo, S., Nassel, D.R., and Rewitz, K.F. (2015). The Neuropeptide Allatostatin A Regulates Metabolism and Feeding Decisions in Drosophila. Sci Rep *5*, 11680.

Hertz, L. (2013). The Glutamate-Glutamine (GABA) Cycle: Importance of Late Postnatal Development and Potential Reciprocal Interactions between Biosynthesis and Degradation. Front Endocrinol (Lausanne) *4*, 59.

Hickey, D.A., Benkel, B.F., Abukashawa, S., and Haus, S. (1988). DNA rearrangement causes multiple changes in gene expression at the amylase locus in Drosophila melanogaster. Biochem Genet *26*, 757-768.

Hinnebusch, A.G. (1984). Evidence for translational regulation of the activator of general amino acid control in yeast. Proc Natl Acad Sci U S A *81*, 6442-6446.

Hinnebusch, A.G. (2005). Translational regulation of GCN4 and the general amino acid control of yeast. Annu Rev Microbiol *59*, 407-450.

Hong, S.P., Leiper, F.C., Woods, A., Carling, D., and Carlson, M. (2003). Activation of yeast Snf1 and mammalian AMP-activated protein kinase by upstream kinases. Proc Natl Acad Sci U S A *100*, 8839-8843.

Horne, I., Haritos, V.S., and Oakeshott, J.G. (2009). Comparative and functional genomics of lipases in holometabolous insects. Insect Biochem Mol Biol *39*, 547-567.

Huang, X., Warren, J.T., Buchanan, J., Gilbert, L.I., and Scott, M.P. (2007). Drosophila Niemann-Pick type C-2 genes control sterol homeostasis and steroid biosynthesis: a model of human neurodegenerative disease. Development *134*, 3733-3742.

Huckesfeld, S., Schoofs, A., Schlegel, P., Miroschnikow, A., and Pankratz, M.J. (2015). Localization of Motor Neurons and Central Pattern Generators for Motor Patterns Underlying Feeding Behavior in Drosophila Larvae. PLoS One *10*, e0135011.

Huergo, L.F., Chandra, G., and Merrick, M. (2013). P(II) signal transduction proteins: nitrogen regulation and beyond. FEMS Microbiol Rev *37*, 251-283.

Inglis, A.J., Masson, G.R., Shao, S., Perisic, O., McLaughlin, S.H., Hegde, R.S., and Williams, R.L. (2019). Activation of GCN2 by the ribosomal P-stalk. Proc Natl Acad Sci U S A *116*, 4946-4954.

Inoki, K., Zhu, T., and Guan, K.L. (2003). TSC2 mediates cellular energy response to control cell growth and survival. Cell *115*, 577-590.

Ishimura, R., Nagy, G., Dotu, I., Chuang, J.H., and Ackerman, S.L. (2016). Activation of GCN2 kinase by ribosome stalling links translation elongation with translation initiation. Elife *5*.

Jackson, E.N., and Yanofsky, C. (1973). Thr region between the operator and first structural gene of the tryptophan operon of Escherichia coli may have a regulatory function. J Mol Biol *76*, 89-101.

Jia, L., Betters, J.L., and Yu, L. (2011). Niemann-pick C1-like 1 (NPC1L1) protein in intestinal and hepatic cholesterol transport. Annu Rev Physiol *73*, 239-259.

Jiang, P., and Ninfa, A.J. (2007). Escherichia coli PII signal transduction protein controlling nitrogen assimilation acts as a sensor of adenylate energy charge in vitro. Biochemistry *46*, 12979-12996.

Jiang, P., Peliska, J.A., and Ninfa, A.J. (1998). The regulation of Escherichia coli glutamine synthetase revisited: role of 2-ketoglutarate in the regulation of glutamine synthetase adenylylation state. Biochemistry *37*, 12802-12810.

Johnson, E.C., Shafer, O.T., Trigg, J.S., Park, J., Schooley, D.A., Dow, J.A., and Taghert, P.H. (2005). A novel diuretic hormone receptor in Drosophila: evidence for conservation of CGRP signaling. J Exp Biol *208*, 1239-1246.

Jouandot, D., 2nd, Roy, A., and Kim, J.H. (2011). Functional dissection of the glucose signaling pathways that regulate the yeast glucose transporter gene (HXT) repressor Rgt1. J Cell Biochem *112*, 3268-3275.

Jung, J., Genau, H.M., and Behrends, C. (2015). Amino Acid-Dependent mTORC1 Regulation by the Lysosomal Membrane Protein SLC38A9. Mol Cell Biol *35*, 2479-2494.

Kaminski, S., Orlowski, E., Berry, K., and Nichols, R. (2002). The effects of three Drosophila melanogaster myotropins on the frequency of foregut contractions differ. J Neurogenet *16*, 125-134.

Kanamori, Y., Saito, A., Hagiwara-Komoda, Y., Tanaka, D., Mitsumasu, K., Kikuta, S., Watanabe, M., Cornette, R., Kikawada, T., and Okuda, T. (2010). The trehalose transporter 1 gene sequence is conserved in insects and encodes proteins with different kinetic properties involved in trehalose import into peripheral tissues. Insect Biochem Mol Biol *40*, 30-37.

Kapan, N., Lushchak, O.V., Luo, J., and Nassel, D.R. (2012). Identified peptidergic neurons in the Drosophila brain regulate insulin-producing cells, stress responses and metabolism by coexpressed short neuropeptide F and corazonin. Cell Mol Life Sci *69*, 4051-4066.

Kaplan, D.D., Zimmermann, G., Suyama, K., Meyer, T., and Scott, M.P. (2008). A nucleostemin family GTPase, NS3, acts in serotonergic neurons to regulate insulin signaling and control body size. Genes Dev *22*, 1877-1893.

Karnani, M.M., Apergis-Schoute, J., Adamantidis, A., Jensen, L.T., de Lecea, L., Fugger, L., and Burdakov, D. (2011). Activation of central orexin/hypocretin neurons by dietary amino acids. Neuron *72*, 616-629.

Kenmoku, H., Ishikawa, H., Ote, M., Kuraishi, T., and Kurata, S. (2016). A subset of neurons controls the permeability of the peritrophic matrix and midgut structure in Drosophila adults. J Exp Biol *219*, 2331-2339.

Kim, E., Goraksha-Hicks, P., Li, L., Neufeld, T.P., and Guan, K.L. (2008). Regulation of TORC1 by Rag GTPases in nutrient response. Nat Cell Biol *10*, 935-945.

Kim, J., and Neufeld, T.P. (2015). Dietary sugar promotes systemic TOR activation in Drosophila through AKH-dependent selective secretion of Dilp3. Nat Commun *6*, 6846.

Kim, S.K., and Rulifson, E.J. (2004). Conserved mechanisms of glucose sensing and regulation by Drosophila corpora cardiaca cells. Nature *431*, 316-320.

King, D.G. (1988). Cellular organization and peritrophic membrane formation in the cardia (proventriculus) of Drosophila melanogaster. J Morphol *196*, 253-282.

Klasson, H., Fink, G.R., and Ljungdahl, P.O. (1999). Ssy1p and Ptr3p are plasma membrane components of a yeast system that senses extracellular amino acids. Mol Cell Biol *19*, 5405-5416.

Klok, M.D., Jakobsdottir, S., and Drent, M.L. (2007). The role of leptin and ghrelin in the regulation of food intake and body weight in humans: a review. Obes Rev *8*, 21-34.

Koehnle, T.J., Russell, M.C., and Gietzen, D.W. (2003). Rats rapidly reject diets deficient in essential amino acids. J Nutr *133*, 2331-2335.

Kondoh, H., Ball, C.B., and Adler, J. (1979). Identification of a methyl-accepting chemotaxis protein for the ribose and galactose chemoreceptors of Escherichia coli. Proc Natl Acad Sci U S A *76*, 260-264.

Kwak, S.J., Hong, S.H., Bajracharya, R., Yang, S.Y., Lee, K.S., and Yu, K. (2013). Drosophila adiponectin receptor in insulin producing cells regulates glucose and lipid metabolism by controlling insulin secretion. PLoS One *8*, e68641.

Lane, N., and Martin, W. (2010). The energetics of genome complexity. Nature *467*, 929-934.

Lee, G., and Park, J.H. (2004). Hemolymph sugar homeostasis and starvation-induced hyperactivity affected by genetic manipulations of the adipokinetic hormone-encoding gene in Drosophila melanogaster. Genetics *167*, 311-323.

Lee, Y.S., Huang, K., Quiocho, F.A., and O'Shea, E.K. (2008). Molecular basis of cyclin-CDK-CKI regulation by reversible binding of an inositol pyrophosphate. Nat Chem Biol *4*, 25-32.

Lee, Y.S., Mulugu, S., York, J.D., and O'Shea, E.K. (2007). Regulation of a cyclin-CDK-CDK inhibitor complex by inositol pyrophosphates. Science *316*, 109-112.

Lehane, M.J. (1997). Peritrophic matrix structure and function. Annu Rev Entomol *42*, 525-550.

Leib, D.E., and Knight, Z.A. (2015). Re-examination of Dietary Amino Acid Sensing Reveals a GCN2-Independent Mechanism. Cell Rep *13*, 1081-1089.

Leib, D.E., and Knight, Z.A. (2016). Rapid Sensing of Dietary Amino Acid Deficiency Does Not Require GCN2. Cell Rep *16*, 2051-2052.

Leung, P.M., Larson, D.M., and Rogers, Q.R. (1972). Food intake and preference of olfactory bulbectomized rats fed amino acid imbalanced or deficient diets. Physiol Behav *9*, 553-557.

Linneweber, G.A., Jacobson, J., Busch, K.E., Hudry, B., Christov, C.P., Dormann, D., Yuan, M., Otani, T., Knust, E., de Bono, M.*, et al.* (2014). Neuronal control of metabolism through nutrient-dependent modulation of tracheal branching. Cell *156*, 69-83.

Liu, G.Y., and Sabatini, D.M. (2020). mTOR at the nexus of nutrition, growth, ageing and disease. Nat Rev Mol Cell Biol *21*, 183-203.

Liu, Q., Tabuchi, M., Liu, S., Kodama, L., Horiuchi, W., Daniels, J., Chiu, L., Baldoni, D., and Wu, M.N. (2017). Branch-specific plasticity of a bifunctional dopamine circuit encodes protein hunger. Science *356*, 534-539.

Lorenz, M.C., and Heitman, J. (1998a). The MEP2 ammonium permease regulates pseudohyphal differentiation in Saccharomyces cerevisiae. EMBO J *17*, 1236-1247.

Lorenz, M.C., and Heitman, J. (1998b). Regulators of pseudohyphal differentiation in Saccharomyces cerevisiae identified through multicopy suppressor analysis in ammonium permease mutant strains. Genetics *150*, 1443-1457.

Luo, J., Becnel, J., Nichols, C.D., and Nassel, D.R. (2012). Insulin-producing cells in the brain of adult Drosophila are regulated by the serotonin 5-HT1A receptor. Cell Mol Life Sci *69*, 471-484.

Luo, J., Lushchak, O.V., Goergen, P., Williams, M.J., and Nassel, D.R. (2014). Drosophila insulin-producing cells are differentially modulated by serotonin and octopamine receptors and affect social behavior. PLoS One *9*, e99732.

Lushchak, O.V., Carlsson, M.A., and Nassel, D.R. (2015). Food odors trigger an endocrine response that affects food ingestion and metabolism. Cell Mol Life Sci *72*, 3143-3155.

Mangum, J.H., Magni, G., and Stadtman, E.R. (1973). Regulation of glutamine synthetase adenylylation and deadenylylation by the enzymatic uridylylation and deuridylylation of the PII regulatory protein. Arch Biochem Biophys *158*, 514-525.

Manson, M.D., Blank, V., Brade, G., and Higgins, C.F. (1986). Peptide chemotaxis in E. coli involves the Tap signal transducer and the dipeptide permease. Nature *321*, 253-256.

Marianes, A., and Spradling, A.C. (2013). Physiological and stem cell compartmentalization within the Drosophila midgut. Elife *2*, e00886.

Marini, A.M., Soussi-Boudekou, S., Vissers, S., and Andre, B. (1997). A family of ammonium transporters in Saccharomyces cerevisiae. Mol Cell Biol *17*, 4282-4293.

Marini, A.M., Vissers, S., Urrestarazu, A., and Andre, B. (1994). Cloning and expression of the MEP1 gene encoding an ammonium transporter in Saccharomyces cerevisiae. EMBO J *13*, 3456-3463.

Martin, J.F., Hersperger, E., Simcox, A., and Shearn, A. (2000). minidiscs encodes a putative amino acid transporter subunit required non-autonomously for imaginal cell proliferation. Mech Dev *92*, 155-167.

Masson, G.R. (2019). Towards a model of GCN2 activation. Biochem Soc Trans *47*, 1481-1488.

Maurin, A.C., Jousse, C., Averous, J., Parry, L., Bruhat, A., Cherasse, Y., Zeng, H., Zhang, Y., Harding, H.P., Ron, D*., et al.* (2005). The GCN2 kinase biases feeding behavior to maintain amino acid homeostasis in omnivores. Cell Metab *1*, 273-277.

Mayack, C., Phalen, N., Carmichael, K., White, H.K., Hirche, F., Wang, Y., Stangl, G.I., and Amdam, G.V. (2019). Appetite is correlated with octopamine and hemolymph sugar levels in forager honeybees. J Comp Physiol A Neuroethol Sens Neural Behav Physiol *205*, 609-617.

Mazumder, M.K., Paul, R., and Borah, A. (2013). beta-phenethylamine--a phenylalanine derivative in brain--contributes to oxidative stress by inhibiting mitochondrial complexes and DT-diaphorase: an in silico study. CNS Neurosci Ther *19*, 596-602.

McLeod, C.J., Wang, L., Wong, C., and Jones, D.L. (2010). Stem cell dynamics in response to nutrient availability. Curr Biol *20*, 2100-2105.

Mesibov, R., Ordal, G.W., and Adler, J. (1973). The range of attractant concentrations for bacterial chemotaxis and the threshold and size of response over this range. Weber law and related phenomena. J Gen Physiol *62*, 203-223.

Meyer, H., Vitavska, O., and Wieczorek, H. (2011). Identification of an animal sucrose transporter. J Cell Sci *124*, 1984-1991.

Micchelli, C.A., and Perrimon, N. (2006). Evidence that stem cells reside in the adult Drosophila midgut epithelium. Nature *439*, 475-479.

Miguel-Aliaga, I., Jasper, H., and Lemaitre, B. (2018). Anatomy and Physiology of the Digestive Tract of Drosophila melanogaster. Genetics *210*, 357-396.

Miller, M.M., Popova, L.B., Meleshkevitch, E.A., Tran, P.V., and Boudko, D.Y. (2008). The invertebrate B(0) system transporter, D. melanogaster NAT1, has unique d-amino acid affinity and mediates gut and brain functions. Insect Biochem Mol Biol *38*, 923-931.

Min, S., Oh, Y., Verma, P., Whitehead, S.C., Yapici, N., Van Vactor, D., Suh, G.S., and Liberles, S. (2021). Control of feeding by Piezo-mediated gut mechanosensation in Drosophila. Elife *10*.

Minokoshi, Y., Alquier, T., Furukawa, N., Kim, Y.B., Lee, A., Xue, B., Mu, J., Foufelle, F., Ferre, P., Birnbaum, M.J.*, et al.* (2004). AMP-kinase regulates food intake by responding to hormonal and nutrient signals in the hypothalamus. Nature *428*, 569-574.

Miyamoto, T., Slone, J., Song, X., and Amrein, H. (2012). A fructose receptor functions as a nutrient sensor in the Drosophila brain. Cell *151*, 1113-1125.

Montgomery, R.K., Mulberg, A.E., and Grand, R.J. (1999). Development of the human gastrointestinal tract: twenty years of progress. Gastroenterology *116*, 702-731.

Mueller, P.P., and Hinnebusch, A.G. (1986). Multiple upstream AUG codons mediate translational control of GCN4. Cell *45*, 201-207.

Narasimhan, J., Staschke, K.A., and Wek, R.C. (2004). Dimerization is required for activation of eIF2 kinase Gcn2 in response to diverse environmental stress conditions. J Biol Chem *279*, 22820-22832.

Nassel, D.R., and Vanden Broeck, J. (2016). Insulin/IGF signaling in Drosophila and other insects: factors that regulate production, release and post-release action of the insulin-like peptides. Cell Mol Life Sci *73*, 271-290.

Ness, T.J., and Gebhart, G.F. (1990). Visceral pain: a review of experimental studies. Pain *41*, 167-234.

Nilsson, A., Haanstra, J.R., Engqvist, M., Gerding, A., Bakker, B.M., Klingmuller, U., Teusink, B., and Nielsen, J. (2020). Quantitative analysis of amino acid metabolism in liver cancer links glutamate excretion to nucleotide synthesis. Proc Natl Acad Sci U S A *117*, 10294-10304.

Nusawardani, T., Kroemer, J.A., Choi, M.Y., and Jurenka, R.A. (2013). Identification and characterization of the pyrokinin/pheromone biosynthesis activating neuropeptide family of G protein-coupled receptors from Ostrinia nubilalis. Insect Mol Biol *22*, 331-340.

Ohlstein, B., and Spradling, A. (2006). The adult Drosophila posterior midgut is maintained by pluripotent stem cells. Nature *439*, 470-474.

Omnus, D.J., and Ljungdahl, P.O. (2013). Rts1-protein phosphatase 2A antagonizes Ptr3-mediated activation of the signaling protease Ssy5 by casein kinase I. Mol Biol Cell *24*, 1480-1492.

Ozcan, S., Dover, J., Rosenwald, A.G., Wolfl, S., and Johnston, M. (1996). Two glucose transporters in Saccharomyces cerevisiae are glucose sensors that generate a signal for induction of gene expression. Proc Natl Acad Sci U S A *93*, 12428-12432.

Palm, W., Sampaio, J.L., Brankatschk, M., Carvalho, M., Mahmoud, A., Shevchenko, A., and Eaton, S. (2012). Lipoproteins in Drosophila melanogaster--assembly, function, and influence on tissue lipid composition. PLoS Genet *8*, e1002828.

Palmer, G.C., Tran, T., Duttlinger, A., and Nichols, R. (2007). The drosulfakinin 0 (DSK 0) peptide encoded in the conserved Dsk gene affects adult Drosophila melanogaster crop contractions. J Insect Physiol *53*, 1125-1133.

Park, J., and Carlson, J.R. (2018). Physiological responses of the Drosophila labellum to amino acids. J Neurogenet *32*, 27-36.

Park, S., Alfa, R.W., Topper, S.M., Kim, G.E., Kockel, L., and Kim, S.K. (2014). A genetic strategy to measure circulating Drosophila insulin reveals genes regulating insulin production and secretion. PLoS Genet *10*, e1004555.

Payne, S.C., Furness, J.B., and Stebbing, M.J. (2019). Bioelectric neuromodulation for gastrointestinal disorders: effectiveness and mechanisms. Nat Rev Gastroenterol Hepatol *16*, 89-105.

Peng, M., Yin, N., and Li, M.O. (2017). SZT2 dictates GATOR control of mTORC1 signalling. Nature *543*, 433-437.

Petersen, M.C., and Shulman, G.I. (2018). Mechanisms of Insulin Action and Insulin Resistance. Physiol Rev *98*, 2133-2223.

Prechtl, J.C., and Powley, T.L. (1990). The fiber composition of the abdominal vagus of the rat. Anat Embryol (Berl) *181*, 101-115.

Prentki, M., Matschinsky, F.M., and Madiraju, S.R. (2013). Metabolic signaling in fuel-induced insulin secretion. Cell Metab *18*, 162-185.

Price, M.D., Merte, J., Nichols, R., Koladich, P.M., Tobe, S.S., and Bendena, W.G. (2002). Drosophila melanogaster flatline encodes a myotropin orthologue to Manduca sexta allatostatin. Peptides *23*, 787-794.

Rabinowitch, I.M. (1938). Diet and Nutrition: Nutritional Requirements of the Mother during Lactation. Can Med Assoc J *39*, 76-79.

Rajan, A., and Perrimon, N. (2012). Drosophila cytokine unpaired 2 regulates physiological homeostasis by remotely controlling insulin secretion. Cell *151*, 123-137.

Reader, R.W., Tso, W.W., Springer, M.S., Goy, M.F., and Adler, J. (1979). Pleiotropic aspartate taxis and serine taxis mutants of Escherichia coli. J Gen Microbiol *111*, 363-374.

Rebsamen, M., Pochini, L., Stasyk, T., de Araujo, M.E., Galluccio, M., Kandasamy, R.K., Snijder, B., Fauster, A., Rudashevskaya, E.L., Bruckner, M.*, et al.* (2015). SLC38A9 is a component of the lysosomal amino acid sensing machinery that controls mTORC1. Nature *519*, 477-481.

Reeds, P.J. (2000). Dispensable and indispensable amino acids for humans. J Nutr *130*, 1835S-1840S.

Ren, G.R., Hauser, F., Rewitz, K.F., Kondo, S., Engelbrecht, A.F., Didriksen, A.K., Schjott, S.R., Sembach, F.E., Li, S., Sogaard, K.C.*, et al.* (2015). CCHamide-2 Is an Orexigenic Brain-Gut Peptide in Drosophila. PLoS One *10*, e0133017.

Renz, P.F., Valdivia-Francia, F., and Sendoel, A. (2020). Some like it translated: small ORFs in the 5'UTR. Exp Cell Res *396*, 112229.

Ribeiro, C., and Dickson, B.J. (2010). Sex peptide receptor and neuronal TOR/S6K signaling modulate nutrient balancing in Drosophila. Curr Biol *20*, 1000-1005.

Rodriguez-Caso, C., Montanez, R., Cascante, M., Sanchez-Jimenez, F., and Medina, M.A. (2006). Mathematical modeling of polyamine metabolism in mammals. J Biol Chem *281*, 21799-21812.

Rolfes, R.J., and Hinnebusch, A.G. (1993). Translation of the yeast transcriptional activator GCN4 is stimulated by purine limitation: implications for activation of the protein kinase GCN2. Mol Cell Biol *13*, 5099-5111.

Roman, G., Meller, V., Wu, K.H., and Davis, R.L. (1998). The opt1 gene of Drosophila melanogaster encodes a proton-dependent dipeptide transporter. Am J Physiol *275*, C857-869.

Rorsman, P., and Braun, M. (2013). Regulation of insulin secretion in human pancreatic islets. Annu Rev Physiol *75*, 155-179.

Rorsman, P., and Renstrom, E. (2003). Insulin granule dynamics in pancreatic beta cells. Diabetologia *46*, 1029-1045.

Roy, A., Shin, Y.J., Cho, K.H., and Kim, J.H. (2013). Mth1 regulates the interaction between the Rgt1 repressor and the Ssn6-Tup1 corepressor complex by modulating PKA-dependent phosphorylation of Rgt1. Mol Biol Cell *24*, 1493-1503.

Rutherford, J.C., Chua, G., Hughes, T., Cardenas, M.E., and Heitman, J. (2008). A Mep2-dependent transcriptional profile links permease function to gene expression during pseudohyphal growth in Saccharomyces cerevisiae. Mol Biol Cell *19*, 3028-3039.

Sakami, W., and Harrington, H. (1963). Amino Acid Metabolism. Annu Rev Biochem *32*, 355-398.

Sancak, Y., Bar-Peled, L., Zoncu, R., Markhard, A.L., Nada, S., and Sabatini, D.M. (2010). Ragulator-Rag complex targets mTORC1 to the lysosomal surface and is necessary for its activation by amino acids. Cell *141*, 290-303.

Sancak, Y., Peterson, T.R., Shaul, Y.D., Lindquist, R.A., Thoreen, C.C., Bar-Peled, L., and Sabatini, D.M. (2008). The Rag GTPases bind raptor and mediate amino acid signaling to mTORC1. Science *320*, 1496-1501.

Sano, H., Nakamura, A., Texada, M.J., Truman, J.W., Ishimoto, H., Kamikouchi, A., Nibu, Y., Kume, K., Ida, T., and Kojima, M. (2015). The Nutrient-Responsive Hormone CCHamide-2 Controls Growth by Regulating Insulin-like Peptides in the Brain of Drosophila melanogaster. PLoS Genet *11*, e1005209.

Sarkar, M.K., Paul, K., and Blair, D. (2010a). Chemotaxis signaling protein CheY binds to the rotor protein FliN to control the direction of flagellar rotation in Escherichia coli. Proc Natl Acad Sci U S A *107*, 9370-9375.

Sarkar, M.K., Paul, K., and Blair, D.F. (2010b). Subunit organization and reversal-associated movements in the flagellar switch of Escherichia coli. J Biol Chem *285*, 675-684.

Savelieva, K.V., Zhao, S., Pogorelov, V.M., Rajan, I., Yang, Q., Cullinan, E., and Lanthorn, T.H. (2008). Genetic disruption of both tryptophan hydroxylase genes dramatically reduces serotonin and affects behavior in models sensitive to antidepressants. PLoS One *3*, e3301.

Saxton, R.A., Chantranupong, L., Knockenhauer, K.E., Schwartz, T.U., and Sabatini, D.M. (2016a). Mechanism of arginine sensing by CASTOR1 upstream of mTORC1. Nature *536*, 229-233.

Saxton, R.A., Knockenhauer, K.E., Wolfson, R.L., Chantranupong, L., Pacold, M.E., Wang, T., Schwartz, T.U., and Sabatini, D.M. (2016b). Structural basis for leucine sensing by the Sestrin2-mTORC1 pathway. Science *351*, 53-58.

Schmidt, P. (2006). Evolution of homochirality by epimerization of random peptide chains. A stochastic model. Orig Life Evol Biosph *36*, 391-411.

Schoofs, A., Huckesfeld, S., and Pankratz, M.J. (2018). Serotonergic network in the subesophageal zone modulates the motor pattern for food intake in Drosophila. J Insect Physiol *106*, 36-46.

Schoofs, A., Huckesfeld, S., Surendran, S., and Pankratz, M.J. (2014). Serotonergic pathways in the Drosophila larval enteric nervous system. J Insect Physiol *69*, 118-125.

Sieber, M.H., and Thummel, C.S. (2012). Coordination of triacylglycerol and cholesterol homeostasis by DHR96 and the Drosophila LipA homolog magro. Cell Metab *15*, 122-127.

Singh, S.R., Zeng, X., Zheng, Z., and Hou, S.X. (2011). The adult Drosophila gastric and stomach organs are maintained by a multipotent stem cell pool at the foregut/midgut junction in the cardia (proventriculus). Cell Cycle *10*, 1109-1120.

Siviter, R.J., Coast, G.M., Winther, A.M., Nachman, R.J., Taylor, C.A., Shirras, A.D., Coates, D., Isaac, R.E., and Nassel, D.R. (2000). Expression and functional characterization of a Drosophila neuropeptide precursor with homology to mammalian preprotachykinin A. J Biol Chem *275*, 23273-23280.

Sourjik, V., and Wingreen, N.S. (2012). Responding to chemical gradients: bacterial chemotaxis. Curr Opin Cell Biol *24*, 262-268.

Spiess, R., Schoofs, A., and Heinzel, H.G. (2008). Anatomy of the stomatogastric nervous system associated with the foregut in Drosophila melanogaster and Calliphora vicina third instar larvae. J Morphol *269*, 272-282.

Stallone, D., and Nicolaidis, S. (1989). Increased food intake and carbohydrate preference in the rat following treatment with the serotonin antagonist metergoline. Neurosci Lett *102*, 319-324.

Stoffolano, J.G., Jr., and Haselton, A.T. (2013). The adult Dipteran crop: a unique and overlooked organ. Annu Rev Entomol *58*, 205-225.

Szurmant, H., and Ordal, G.W. (2004). Diversity in chemotaxis mechanisms among the bacteria and archaea. Microbiol Mol Biol Rev *68*, 301-319.

Talsma, A.D., Christov, C.P., Terriente-Felix, A., Linneweber, G.A., Perea, D., Wayland, M., Shafer, O.T., and Miguel-Aliaga, I. (2012). Remote control of renal physiology by the intestinal neuropeptide pigment-dispersing factor in Drosophila. Proc Natl Acad Sci U S A *109*, 12177-12182.

Tavares, M.R., Lemes, S.F., de Fante, T., Saenz de Miera, C., Pavan, I.C.B., Bezerra, R.M.N., Prada, P.O., Torsoni, M.A., Elias, C.F., and Simabuco, F.M. (2020). Modulation of hypothalamic S6K1 and S6K2 alters feeding behavior and systemic glucose metabolism. J Endocrinol *244*, 71-82.

Tejero, J., Biswas, A., Wang, Z.Q., Page, R.C., Haque, M.M., Hemann, C., Zweier, J.L., Misra, S., and Stuehr, D.J. (2008). Stabilization and characterization of a heme-oxy reaction intermediate in inducible nitric-oxide synthase. J Biol Chem *283*, 33498-33507.

Tian, A., and Jiang, J. (2014). Intestinal epithelium-derived BMP controls stem cell self-renewal in Drosophila adult midgut. Elife *3*, e01857.

Tian, Y., and Wang, L. (2018). Octopamine mediates protein-seeking behavior in mated female Drosophila. Cell Discov *4*, 66.

Tomar, P., and Sinha, H. (2014). Conservation of PHO pathway in ascomycetes and the role of Pho84. J Biosci *39*, 525-536.

Tsang, F., and Lin, S.J. (2015). Less is more: Nutrient limitation induces cross-talk of nutrient sensing pathways with NAD(+) homeostasis and contributes to longevity. Front Biol (Beijing) *10*, 333-357.

Tsun, Z.Y., Bar-Peled, L., Chantranupong, L., Zoncu, R., Wang, T., Kim, C., Spooner, E., and Sabatini, D.M. (2013). The folliculin tumor suppressor is a GAP for the RagC/D GTPases that signal amino acid levels to mTORC1. Mol Cell *52*, 495-505.

Turner, L., Ryu, W.S., and Berg, H.C. (2000). Real-time imaging of fluorescent flagellar filaments. J Bacteriol *182*, 2793-2801.

Tzou, P., Ohresser, S., Ferrandon, D., Capovilla, M., Reichhart, J.M., Lemaitre, B., Hoffmann, J.A., and Imler, J.L. (2000). Tissue-specific inducible expression of antimicrobial peptide genes in Drosophila surface epithelia. Immunity *13*, 737-748.

Valk, E., and Loog, M. (2013). Multiple Pho85-dependent mechanisms control G1 cyclin abundance in response to nutrient stress. Mol Cell Biol *33*, 1270-1272.

van de Wouw, M., Schellekens, H., Dinan, T.G., and Cryan, J.F. (2017). Microbiota-Gut-Brain Axis: Modulator of Host Metabolism and Appetite. J Nutr *147*, 727-745.

Vargas, M.A., Luo, N., Yamaguchi, A., and Kapahi, P. (2010). A role for S6 kinase and serotonin in postmating dietary switch and balance of nutrients in D. melanogaster. Curr Biol *20*, 1006-1011.

Veenstra, J.A., Agricola, H.J., and Sellami, A. (2008). Regulatory peptides in fruit fly midgut. Cell Tissue Res *334*, 499-516.

Veenstra, J.A., and Ida, T. (2014). More Drosophila enteroendocrine peptides: Orcokinin B and the CCHamides 1 and 2. Cell Tissue Res *357*, 607-621.

Wachter, A., Tunc-Ozdemir, M., Grove, B.C., Green, P.J., Shintani, D.K., and Breaker, R.R. (2007). Riboswitch control of gene expression in plants by splicing and alternative 3' end processing of mRNAs. Plant Cell *19*, 3437-3450.

Wang, E.A., and Koshland, D.E., Jr. (1980). Receptor structure in the bacterial sensing system. Proc Natl Acad Sci U S A *77*, 7157-7161.

Wang, P., Jia, Y., Liu, T., Jan, Y.N., and Zhang, W. (2020). Visceral Mechano-sensing Neurons Control Drosophila Feeding by Using Piezo as a Sensor. Neuron *108*, 640-650 e644.

Wang, S., Tsun, Z.Y., Wolfson, R.L., Shen, K., Wyant, G.A., Plovanich, M.E., Yuan, E.D., Jones, T.D., Chantranupong, L., Comb, W.*, et al.* (2015). Metabolism. Lysosomal amino acid transporter SLC38A9 signals arginine sufficiency to mTORC1. Science *347*, 188-194.

Warchol, M., Krauss, H., Wojciechowska, M., Opala, T., Pieta, B., Zukiewicz-Sobczak, W., Kupsz, J., and Grochowalska, A. (2014). The role of ghrelin, leptin and insulin in foetal development. Ann Agric Environ Med *21*, 349-352.

Wek, R.C., Jackson, B.M., and Hinnebusch, A.G. (1989). Juxtaposition of domains homologous to protein kinases and histidyl-tRNA synthetases in GCN2 protein suggests a mechanism for coupling GCN4 expression to amino acid availability. Proc Natl Acad Sci U S A *86*, 4579-4583.

Wek, S.A., Zhu, S., and Wek, R.C. (1995). The histidyl-tRNA synthetase-related sequence in the eIF-2 alpha protein kinase GCN2 interacts with tRNA and is required for activation in response to starvation for different amino acids. Mol Cell Biol *15*, 4497-4506.

Wiczer, B.M., and Thomas, G. (2010). The role of the mTOR pathway in regulating food intake. Curr Opin Drug Discov Devel *13*, 604-612.

Winkler, W.C. (2005). Riboswitches and the role of noncoding RNAs in bacterial metabolic control. Curr Opin Chem Biol *9*, 594-602.

Winkler, W.C., and Breaker, R.R. (2005). Regulation of bacterial gene expression by riboswitches. Annu Rev Microbiol *59*, 487-517.

Wolfson, R.L., Chantranupong, L., Saxton, R.A., Shen, K., Scaria, S.M., Cantor, J.R., and Sabatini, D.M. (2016). Sestrin2 is a leucine sensor for the mTORC1 pathway. Science *351*, 43-48.

Wolfson, R.L., Chantranupong, L., Wyant, G.A., Gu, X., Orozco, J.M., Shen, K., Condon, K.J., Petri, S., Kedir, J., Scaria, S.M.*, et al.* (2017). KICSTOR recruits GATOR1 to the lysosome and is necessary for nutrients to regulate mTORC1. Nature *543*, 438-442.

Wu, G. (2009). Amino acids: metabolism, functions, and nutrition. Amino Acids *37*, 1-17.

Wyant, G.A., Abu-Remaileh, M., Wolfson, R.L., Chen, W.W., Freinkman, E., Danai, L.V., Vander Heiden, M.G., and Sabatini, D.M. (2017). mTORC1 Activator SLC38A9 Is Required to Efflux Essential Amino Acids from Lysosomes and Use Protein as a Nutrient. Cell *171*, 642-654 e612.

Wylie, D., Stock, A., Wong, C.Y., and Stock, J. (1988). Sensory transduction in bacterial chemotaxis involves phosphotransfer between Che proteins. Biochem Biophys Res Commun *151*, 891-896.

Xiao, B., Heath, R., Saiu, P., Leiper, F.C., Leone, P., Jing, C., Walker, P.A., Haire, L., Eccleston, J.F., Davis, C.T.*, et al.* (2007). Structural basis for AMP binding to mammalian AMP-activated protein kinase. Nature *449*, 496-500.

Yadav, V.K., Oury, F., Tanaka, K.F., Thomas, T., Wang, Y., Cremers, S., Hen, R., Krust, A., Chambon, P., and Karsenty, G. (2011). Leptin-dependent serotonin control of appetite: temporal specificity, transcriptional regulation, and therapeutic implications. J Exp Med *208*, 41-52.

Yang, Y., Atasoy, D., Su, H.H., and Sternson, S.M. (2011). Hunger states switch a flip-flop memory circuit via a synaptic AMPK-dependent positive feedback loop. Cell *146*, 992-1003.

Yang, Z., Huang, R., Fu, X., Wang, G., Qi, W., Mao, D., Shi, Z., Shen, W.L., and Wang, L. (2018). A post-ingestive amino acid sensor promotes food consumption in Drosophila. Cell Res *28*, 1013-1025.

Yanofsky, C., Konan, K.V., and Sarsero, J.P. (1996). Some novel transcription attenuation mechanisms used by bacteria. Biochimie *78*, 1017-1024.

Yoon, J.G., and Stay, B. (1995). Immunocytochemical localization of Diploptera punctata allatostatin-like peptide in Drosophila melanogaster. J Comp Neurol *363*, 475-488.

York, J.D., and Lew, D.J. (2008). IP7 guards the CDK gate. Nat Chem Biol *4*, 16-17.

Yuan, H.X., Xiong, Y., and Guan, K.L. (2013). Nutrient sensing, metabolism, and cell growth control. Mol Cell *49*, 379-387.

Zhang, H., Liu, J., Li, C.R., Momen, B., Kohanski, R.A., and Pick, L. (2009). Deletion of Drosophila insulin-like peptides causes growth defects and metabolic abnormalities. Proc Natl Acad Sci U S A *106*, 19617-19622.

Zhang, L., Han, W., Lin, C., Li, F., and de Araujo, I.E. (2018). Sugar Metabolism Regulates Flavor Preferences and Portal Glucose Sensing. Front Integr Neurosci *12*, 57.

Zhang, T., Branch, A., and Shen, P. (2013). Octopamine-mediated circuit mechanism underlying controlled appetite for palatable food in Drosophila. Proc Natl Acad Sci U S A *110*, 15431-15436.

Zhang, Z., and Kishino, H. (2004). Genomic background drives the divergence of duplicated amylase genes at synonymous sites in Drosophila. Mol Biol Evol *21*, 222-227.

Chapter 2

SAMTOR is an S-adenosylmethionine sensor for the mTORC1 pathway

---

Parts of this chapter were first published as:

Xin Gu*, Jose M. Orozco*, Robert A. Saxton, Kendall J. Condon, Grace Y. Liu, Sonia M. Scaria, J. Wade Harper, Steven P. Gygi, David M. Sabatini, SAMTOR is an S-adenosylmethionine sensor for the mTORC1 pathway. ***Science*****,** doi:10.1126/science.aao3265 (2017)

(*: Contribute equally to the work)
My contributions: Figure 1, Figure 2B-D, Figure 3, Supplement figure 1-3.

Abstract

mTOR complex 1 (mTORC1) regulates cell growth and metabolism in response to multiple environmental cues. Nutrients signal via the Rag GTPases to promote the localization of mTORC1 to the lysosomal surface, its site of activation. Here, we identified SAMTOR as a previously uncharacterized protein that inhibits mTORC1 signaling by interacting with GATOR1, the GTPase activating protein (GAP) for RagA/B. The methyl donor S-adenosylmethionine (SAM) disrupts the SAMTOR-GATOR1 complex by binding directly to SAMTOR with a dissociation constant of approximately 7 μM. In cells, methionine starvation reduces SAM levels below this dissociation constant and promotes the association of SAMTOR with GATOR1, thereby inhibiting mTORC1 signaling in a SAMTOR-dependent fashion. Methionine-induced activation of mTORC1 requires the SAM binding capacity of SAMTOR. Thus, SAMTOR is a SAM sensor that links methionine and one carbon metabolism to mTORC1 signaling.

Introduction

The mechanistic target of rapamycin complex 1 (mTORC1) protein kinase is the central component of a pathway that regulates anabolic and catabolic processes in response to environmental signals, including growth factors and nutrients (Dibble and Manning, 2013; Jewell et al., 2013; Saxton and Sabatini, 2017). Amino acids promote the translocation of mTORC1 to the lysosomal surface, where its activator Rheb resides. This localization depends on the heterodimeric Rag GTPases, which consist of RagA or RagB bound to RagC or RagD (Kim et al., 2008; Sancak et al., 2008).

The amino acid sensing pathway upstream of mTORC1 is complicated, with several multi-component complexes regulating the Rag heterodimer, each likely conveying a distinct amino acid input. GATOR1 and FLCN-FNIP are GAPs for RagA/B and RagC/D, respectively (Bar-Peled et al., 2013; Tsun et al., 2013), while Ragulator tethers the Rags to the lysosomal surface and also has nucleotide exchange activity (Bar-Peled et al., 2012; Sancak et al., 2010). The KICSTOR complex binds GATOR1 and recruits it to the lysosome, and, like GATOR1, is necessary for amino acid starvation to inhibit mTORC1 signaling (Bar-Peled et al., 2013; Peng et al., 2017; Wolfson et al., 2017). The molecular function of GATOR2 is unknown, but it is required for pathway activity and might act upstream of GATOR1 (Bar-Peled et al., 2013).

Leucine and arginine are well-established activators of mTORC1 signaling, and recent work has shed light on the molecular mechanisms involved. The lysosomal transmembrane protein SLC38A9 interacts with Ragulator (Jung et al., 2015; Rebsamen et al., 2015; Wang et al., 2015a) and is a lysosomal arginine sensor (Wyant et al.),while Sestrin2 and CASTOR1 are cytosolic leucine and arginine sensors, respectively, that bind to and inhibit the function of GATOR2 in the absence of their cognate amino acids (Chantranupong et al., 2016; Saxton et al., 2016a; Saxton et al., 2016b; Wolfson et al., 2016). If, and how, other amino acids impact mTORC1 signaling is unclear.

Results

To search for proteins that bind to GATOR1 or KICSTOR, we mined the BioPlex protein-protein interaction database generated by immunoprecipitation followed by mass spectrometry of more than 5000 proteins stably expressed in HEK-293T cells (Huttlin et al., 2017). This analysis revealed C7orf60, a previously unstudied protein, as a putative interaction partner of all known components of GATOR1 (Depdc5, Nprl3, Nprl2) and KICSTOR (Kaptin, ITFG2, C12orf66, SZT2). For reasons described below, we renamed C7orf60 as S-adenosylmethionine sensor upstream of mTORC1 (SAMTOR).

Figure 1

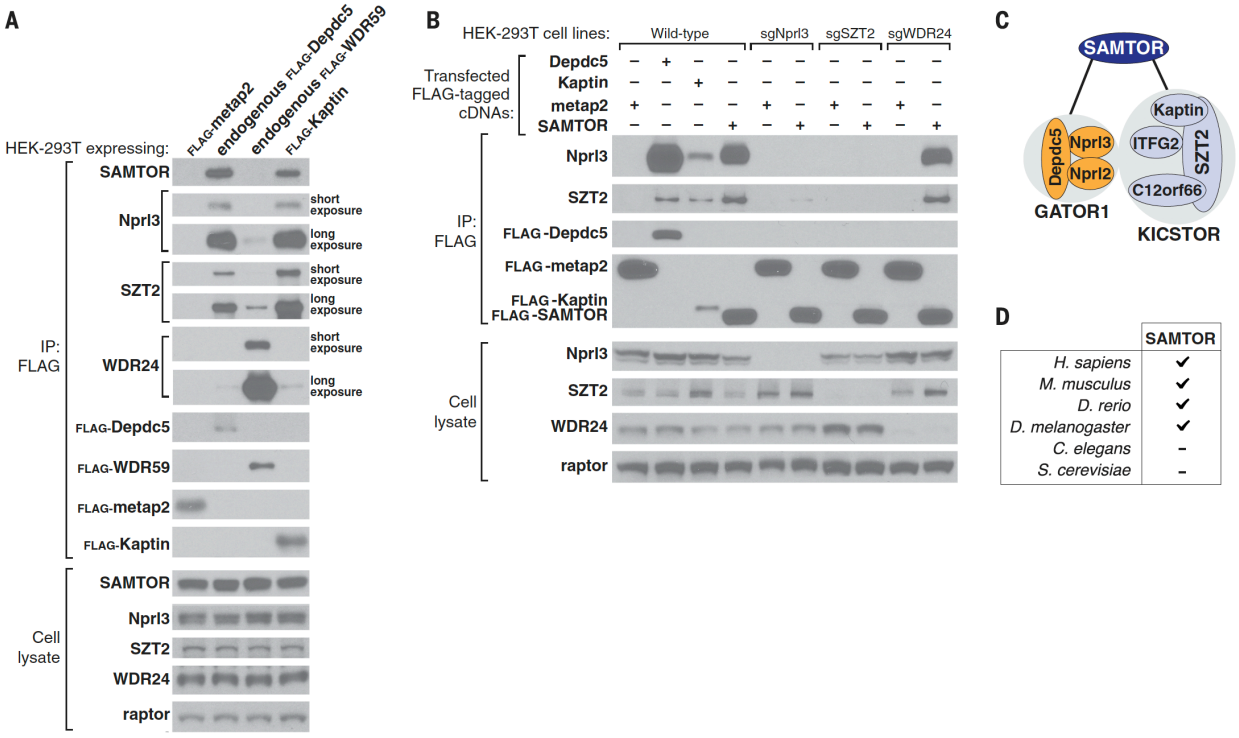

Figure 1. SAMTOR interacts with GATOR1 and KICSTOR
(A) GATOR1 and KICSTOR, but not GATOR2, co-immunoprecipitate SAMTOR. FLAG-immunoprecipitates were prepared from HEK-293T cell lines that stably expressed FLAG-tagged metap2 or Kaptin, or had endogenously FLAG-tagged Depdc5 or WDR59. FLAG-immunoprecipitates and lysates were analyzed by immunoblotting for the indicated proteins. FLAG-metap2 served as a negative control. Depdc5 and Nprl3, WDR59 and WDR24, and Kaptin and SZT2 were used as representative components of the GATOR1, GATOR2, and KICSTOR complexes respectively. Short or long exposure indicates relative blot exposure times.
(B) SAMTOR co-immunoprecipitates GATOR1 and KICSTOR and the interaction requires both GATOR1 and KICSTOR but not GATOR2. FLAG-immunoprecipitates were prepared from wild-type, Nprl3-deficient,

SZT2-deficient, or WDR24-deficient HEK-293T cells transiently expressing the indicated cDNAs. FLAG-immunoprecipitates and lysates were analyzed as in (A).
(C) Model showing that SAMTOR interacts with GATOR1 and KICSTOR.
(D) Presence or absence of gene orthologs of SAMTOR in several model organisms.

Using an antibody against SAMTOR to probe anti-FLAG immunoprecipitates prepared from cells having endogenously Flag-tagged components of GATOR1 (Depdc5) or GATOR2 (WDR59) or stably expressing a KICSTOR component (Flag-Kaptin), we validated that SAMTOR co-immunoprecipitated GATOR1 and KICSTOR, but not GATOR2 (Fig. 1A). Moreover, transiently expressed SAMTOR co-immunoprecipitated endogenous GATOR1 and KICSTOR, as detected by the presence of their Nprl3 and SZT2 components, respectively. Loss of a component of GATOR1 or KICSTOR, but not of GATOR2, severely reduced the interaction of SAMTOR with KICSTOR or GATOR1, respectively (Fig. 1B). Furthermore, overexpressed GATOR1 co-immunoprecipitated SAMTOR only when KICSTOR was co-expressed (Fig. S1A). Thus, SAMTOR binds to the supercomplex of GATOR1 and KICSTOR and both complexes are required for the interaction to occur (Fig. 1C).

Figure S1

A

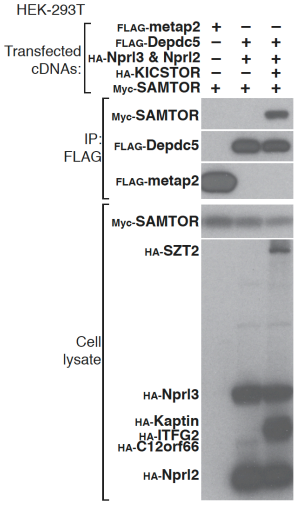

Figure S1.
(A) Overexpressed GATOR1 co-immunoprecipitated transiently expressed SAMTOR only when KICSTOR was also transfected. FLAG-immunoprecipitates were prepared from wild-type HEK-293T cells transiently expressing the indicated cDNAs. FLAG-immunoprecipitates and lysates were analyzed as in Fig 1(A).

Orthologs of SAMTOR are encoded in the genomes of vertebrates and some invertebrates, such as *Drosophila melanogaster*. We could not identify SAMTOR orthologs in *Caenorhabditis elegans or Saccharomyces cerevisiae* (Fig. 1D).

To determine whether SAMTOR regulates mTORC1 signaling, we overexpressed SAMTOR in HEK-293T cells and monitored the phosphorylation of S6 Kinase 1 (S6K1), a canonical mTORC1 substrate. SAMTOR expression suppressed mTORC1 signaling in a dose-dependent fashion (Fig. 2A), establishing SAMTOR as a negative regulator of the pathway. Amino acids activate mTORC1 by promoting its localization to the lysosomal surface (Sancak et al., 2010; Sancak et al., 2008). Consistent with SAMTOR inhibiting the amino acid sensing pathway upstream of mTORC1, overexpression of GFP-tagged SAMTOR displaced mTOR from lysosomes to an extent similar to that of GFP-Sestrin2, an inhibitor of GATOR2 (Chantranupong et al., 2014; Parmigiani et al., 2014) (Fig. 2B).

Figure 2

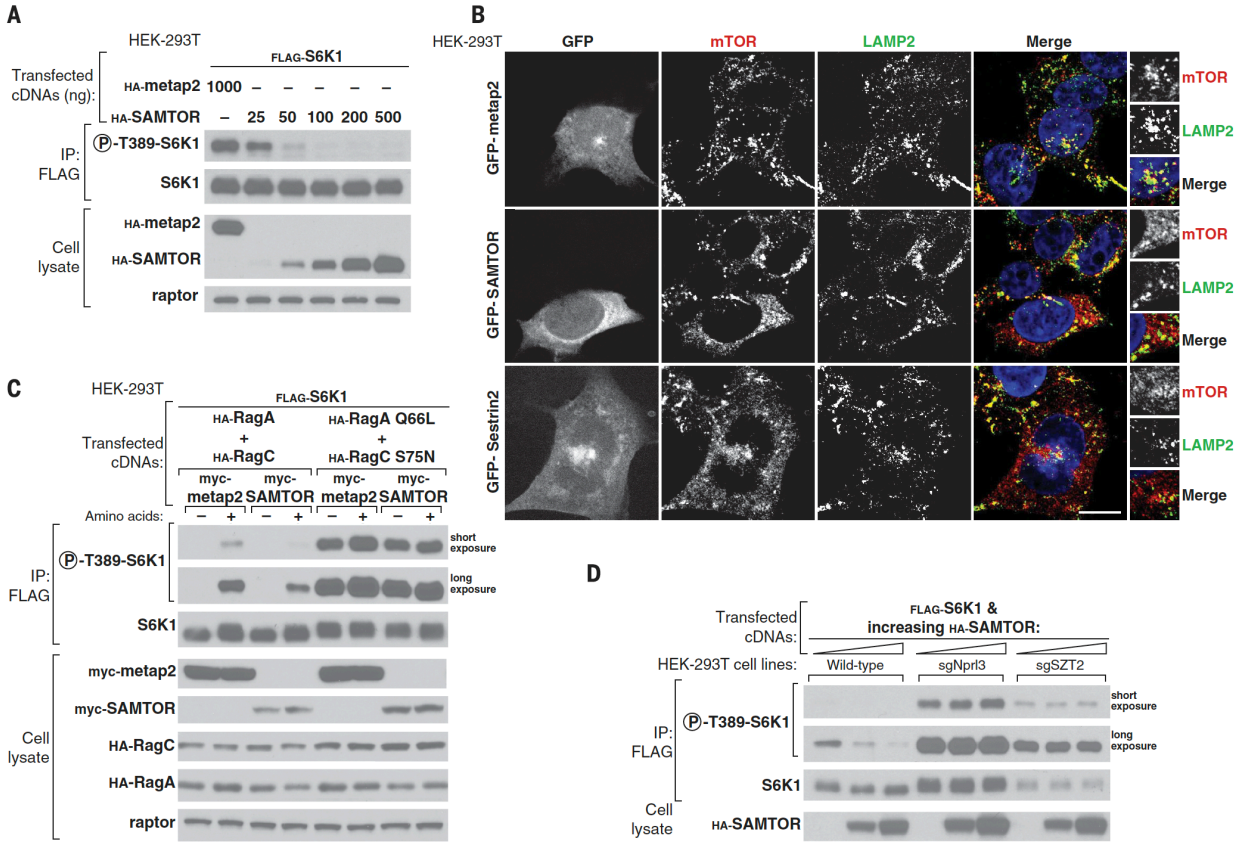

Figure 2. SAMTOR is a negative regulator of mTORC1 signaling that acts upstream of the Rag GTPases, GATOR1, and KICSTOR
(A) Transient overexpression of SAMTOR inhibits mTORC1 signaling. FLAG-immunoprecipitates were prepared from HEK-293T cells transfected with 2 ng of the FLAG-S6K1 cDNA along with either the HA-metap2 cDNA or increasing amounts of the HA-SAMTOR cDNA. FLAG-immunoprecipitates and cell lysates were analyzed by immunoblotting for the phosphorylation states and levels of the indicated proteins.
(B) Overexpression of GFP-SAMTOR displaces mTOR from lysosomes, similar to that of GFP-Sestrin2. Wild-type HEK-293T cells transiently expressing GFP-metap2, GFP-SAMTOR, or GFP-Sestrin2 were processed for immunofluorescence detection of mTOR and the lysosomal marker LAMP2. In all images, insets represent selected fields magnified 5.12X as well as their overlays. Scale bar represents 10 μm.
(C) SAMTOR functions upstream of the Rag GTPases to regulate the mTORC1 pathway. HEK-293T cells expressing the indicated cDNAs were starved of amino acids for 50 minutes or starved and restimulated with amino acids for 10 minutes. FLAG-immunoprecipitates and cell lysates were analyzed as in (A).
(D) SAMTOR functions upstream of GATOR1 and KICSTOR. FLAG-immunoprecipitates and cell lysates prepared from wild-type or Nprl3-deficient or SZT2-deficient HEK-293T cell lines expressing the indicated cDNAs were analyzed as in (A).

To understand where in the mTORC1 pathway SAMTOR functions, we performed epistasis experiments with established mTORC1 regulators. Overexpression of SAMTOR inhibited mTORC1 signaling when co-expressed with the wild type RagA and RagC heterodimer, but not with the constitutively active mutant one (RagA Q66L and RagC S75N) that bypasses the requirement for amino acids for maintaining mTORC1 active (Fig. 2C) (Kim et al., 2008; Sancak et al., 2008). In addition, SAMTOR did not inhibit mTORC1 signaling in cells lacking either a GATOR1 or KICSTOR component. Thus, SAMTOR acts upstream of the Rag GTPases and requires GATOR1 and KICSTOR to inhibit mTORC1 signaling (Fig. 2D). In combination with the interaction data, these results are consistent with SAMTOR promoting the function of GATOR1 and/or KICSTOR, which are both negative regulators of mTORC1 signaling.

Sequence analyses predict that SAMTOR contains a class I Rossmann fold methyltransferase domain (PF13489) (Fig. 3A and fig. S2) (Hildebrand et al., 2009). These domains are known to bind S-adenosylmethionine (SAM) and exist in methyltransferases in bacteria, archaea, and eukarya (Kozbial and Mushegian, 2005). In order to determine if SAMTOR binds SAM, we developed an equilibrium binding assay based on one we used to detect the binding of leucine to Sestrin2 (Wolfson et al., 2016) and determined that SAMTOR binds SAM with a dissociation constant of approximately 7 μM (Fig. 3B). A

competition binding assay revealed that, as with other SAM-binding proteins, SAMTOR can also bind S-adenosylhomocysteine (SAH), the demethylated form of SAM (Fig. 3B).

Figure 3

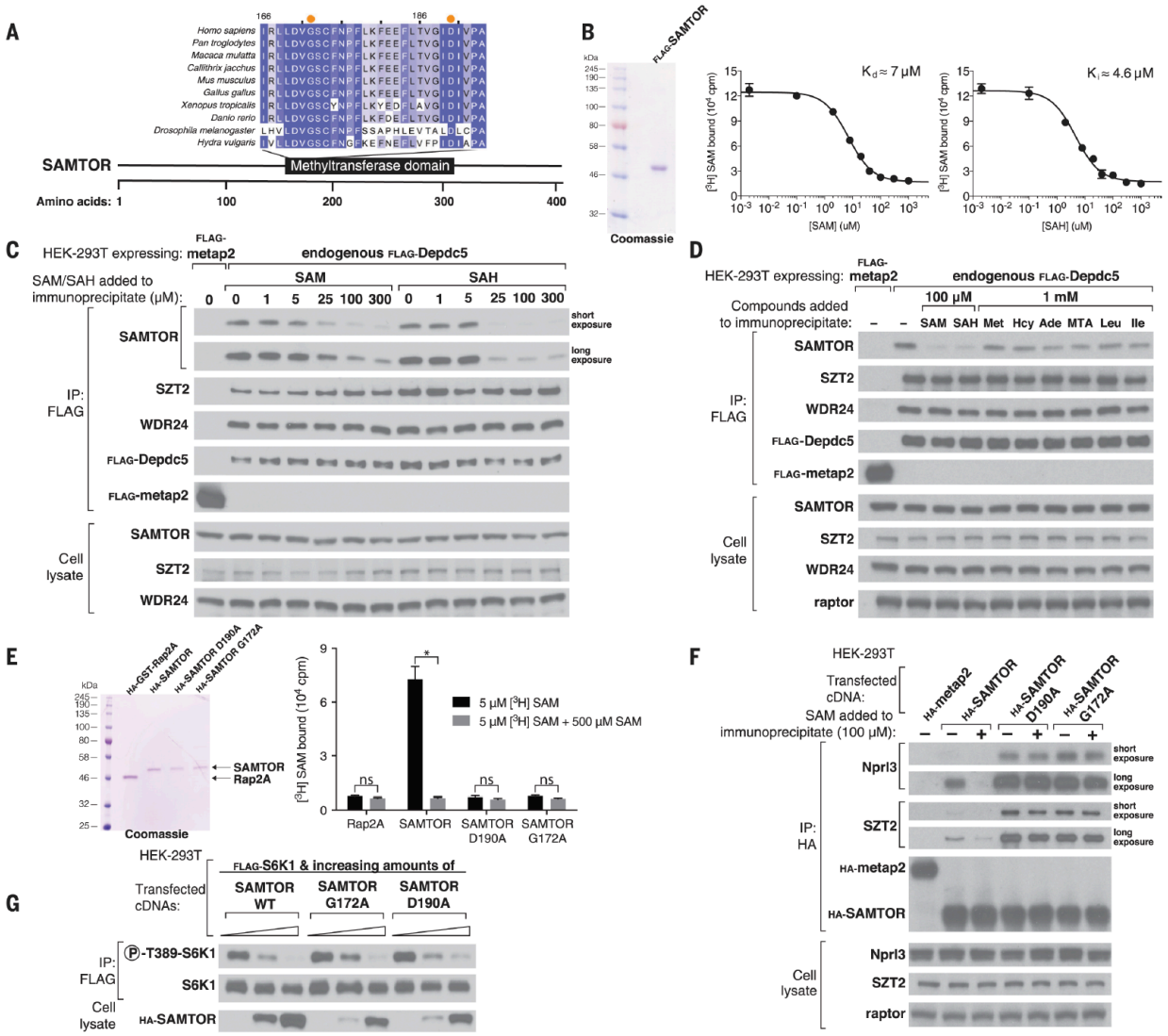

Figure 3. S-adenosylmethionine binds SAMTOR to disrupt its interaction with GATOR1 and KICSTOR
(A) Schematic of the human SAMTOR protein indicating the Class I Rossmann fold methyltransferase domain. Shown is an alignment of partial sequences of this domain from SAMTOR in indicated species. Amino acid positions are colored from white to blue in order of increasing sequence similarity. Orange dots denote the G172 and D190 residues of human SAMTOR.
(B) SAMTOR binds SAM and SAH. Purified FLAG-SAMTOR protein was analyzed by SDS-PAGE followed by Coomassie blue staining. Binding assays were performed with purified FLAG-SAMTOR incubated with indicated concentrations of [^{3}H] SAM, unlabeled SAM or SAH. Values for each point are mean ± SD of three technical replicates from one representative experiment. The experiment was performed twice.

(C) SAM and SAH disrupt the interaction of SAMTOR with GATOR1 in vitro. FLAG-immunoprecipitates were prepared from the endogenously FLAG-tagged Depdc5 HEK-293T cells. SAM and SAH were added directly to the immunoprecipitates at the indicated concentrations. FLAG-immunoprecipitates and cell lysates were analyzed by immunoblotting for the levels of the indicated proteins.
(D) 100 μM SAM or SAH, but not 1 mM methionine, homocysteine, adenosine, 5-methylthioadenosine, leucine, or isoleucine, disrupt the interaction between SAMTOR and GATOR1. The experiment was performed and analyzed as in (C).
(E) Wild type HA-SAMTOR, but not HA-SAMTOR G172A or D190A, binds SAM. HA tagged wild-type and mutant SAMTOR proteins were prepared from HEK-293T cells expressing the indicated cDNAs and binding assays were performed as in (B). A representative experiment is shown and values are mean ± SD of three technical replicates. Two-tailed t tests were used for comparisons between two groups. The asterisk denotes $p < 0.001$; ns, not significant. The experiment was repeated three times.
(F) HA-SAMTOR G172A and D190A co-immunoprecipitate more endogenous GATOR1 and KICSTOR than wild-type SAMTOR and the interactions are insensitive to SAM added in vitro. HA-immunoprecipitates and cell lysates were prepared from HEK-293T cells transiently expressing wild-type or the G172A or D190A mutant HA-SAMTOR. SAM was added to the immunoprecipitates where indicated. HA-immunoprecipitates and cell lysates were analyzed as (C).
(G) HA-SAMTOR G172A and D190A inhibit mTORC1 activity to similar extents as wild-type SAMTOR. FLAG-immunoprecipitates were prepared from HEK-293T cells transfected with the indicated cDNAs. FLAG-immunoprecipitates and cell lysates were analyzed by immunoblotting for the phosphorylation states and levels of the indicated proteins.

Given these findings, we asked if SAM and SAH regulate the interaction of SAMTOR with GATOR1-KICSTOR. Indeed, SAM and SAH, but not methionine, homocysteine, adenosine, 5-methylthioadenosine, leucine, or isoleucine, disrupted the interaction when added directly to the immunopurified complex kept at 4°C (Fig. 3 C and D). Thus, SAM disrupts the interaction between SAMTOR and GATOR1-KICSTOR analogously to how leucine and arginine induce the release of Sestrin2 and CASTOR1 from GATOR2, respectively (Chantranupong et al., 2016; Wolfson et al., 2016). Given that SAH has the same effect, it is unlikely that a methylation event is required for SAM to dissociate GATOR1-KICSTOR.

Mutagenesis of highly conserved residues in human SAMTOR yielded two mutants, G172A and D190A, which no longer bound SAM (Fig. 3E and fig. S2 A and B). These mutants co-immunoprecipitated greater amounts of endogenous GATOR1 and KICSTOR than wild-type SAMTOR and the purified complexes were insensitive to SAM in vitro (Fig. 3F). Moreover, these mutants inhibited mTORC1 signaling to a similar extent as wild-type SAMTOR, despite their lower expression (Fig. 3G). Thus, SAMTOR must be able to bind SAM for SAM to disrupt the interaction of SAMTOR with GATOR1-

KICSTOR. In contrast, SAMTOR does not have to bind SAM to inhibit mTORC1 signaling, indicating that this function of SAMTOR does not require a methylation event.

Figure S2

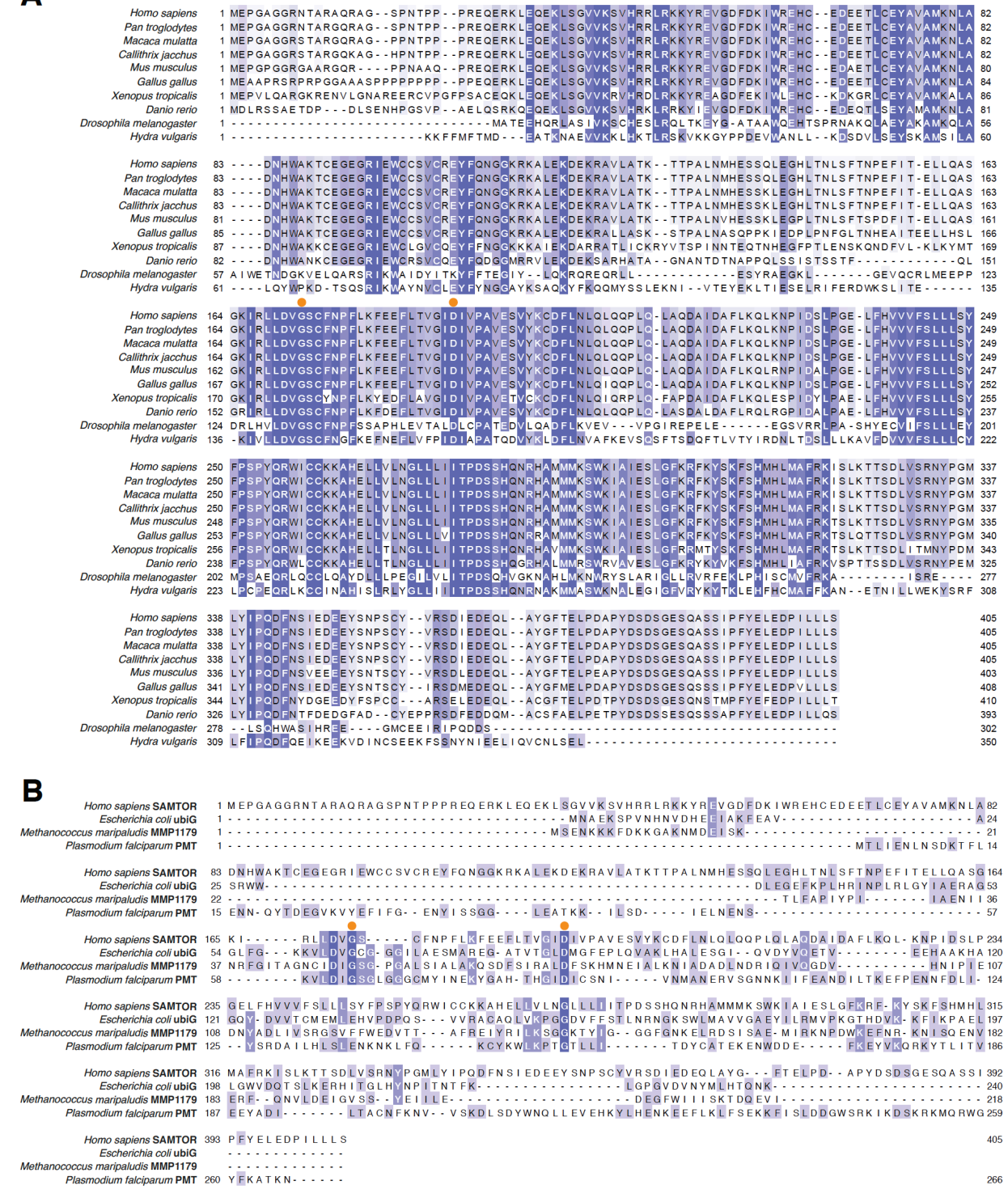

Figure S2.
(A) Sequence alignment of SAMTOR homologues from various organisms. Amino acid positions are colored white and blue according to increasing sequence similarity. Two residues (G172 and D190) significant for SAM binding capacity are indicated with orange dots.
(B) Sequence alignment of human SAMTOR with three methyltransferases selected from the list of proteins predicted by HHPred as having secondary structure similarity to SAMTOR. Two residues (G172 and D190) significant for SAM binding capacity are indicated with orange dots.

Because SAM and SAH disrupt the interaction of SAMTOR with GATOR1-KICSTOR in vitro, we sought to determine if this is also true in cells. The enzyme methionine adenosyltransferase (MAT) synthesizes SAM from ATP and methionine, an essential amino acid, so that starvation for methionine should lower SAM levels, as has been observed previously in other systems (Mentch et al., 2015; Quinlan et al., 2017). Indeed, SAM concentrations in HEK-293T cells decreased upon methionine starvation, falling from above the dissociation constant of SAMTOR for SAM to below it (Fig. 4A). In contrast, in both methionine replete and starved cells, SAH concentrations were lower than the affinity of SAMTOR for SAH (Fig. 4A), making it unlikely that SAH is a physiologically relevant modulator of the binding of SAMTOR to GATOR1-KICSTOR.

Consistent with the effects of SAM on the interaction between SAMTOR and GATOR1-KICSTOR in vitro, methionine starvation strongly increased this interaction in cells. Importantly, the addition to the methionine-starved cells of either methionine or SAM, which can enter cells when used at high concentrations, reduced the interaction to baseline levels (Fig. 4B). Interestingly, methionine starvation weakened the interaction between GATOR1 and GATOR2 in a SAMTOR-dependent fashion, while methionine addition restored the interaction to normal levels (Fig. S3 A and B). In addition, in a dose-dependent manner SAMTOR overexpression was sufficient to disrupt the interaction between GATOR1 and GATOR2 (Fig. S3 C and D).

Given that SAMTOR is an inhibitor of mTORC1 signaling and methionine starvation promotes the interaction between SAMTOR and GATOR1-KICSTOR, we hypothesized that methionine starvation would also inhibit mTORC1 signaling. Indeed, in multiple cell types, methionine starvation inhibited mTORC1

signaling in a SAMTOR-dependent fashion, as measured by the phosphorylation of the mTORC1 substrates S6K1 and 4E-BP1 (Fig. 4C; fig. S4 A, B and C). In contrast, loss of SAMTOR did not prevent the inhibition of mTORC1 signaling caused by withdrawal of leucine, arginine (Fig. 4D) or growth factors (Fig. S4D).

Figure 4

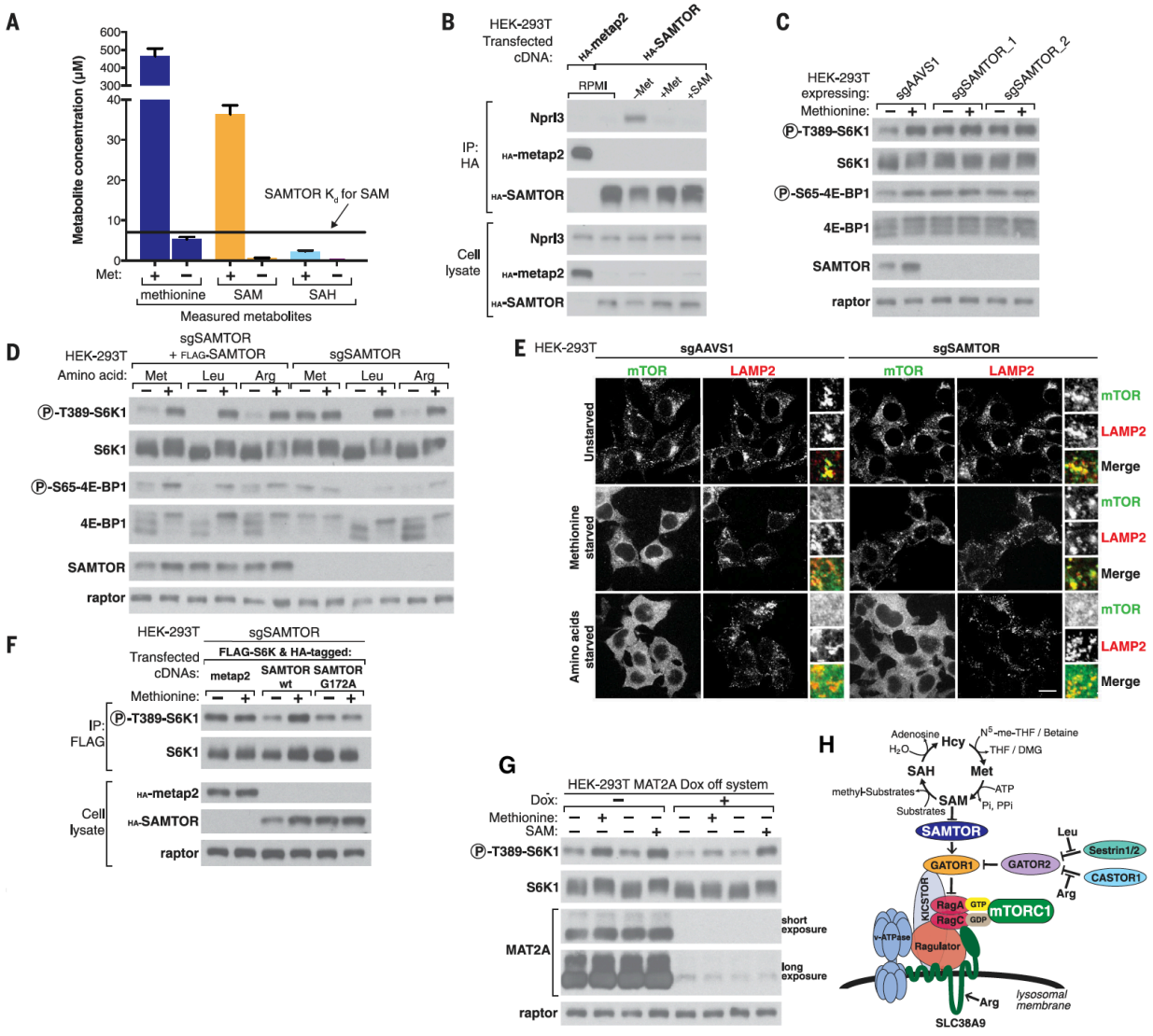

Figure 4. SAMTOR senses SAM to signal methionine sufficiency to mTORC1
(A) HEK-293T cells were incubated with or without methionine for 2 hours prior to sample preparation for LC/MS-based measurements of the absolute amounts of the indicated metabolites.
(B) Methionine starvation increases the interaction between SAMTOR and GATOR1. HEK-293T cells transiently expressing HA-tagged metap2 or SAMTOR were kept in growth media (RPMI) or starved of methionine for 2 hours (-Met) or starved for methionine for 2 hours and then restimulated for 20

minutes with 100 µM methionine (+Met) or 1 mM SAM (+SAM). HA-immunoprecipitates and cell lysates were analyzed by immunoblotting for the levels of the indicated proteins.
(C) In SAMTOR-depleted cells, the mTORC1 pathway is resistant to methionine starvation. HEK-293T cells stably co-expressing Cas9 and the indicated guides were incubated in media with or without methionine for 2 hours. Cell lysates were analyzed by immunoblotting for the phosphorylation states and the levels of the indicated proteins.
(D) The loss of SAMTOR does not affect the sensitivity of the mTORC1 pathway to leucine or arginine starvation. SAMTOR-deficient HEK-293T cells with or without FLAG-SAMTOR expression were starved for the indicated amino acid for 2 hours. Cell lysates were analyzed as in (C).
(E) In cells without SAMTOR, mTOR co-localizes with lysosomes even upon methionine starvation. SAMTOR-deficient or control HEK-293T cells were treated as indicated for 2 hours prior to processing for immunofluorescence detection of mTOR and the lysosomal marker LAMP2. In all images, insets represent selected fields magnified 3.07X as well as their overlays. Scale bar represents 10 µm.
(F) Re-expression in SAMTOR-null cells of wild-type SAMTOR, but not the SAM-binding G172A mutant of SAMTOR, restored the capacity of the mTORC1 pathway to sense methionine sufficiency. SAMTOR-null cells were transfected with the indicated cDNAs and the cells were treated as in (C) prior to preparing lysates and FLAG-immunoprecipitates. FLAG-immunoprecipitates and cell lysates were analyzed as in (C).
(G) Acute loss of MAT2A using a doxycycline-suppressible system attenuates the capacity of mTORC1 to sense methionine, but leaves SAM signaling largely intact. MAT2A dox-off HEK-293T cells were treated with 30 ng/mL doxycycline for 50 hours prior to starving them as in (C). Cell lysates were analyzed as in (C).
(H) A model depicting how SAM sensing by SAMTOR signals methionine levels to mTORC1. Substrates receiving methyl group from SAM include: DNA, RNA, proteins, phospholipids, etc.

Consistent with the effects of SAMTOR overexpression (Fig. 2B), methionine starvation also reduced the co-localization of mTOR with lysosomes in wild-type but not SAMTOR-null cells (Fig. 4E). Furthermore, re-expression of wild type SAMTOR, but not a SAM-binding deficient mutant, restored the capacity of the mTORC1 pathway to sense methionine in the SAMTOR-null HEK-293T cells (Fig. 4F). Interestingly, methionine starvation partially reduced SAMTOR levels in a proteasome dependent manner (Fig. 4, B, C, and F, and fig. S4D) but this degradation was not required for mTORC1 to respond to methionine starvation (Fig. S4E).

Our results show that SAMTOR is required for the mTORC1 pathway to detect changes in methionine levels and that this function requires its capacity to bind SAM. Moreover, the addition of SAM to methionine-starved cells reactivated mTORC1 signaling (Fig. 4G), indicating that it is the drop in SAM levels that mediates the inhibitory effects of methionine restriction on mTORC1. Given these

findings, we predicted that the loss of methionine adenosyltransferase (MAT2A) would prevent mTORC1 from sensing methionine by blocking its conversion to SAM. Because MAT2A is essential in human cells (Wang et al., 2015b; Wang et al., 2017), we generated a doxycycline-repressible system in order to acutely suppress MAT2A expression (Gossen and Bujard, 1992). Consistent with SAMTOR sensing SAM rather than methionine directly, the loss of MAT2A greatly attenuated the capacity of mTORC1 to sense methionine while leaving its activation by SAM largely intact (Fig. 4G).

Figure S3

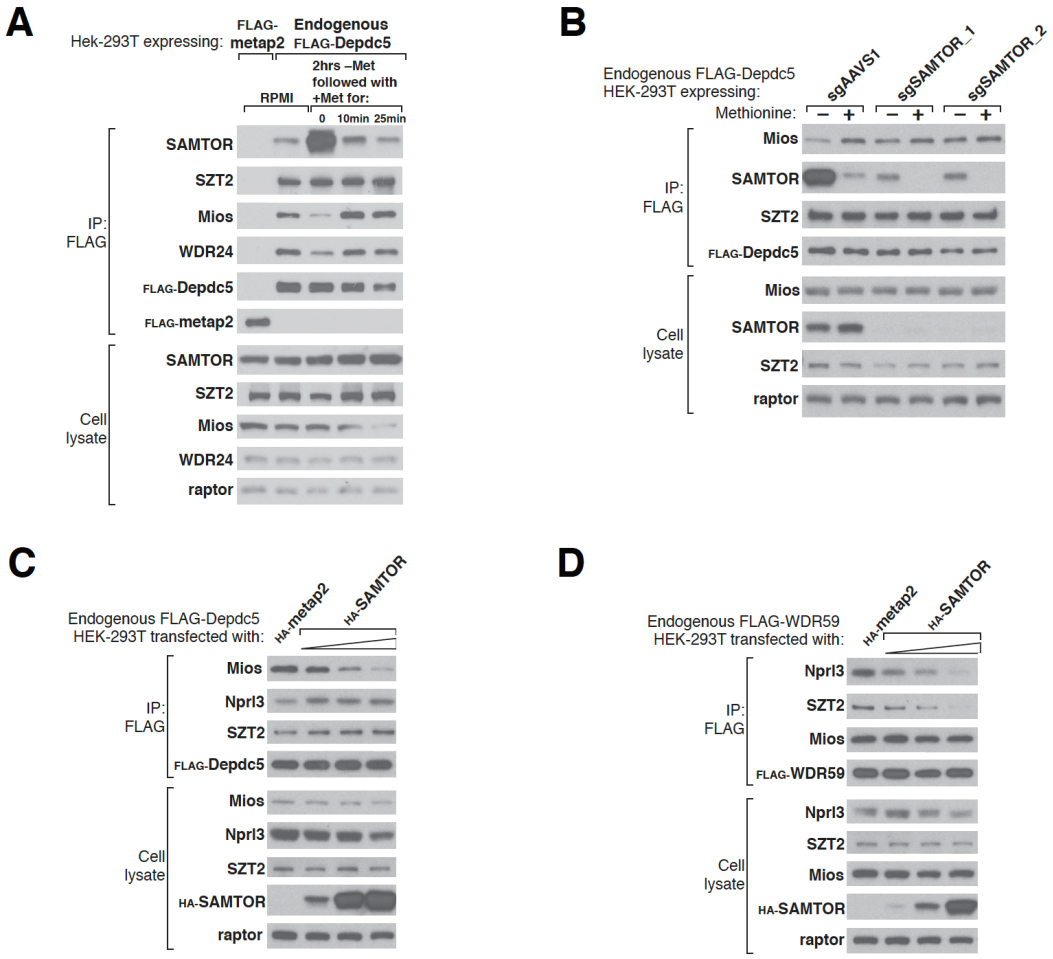

Figure S3.
(A) Methionine starvation increases the interaction between SAMTOR and GATOR1 but weakens that between GATOR1 and GATOR2. Stably expressed FLAG-metap2 or endogenously FLAG-tagged Depdc5 HEK-293T cells were kept in growth media (RPMI) or starved of methionine for 2 hours or starved for methionine for 2 hours and then restimulated for either 10 or 25 minutes with 100 µM methionine.

FLAG-immunoprecipitates and cell lysates were analyzed by immunoblotting for the levels of the indicated proteins.
(B) Loss of SAMTOR weakens the regulation by methionine starvation of the GATOR1-GATOR2 interaction. The control and SAMTOR-deficient HEK-293T cells were treated and analyzed as in (A).
(C and D) Transiently overexpresed SAMTOR decreases the interaction between GATOR1 and GATOR2. Endogenously FLAG-tagged-Depdc5 (C) and -WDR59 (D) HEK-293T cells were transfected with a control cDNA or increasing amounts of the SAMTOR cDNA. FLAG-immunoprecipitates were analyzed as in (A).

Figure S4

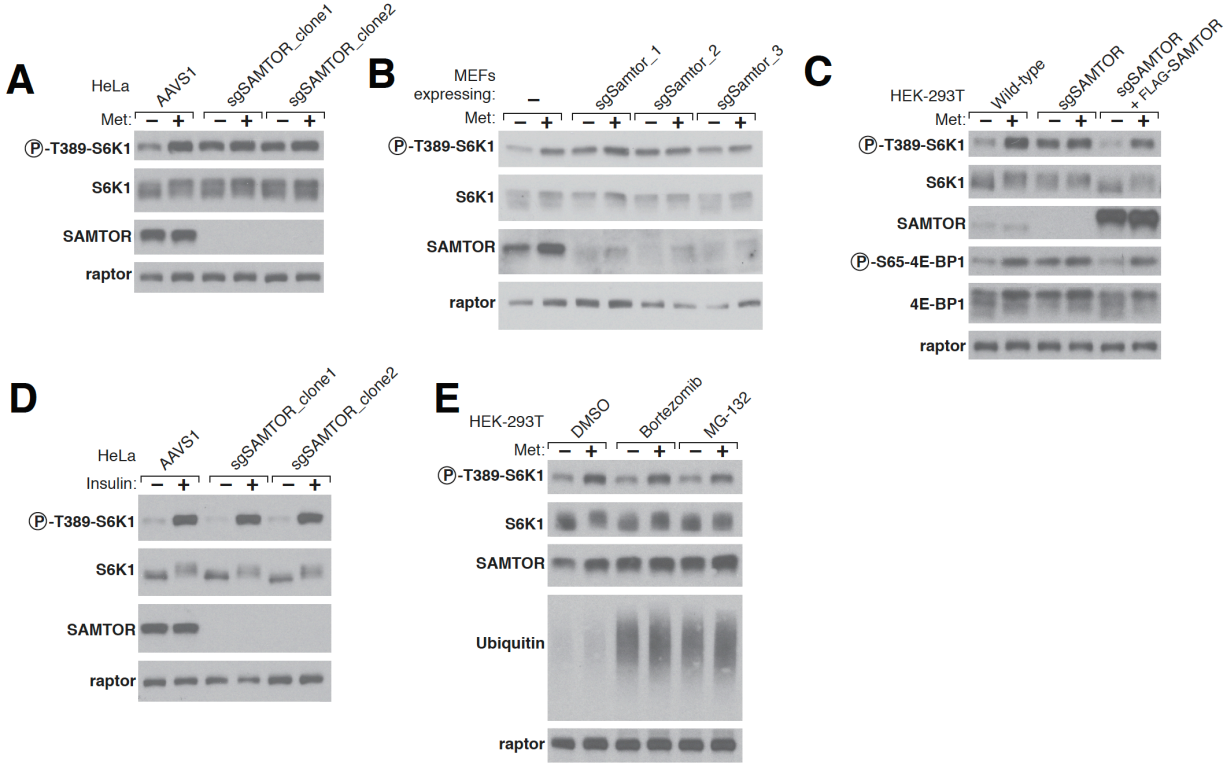

Figure S4.
(A) In HeLa cells with reduced SAMTOR expression, the mTORC1 pathway is resistant to methionine starvation. Two SAMTOR-deficient HeLa cell lines generated using CRISPR/Cas9 were treated as in Fig 4(C). Cell lysates were analyzed by immunoblotting for the phosphorylation states and levels of the indicated proteins.
(B) In MEFs with reduced SAMTOR expression, the mTORC1 pathway is resistant to methionine starvation. Cells were prepared via the stable expression of Cas9 along with the indicated guide. Cells were treated as in Fig. 4(C) and the lysates were analyzed by immunoblotting for the phosphorylation states and levels of the indicated proteins.
(C) In HEK-293T cells, restoration of SAMTOR expression in SAMTOR-deficient cells rescues methionine starvation phenotype to similar level as in wild-type cells. Wild-type, SAMTOR-deficient cell line and FLAG-SAMTOR stably expressed SAMTOR-deficient cell line were prepared and treated as in Fig. 4(C) and the lysates were analyzed by immunoblotting for the phosphorylation states and the levels of the indicated proteins.

(D) The loss of SAMTOR in HeLa cells does not impact the regulation of mTORC1 by growth factors. SAMTOR-deficient cells were incubated in the presence or absence of insulin for 1 hour. Cell lysates were analyzed by immunoblotting for the indicated proteins.
(E) Methionine starvation causes SAMTOR protein levels to drop in a proteasome dependent fashion. 10 μM of the indicated proteasome inhibitors was added to HEK-293T cells cultured in media with or without methionine for 2 hours. Cell lysates were analyzed by immunoblotting for the phosphorylation states and levels of the indicated proteins.

Conclusions

SAMTOR has several properties suggesting that it functions as a SAM sensor that signals methionine sufficiency to mTORC1 (Fig. 4H): (i) it binds SAM with an affinity that is compatible with the drop in intracellular SAM concentrations caused by methionine starvation, (ii) SAMTOR is required for methionine starvation to inhibit mTORC1 signaling, and (iii) SAMTOR mutants that do not bind SAM cannot signal methionine sufficiency to mTORC1. As SAM levels can be affected by the availability of folate, betaine, and vitamin B12, SAMTOR may also link mTORC1 signaling to the availability of these metabolites (Locasale, 2013).

The Rag GTPase pathway senses and integrates the presence of multiple amino acids upstream of mTORC1 (Sancak et al., 2010; Sancak et al., 2008). Sestrin1 and Sestrin2 detect leucine, while CASTOR1 and SLC38A9 sense cytosolic and lysosomal arginine, respectively (Chantranupong et al., 2016; Wolfson et al., 2016). In contrast to the Sestrins and CASTOR1, which bind to GATOR2, SAMTOR interacts with GATOR1-KICSTOR. Our genetic data suggest that SAMTOR potentiates GATOR1 function, but the mechanism through which this occurs is unknown but may involve disruption of the binding of GATOR1 to GATOR2. The interaction between SAMTOR and GATOR1 requires KICSTOR, which may reflect either a composite binding site or the requirement for KICSTOR to localize GATOR1 to the lysosomal surface. In addition, structural information will be needed to understand how the binding of SAM to SAMTOR disrupts its interaction with GATOR1 and KICSTOR.

Unlike leucine and arginine, which directly bind sensors upstream of mTORC1, methionine is sensed indirectly through SAM. SAM is a central metabolite required for most methylation reactions,

including that of DNA(Law and Jacobsen, 2010), histones (Locasale, 2013; Mentch et al., 2015), and phospholipids (Ye et al., 2017), and our work highlights its additional role as a signaling molecule. While *Saccharomyces cerevisiae* does not have a SAMTOR homologue, the yeast TOR pathway does sense methionine through the regulated methylation of the PP2A family of phosphatases (Sutter et al., 2013).

In metazoans the mTORC1 pathway senses multiple amino acids, suggesting that these nutrients were, at times, scarce during their evolution. Two predictions can be made based on the existence of SAMTOR: (i) SAM can become limiting in certain nutritional states, and (ii) modulation of mTORC1 under these conditions is beneficial for maintaining organismal homeostasis. Indeed, diets low in methionine reduce tissue SAM levels and improve insulin sensitivity and extend lifespan in mice and rats (Brown-Borg et al., 2014; Miller et al., 2005; Orentreich et al., 1993; Sun et al., 2009; Wanders et al., 2016). It is intriguing to speculate that these benefits might be mediated in part via the SAMTOR-dependent inhibition of mTORC1, which is well appreciated to impact glucose metabolism and the aging process (Saxton and Sabatini, 2017). Given that SAMTOR has a SAM-binding pocket, it may be possible to modulate SAMTOR function pharmacologically.

Acknowledgements

We thank all members of the Sabatini Lab for helpful insights and suggestions, in particular C. Lewis, B. Chan and T. Kunchok for performing the LC/MS analysis. The pCW57.1 vector was a gift from C. Thoreen. This work was supported by grants from the NIH to D.M.S. (R01 CA103866 and R37 AI47389), Department of Defense (W81XWH-07-0448) to D.M.S., and fellowship support from the NIH to J.M.O. (T32 GM007753 and F30 CA210373), from the NIH to R.A.S. (F31 GM121093-01A1), from the NSF to K.J.C. (2016197106), from the Paul Gray UROP Fund to S.M.S. (3143900), and from the NIH to S.P.G. and J.W.H. (U41 HG006673). D.M.S. is an investigator of the Howard Hughes Medical Institute.

Author Contributions

X.G., J.M.O. and D.M.S. designed the research plan and interpreted experimental results. X.G. and J.M.O. designed and performed most experiments with assistance from R.A.S., P.A.K., K.J.C., G.Y.L. and S.M.S. R.A.S. purified FLAG-tagged SAMTOR protein. K.J.C., G.Y.L. and S.M.S. helped with generating plasmid constructs. J.W.H. and S.P.G. generated the BioPlex dataset. X.G., J.M.O. and D.M.S. wrote the manuscript and R.A.S. helped with editing it.

Methods

Materials

Reagents were obtained from the following sources: the antibody against SAMTOR (NBP1-94062) from Novus Biologicals; the antibody against Nprl3 (HPA011741) from Atlas Antibodies; antibodies against LAMP2 (sc-18822), MAT2A (sc-166452), ubiquitin (sc-8017), and HRP-labeled anti-mouse and anti-rabbit secondary antibodies from Santa Cruz Biotechnology; the antibody against raptor (2818718) from EMD Millipore; antibodies against phospho-T389 S6K1 (9234), S6K1 (2708), phospho-T398 dS6K, phospho-S65 4E-BP1 (9451), 4E-BP1 (9644), mTOR (2983), HRP-labeled anti-rabbit secondary antibody and the myc (2278) and FLAG (2368) epitopes from Cell Signaling Technology (CST); antibodies against the HA epitope from CST (3724) and Bethyl laboratories (A190208A); SAM (13956) from Cayman Chemical; [^{3}H] SAM from American Radiolabeled Chemicals, Inc. SAH (A9384), RPMI, anti-FLAG M2 affinity gel, and amino acids from Sigma Aldrich; DMEM from SAFC Biosciences; Effectene transfection reagent from Qiagen; XtremeGene9 and Complete Protease Cocktail from Roche; Alexa 488, 568 and 647-conjugated secondary antibodies, Schneider's media, and Inactivated Fetal Bovine Serum (IFS) from Invitrogen; amino acid-free RPMI, and amino acid-free Schneider's media from US Biologicals; and anti-HA magnetic beads, methionine-free RPMI from ThermoFisher Scientific. Antibodies against Wdr24 and

SZT2 were generously provided by Jianxin Xie of Cell Signaling Technology, Inc. The dS6K antibody was a generous gift from Mary Stewart (North Dakota State University).

Plasmids used

Plasmid name	Addgene ID	Reference
FLAG-SAMTOR in pRK5	100508	This study
FLAG-Kaptin in pRK5	87041	Wolfson et al. 2017
FLAG-metap2 in pRK5	32004	Peterson et al. 2011
FLAG-DEPDC5 in pRK5	46340	Bar-Peled et al. 2013
FLAG-S6K1 in pRK5	100509	Burnett et al. 1998
FLAG-metap2 in pLJM1	100510	This study
FLAG-Kaptin in pLJM1	100511	This study
HA-metap2 in pRK5	100512	This study
HA-SAMTOR in pRK5	100513	This study
HA-SAMTOR(G172A) in pRK5	100514	This study
HA-SAMTOR(D190A) in pRK5	100515	This study
HA-RagA in pRK5	99710	Sancak et al.
HA-RagC in pRK5	99718	Sancak et al.
HA-RagA(Q66L) in pRK5	99712	Sancak et al.
HA-RagC(S75N) in pRK5	99719	Sancak et al.
Myc-metap2 in pRK5	100516	This study
Myc-SAMTOR in pRK5	100517	This study
GFP-metap2 pLC242	100518	This study

GFP-Sestrin2 pLC242	100519	This study
GFP-SAMTOR pLC242	100520	This study
MAT2A (sg1_resistant) in pCW57.1	100521	This study
pLJC5-FLAG-SAMTOR	102420	This study

Cell lines and tissue culture

HeLa, HEK-293T, p53 -/- MEFs were cultured in DMEM with 10% IFS and supplemented with 2 mM glutamine. These cell lines were maintained at 37°C and 5% CO_2. Drosophila S2R+ cells were cultured in Schneider's media with 10% IFS at 25°C and 5% CO_2.

Transfections

For the transfection of cDNA expression constructs into HEK-293T cells, 1.5 – 2 million cells were seeded in 10 cm dishes. Using the polyethylenimine method (Boussif et al., 1995), cells were transfected 24 hours after seeding with the indicated pRK5 based expression vectors. Experiments were done 36-48 hours after transfection. The total amount of DNA transfected was normalized to 5 µg with the empty pRK5 vector. The following amounts of cDNA were used in the indicated figures.

Fig1C: 250 ng FLAG-metap2, 250 ng FLAG-SAMTOR, 350 ng FLAG-DEPDC5, or 75 ng FLAG-KPTN.

Fig 2A: 2 ng FLAG-S6K1 and the amounts as indicated in the figure for the HA-tagged constructs.

Fig 2C: 2 ng FLAG-S6K1, 150 ng HA-RagA/C, or HA-RagA (Q66L) and HA-RagC (S75N).

Fig 2D: 2 ng FLAG-S6K1 and 0 ng, 25 ng, or 50 ng HA-SAMTOR.

Fig 3F: 150 ng HA-metap2, 150 ng HA-SAMTOR, 200 ng HA-SAMTOR (G172A), or 190 ng HA-SAMTOR (D190A).

Fig 3G: 2 ng FLAG-S6K and 0 ng, 25 ng, or 100 ng HA-tagged SAMTOR wild-type or mutant.

Fig 4B: 50 ng HA-metap2 or 25 ng HA-SAMTOR.

Fig 4F: 2 ng FLAG-S6K, 25 ng HA-metap2, 10 ng HA-SAMTOR, or 40 ng of HA-SAMTOR (G172A).

Fig S1A: 150ng FLAG-metap2, 250ng FLAG-Depdc5, 150ng HA-Nprl3, 150ng HA-Nprl2, 750ng HA-SZT2, 50ng HA-KPTN, 50ng HA-ITFG2, 50ng C12orf66, 150ng Myc-SAMTOR.

Lentiviral production and lentiviral infections

HEK-293T cells were seeded at a density of 750,000 cells per well of a 6-well plate in DMEM with 20% IFS. 24 hours after seeding, VSV-G envelope and CMV ΔVPR packaging plasmids were co-transfected with either pLJM1 containing cDNAs, pLentiCRISPRv2 with indicated guide sequences, or pCW57.1_tTA with the MAT2A (sg1_resistant) cDNA, using XTremeGene 9 transfection reagent (Roche). 12 hours after transfection, the media was changed to DMEM 20% IFS. 36 hours after the media change, the virus-containing supernatant was collected and passed through a 0.45 μm filter. Target cells were plated in 6-well plates with 8 μg/mL polybrene and incubated with virus containing media. Infections with pLentiCRISPRv2 were spinfected at 2200 rpm for 45 minutes at 37°C. 24-48 hours later, the media was changed to fresh media containing either puromycin for pLJM1 or pLentiCRISPR or blasticidin for pCW57.1_tTA.

Cell lysis and immunoprecipitations

Cells were rinsed with cold PBS and lysed in lysis buffer (1% Triton, 10 mM β-glycerol phosphate, 10 mM pyrophosphate, 40 mM Hepes pH 7.4, 2.5 mM MgCl2 and 1 tablet of EDTA-free protease inhibitor [Roche] (per 25 ml buffer)). Cell lysates were cleared by centrifugation in microcentrifuge (15,000 rpm for 10 minutes at 4°C). Cell lysate samples were prepared by addition of 5X sample buffer (0.242 M Tris, 10% SDS, 25% glycerol, 0.5 M DTT, and bromophenol blue), resolved by 8%-16% SDS-PAGE, and analyzed by immunoblotting.

For anti-FLAG immunoprecipitations, anti-FLAG M2 Affinity Gel (SIGMA A2220) was washed with lysis buffer three times then resuspended to a ratio of 50:50 affinity gel to lysis buffer. 25 µL of a well-mixed slurry was added to cleared lysates and incubated at 4°C in a shaker for 90-120 minutes. For anti-HA immunoprecipitations, magnetic anti-HA beads (Pierce) were washed three times with lysis buffer. 30 µL of resuspended beads in lysis buffer was added to cleared lysates and incubated at 4°C in a shaker for 90-120 minutes.

Immunoprecipitates were then washed three times, once with lysis buffer and twice with lysis buffer with 500 mM NaCl. Immunoprecipitated proteins were denatured by addition of 50 µL of SDS-containing sample buffer (0.121 M Tris, 5% SDS, 12.5% glycerol, 0.25 M DTT, and bromophenol blue) and boiled for 5 minutes. Denatured samples were resolved by 8%-12% SDS-PAGE, and analyzed by immunoblotting.

RNAi in Drosophila S2R+ cells and qPCR

The dsRNA against dSesn was designed as described in (Bar-Peled et al., 2013). To minimize off-target effects, we used the DRSC tool at http://flyrnai.org/RNAi_find_frag-free.html and excluded regions of 19-mer-or-greater identity to any other Drosophila transcripts. The dsRNA targeting GFP was used as a negative control. The dsRNA against dSamtor was picked from searching CG3570 at DRSC/TRiP Functional Genomics Resources website: http://www.flyrnai.org/cgi-bin/DRSC_gene_lookup.pl. DRSC24231 was used in this work. Primer sequences used to amplify DNA templates for dsRNA synthesis for GFP, dSamtor and dSesn, including underlined 5' and 3' T7 promoter sequences, are as follows:

F-dsGFP primer: GAATTAATACGACTCACTATAGGGAGAAGCTGACCCTGAAGTTCATCTG

R-dsGFP primer: GAATTAATACGACTCACTATAGGGAGATATAGACGTTGTGGCTGTTGTAGTT

F-dsdSamtor primer: GAATTAATACGACTCACTATAGGGAGATGGAATCCTACAGAGCCGAGGG

R-dsdSamtor primer: GAATTAATACGACTCACTATAGGGAGACGTACCCGTAGCAGTCCAATCCTG

F-dsdSesn primer: GAATTAATACGACTCACTATAGGGAGAGACTACGACTATGGCGAAGTGAA

R-dsdSesn primer: GAATTAATACGACTCACTATAGGGAGATCAAGTCATATAGCGCATTATCTCG

On day one, 2 million S2R+ cells were plated in 6-well culture dishes in 1.5 ml of Schneider's media with 10% IFS. Cells were transfected with 2 µg of each dsRNA using Effectene transfection reagent (Qiagen) after 12-24 hours. On day three, a second round of dsRNA transfection was performed. On day five, 1.2 million cells were plated in 12-well culture dishes coated with fibronectin in advance. 3-4 hours later, cells were rinsed once with amino acid-free Schneider's media, and starved for either methionine or leucine by replacing the media with methionine or leucine-free media for 1 hour. To stimulate with methionine or leucine, the media was replaced with complete Schneider's media for 30 minutes. Cells were then rinsed with cold PBS once, lysed in lysis buffer, and subjected to immunoblotting for the levels of phospho-T398 dS6K and total dS6K.

To validate knockdown of dSamtor and dSesn, the following primer pairs were used in qPCR reactions due to the lack of available antibodies to these proteins. We used alpha-tubulin as internal standard control. The data were analyzed via the ΔΔCt method as described previously (Chantranupong et al., 2014).

F-alpha-tubulin: CAACCAGATGGTCAAGTGCG

R-alpha-tubulin: ACGTCCTTGGGCACAACATC

F-dSamtor: GACCAACGATGGGAAGGTGG

R-dSamtor: GCTCTGTAGGATTCCAGGAGT

F-dSesn: TCCGCTGCCTAACGATTACAG

R-dSesn: TTCACCAGATACGGACACTGA

Sequence analyses of SAMTOR

We assessed the sequence conservation of SAMTOR with the PHMMER online tool (https://www.ebi.ac.uk/Tools/hmmer/search/phmmer) and performed secondary structure predictions using the HHPred online tool (https://toolkit.tuebingen.mpg.de/#/tools/hhpred). Note: the name for SAMTOR in the BioPlex dataset is C7orf60. When we searched C7orf60 on multiple websites, including Genecards and Uniprot, we found that C7orf60 is also associated with another name: Probable BMT2 (Base Methyltransferase Of 25S rRNA 2) homolog. BMT2 is a nuclear RNA methyltransferase in *Saccharomyces cerevisiae* (Sharma et al., 2013). However, in our own extensive analyses we could find no similarity between human C7orf60 (SAMTOR) and yeast BMT2 at the protein sequence level. We suspect that the BMT2 name was erroneously assigned in an automated fashion to C7orf60 because both contain a predicted Class I Rossmann fold methyltransferase domain.

Generation of CRISPR/Cas9 genetically modified cells with loss of SAMTOR or MAT2A

To generate HEK-293T or HeLa cells with loss of SAMTOR, the following sense (S) and antisense (AS) oligonucleotides encoding the guide RNAs were cloned into pX330:

sgSAMTOR_guide1_S: caccgGAAATACTGCTCGTGCGCAG

sgSAMTOR_guide1_AS: aaacCTGCGCACGAGCAGTATTTCc

Control cells were generated by targeting the AAVS1 locus as described before (Kim et al., 2002; Wolfson et al., 2017). On day one, 2 million HEK-293T cells were seeded in a 10-cm plate. Twenty-four hours after seeding, each well was transfected with 1µg shGFP pLKO, 1 µg of the pX330 guide construct and 3 µg of empty pRK5 using XtremeGene9. Two days after transfection, cells were moved to a new 10-cm plate into puromycin containing media. Forty-eight hours after selection, the media was switched to

media not containing puromycin. Cells were allowed to recover for 1 week after selection prior to single-cell sorting with a flow cytometer into the wells of a 96-well plate containing 150 µl of DMEM supplemented with 30% IFS.

For HeLa cells, on day one, 1 million cells were plated in a 10-cm dish. 24 hours later, the cells were transfected with 1 µg shGFP pLKO and 1 µg of the pX330 guide construct using FuGENE. Selection with puromycin was started the following day to eliminate untransfected cells. 48 hours after selection, the medium was aspirated and replenished with fresh medium without puromycin and the cells were single-cell sorted as described above. Cells were grown for two weeks and the resultant colonies were trypsinized and expanded. Cell clones were validated via immunoblotting.

Human SAMTOR, mouse SAMTOR, and MAT2A were depleted using the lentiviral pLentiCRISPRv2 system. The following sense (S) and antisense (AS) oligonucleotides were cloned into pLentiCRISPRv2:

Human SAMTOR

sgSAMTOR_1 (S): caccgGAAATACTGCTCGTGCGCAG

sgSAMTOR_1 (AS): aaacCTGCGCACGAGCAGTATTTCc

sgSAMTOR_2 (S): caccgGATATGGAGCCAGGGGCCGG

sgSAMTOR_2 (AS): aaacCCGGCCCCTGGCTCCATATCc

Mouse Samtor

sg*Mm*Samtor_1 (S): caccgGCAGGAGAAGCTGTCCGGGG

sg*Mm*Samtor_1 (AS): aaacCGCCACTAAGACCACTCCAGc

sg*Mm*Samtor_2 (S): caccgCTCCGCAAGAAGTACCGCGA

sg*Mm*Samtor_2 (AS): aaacTCGCGGTACTTCTTGCGGAGc

sg*Mm*Samtor_3 (S): caccgATGAACGCTCTTCACCACCC

sg*Mm*Samtor_3 (AS): aaacGGGTGGTGAAGAGCGTTCATc

Human MAT2A

sgMAT2A_1 (S): caccgTTAAAGGAGGTCTGTGCCGG

sgMAT2A_1 (AS): aaacCCGGCACAGACCTCCTTTAAc

Lentivirus was produced and used to infect cells as described above. To give Cas9 time to cut the targeted locus, experiments were performed at least one week after transduction.

Generation of the MAT2A doxycycline-repressible system

The MAT2A cDNA was amplified from cDNA prepared from total cell HEK-293T RNA. The following synonymous mutations were introduced by overhang extension PCR into the MAT2A coding sequence: 144G>A to remove a BamHI restriction site and 939G>A to mutate the protospacer adjacent motif of the sgMAT2A_1 sgRNA sequence. Using NheI and BamHI restriction sites, the MAT2A_sg1 cDNA was cloned downstream of the tetO element in the lentiviral pCW57.1 vector, which encodes the tet/dox-repressible tTA trans-factor and a blasticidin resistance gene. Lentivirus was produced as described above and was used to transduce wild-type HEK-293T cells. After 24 hours, blasticidin was added to the cells to remove untransduced cells. After 48 hours of selection, cells were transduced with lentivirus produced from pLentiCRISPRv2 with the MAT2A_sg1 guide sequence. After puromycin selection, cells were single cell sorted using flow cytometry into 96-well plates containing DMEM 30% IFS. Resulting clones were expanded and screened by replica plating for sensitivity to 30 ng/mL doxycycline. Positive clones were then screened by immunoblotting for MAT2A protein in whole cell lysates.

Immunofluorescence assays

Immunofluorescence assays were performed as described previously (Wolfson et al., 2017). Briefly, for the experiment in Figure 2B, 2 million cells growing in a 10 cm dish and plated 24 hours before were transfected with 150 ng of the cDNAs for GFP-metap2, GFP-SAMTOR, or GPF-Sestrin2 in pIC242. After 24 hours, 400,000 cells were counted and plated on fibronectin-coated glass coverslips (TED PELLA, Inc.) in 6-well tissue culture plates. For the experiment in Figure 4E, 400,000 HEK-293T cells were plated on fibronectin-coated glass coverslips in 6-well tissue culture plates. After 24 hours, the slides were rinsed once with PBS and fixed with 4% paraformaldehyde in PBS for 15 minutes at room temperature. The slides were then rinsed three times with PBS and the cells permeabilized with 0.05% Triton X-100 in PBS for 5 minutes at room temperature. The slides were rinsed three times with PBS and then blocked for 1 hour in Odyssey blocking buffer at room temperature. The slides were incubated with primary antibody in Odyssey blocking buffer at 4°C overnight, rinsed three times with PBS, and incubated with secondary antibodies produced in donkey (diluted 1:1000 in Odyssey blocking buffer) for 50 minutes at room temperature in the dark, and washed three times with PBS. The primary antibodies used were directed against mTOR (CST; 1:100-1:300 dilution), LAMP2 (Santa Cruz Biotechnology; 1:300 dilution). Slides were mounted on glass coverslips using Vectashield (Vector Laboratories) containing DAPI.

Images were acquired on a Zeiss AxioVert200M microscope with a 63X oil immersion objective and a Yokogawa CSU-22 spinning disk confocal head with a Borealis modification (Spectral Applied Research/Andor) and a Hamamatsu ORCA-ER CCD camera. The MetaMorph software package (Molecular Devices) was used to control the hardware and image acquisition. The excitation lasers used to capture the images were 405 nm, 488 nm, 561 nm and 640 nm. DAPI channel is not shown in the main images, but it is in the insets as a blue signal.

In the experiment in Figure 2B, an Alexa568-conjugated secondary antibody was used for the mTOR staining and the excitation wavelength was 561 nm, while an Alexa647-conjugated secondary antibody was used for the LAMP2 staining and the excitation wavelength was 640 nm. The GFP signal was detected by excitation with the 488 nm laser without use of a primary or secondary antibody.

In the experiment in Figure 4E, an Alexa488-conjugated secondary antibody was used for mTOR staining and the excitation wavelength was 488 nm, while an Alexa568-conjugated secondary antibody was used for the LAMP2 staining and the excitation wavelength was 561 nm.

Purification of proteins expressed in human cells for SAM binding assays

For radiolabelled SAM binding assays using FLAG-tagged wild-type SAMTOR (figure 3B), suspension HEK-293F cells were seeded at 2.5 million cells/ml, and the pRK5-FLAG-SAMTOR cDNA was transfected using polyethylenimine. 72-96 hours after transfection, cells were rinsed one time in cold PBS and lysed in 1% Triton lysis buffer (1% Triton, 40 mM Hepes pH 7.4, 2.5 mM MgCl2 and 1 tablet of EDTA-free protease inhibitor [Roche] per 25 ml buffer). Following anti-FLAG immunoprecipitation, the beads were washed 4 times with lysis buffer containing 500 mM NaCl and the protein was eluted in FLAG Elution Buffer (40 mM Hepes pH 7.4, 150 mM NaCl, 2.5 mM MgCl2 and 0.5 mg/ml FLAG peptide) for 1 hour at 4°C. The eluted protein was further purified via size-exclusion chromatography on a Superdex S75 10/300 column (GE Healthcare) equilibrated in running buffer (20 mM Hepes pH 7.4, 150 mM NaCl, 1 mM DTT) and concentrated to approximately 1 mg/ml. 1 µl of the protein was examined by SDS-PAGE followed by Coomassie blue staining for purity analysis. 5 µg of purified FLAG-SAMTOR protein was used in each sample in the experiment in Figure 3B.

For radiolabeled SAM binding assays using HA tagged SAMTOR (wild-type, D190A and G172A) (Figure 3E), 6 million HEK-293T cells were plated in a 15 cm plate. 24 hours after plating, the cells were transfected using polyethylenimine with the pRK5-based cDNA expression plasmids indicated in the

figures in the following amounts: 12 µg HA-GST Rap2A, 15 µg HA-SAMTOR wild-type or mutants. The total amount of plasmid DNA in each plate was normalized to 20 µg total DNA with empty-pRK5. In figure 3E, each plasmid was transfected to five plates. 48 hours after transfection, cells were lysed as previously described and the lysates with same plasmid transfected was mixed and combined.

SAM binding assay

Anti-FLAG (Sigma) or anti-HA magnetic beads (Pierce) were blocked by rotating in 1 µg/µl bovine serum albumin (BSA) for 30 minutes at 4 °C, then washed three times in lysis buffer, and re-suspended in an equal volume of lysis buffer.

30 µl of a bead slurry was added to each of the purified proteins or clarified cell lysates and incubated for 90 minutes at 4°C. The beads were then washed as previously and incubated for one hour on ice in cytosolic buffer (0.1% Triton, 40 mM HEPES pH 7.4, 10 mM NaCl, 150 mM KCl, 2.5 mM $MgCl_2$) with the indicated amount of [^{3}H]-labeled SAM and unlabeled SAM or SAH. At the end of one hour, the beads were aspirated dry and rapidly washed four times with binding wash buffer (0.1% Triton, 40 mM HEPES pH 7.4, 300 mM NaCl, 2.5 mM MgCl2). The beads were aspirated dry again and resuspended in 80 µl of cytosolic buffer. Each sample was mixed well and then 15 µl aliquots were separately quantified using a TriCarb scintillation counter (Perkin Elmer). This process was repeated in pairs for each sample, to ensure similar incubation and wash times for all samples analyzed across different experiments.

For radiolabeled SAM binding assays using HA tagged SAMTOR (wild-type, D190A and G172A), an immunoprecipitation for each sample was performed in parallel. After washing three times as previously described, the proteins were eluted in lysis buffer with 500 mM NaCl and 1 mg/ml HA peptide for 1 hour at 30°C. The eluted proteins were denatured by the addition of sample buffer and boiled for 5 minutes at 95°C, resolved by 10 % SDS-PAGE, and analyzed with Coomassie blue staining.

K_d and K_i calculations

The affinities for SAM and SAH of human FLAG-SAMTOR were determined by first normalizing the bound [^{3}H]-labeled SAM concentrations across three separate binding assays performed with varying amounts of cold SAM or SAH. These values were plotted and fit to a hyperbolic equation (Cheng-Prusoff equation) to estimate the IC_{50} value. K_d or K_i values were derived from the IC50 value using the equation: K_d or $K_i = IC_{50} / (1+([^3H]SAM)/K_d)$.

In vitro GATOR1-SAMTOR dissociation assay

HEK-293T cells stably expressing endogenous FLAG-tagged Depdc5 were lysed and subjected to anti-FLAG immunoprecipitations as described above. The GATOR1-SAMTOR complexes immobilized on the FLAG beads were washed twice in lysis buffer with 250 mM NaCl, and then incubated for 25 minutes in 0.3 ml of cytosolic buffer (0.1% Triton, 40 mM HEPES pH7.4, 10 mM NaCl, 150 mM KCl, 2.5 mM MgCl2) with the indicated concentrations of SAM or SAH in the cold. The amount of GATOR1, SAMTOR, GATOR2, and KICSTOR that remained bound was assayed by SDS-PAGE and immunoblotting as described previously.

LC/MS-based metabolomics and quantification of metabolite abundance

LC/MS-based metabolomics were performed and analyzed as previously described (Birsoy et al., 2015; Chen et al., 2016), with 500 nM isotope-labeled internal standards were used. SAM standards were purchased from Cayman Chemical (13956), and SAH from SIGMA (A9384). Briefly, 80% methanol extraction buffer with 500 nM isotope-labeled internal standards was used for whole cell metabolite extraction. Samples were briefly vortexed and dried by vacuum centrifugation. Samples were stored at -80°C until analyzed. On the day of analysis, samples were resuspended in 100 µL of LC/MS grade water

and the insoluble fraction was cleared by centrifugation at 15,000 rpm. The supernatant was then analyzed as previously described by LC/MS (Birsoy et al., 2015; Chen et al., 2016).

Statistical analyses

Two-tailed t tests were used for comparison between two groups. All comparisons were two-sided, and P values of less than 0.001 were considered to indicate statistical significance.

References

Bar-Peled, L., Chantranupong, L., Cherniack, A.D., Chen, W.W., Ottina, K.A., Grabiner, B.C., Spear, E.D., Carter, S.L., Meyerson, M., and Sabatini, D.M. (2013). A Tumor suppressor complex with GAP activity for the Rag GTPases that signal amino acid sufficiency to mTORC1. Science *340*, 1100-1106.

Bar-Peled, L., Schweitzer, L.D., Zoncu, R., and Sabatini, D.M. (2012). Ragulator is a GEF for the rag GTPases that signal amino acid levels to mTORC1. Cell *150*, 1196-1208.

Birsoy, K., Wang, T., Chen, W.W., Freinkman, E., Abu-Remaileh, M., and Sabatini, D.M. (2015). An Essential Role of the Mitochondrial Electron Transport Chain in Cell Proliferation Is to Enable Aspartate Synthesis. Cell *162*, 540-551.

Boussif, O., Lezoualc'h, F., Zanta, M.A., Mergny, M.D., Scherman, D., Demeneix, B., and Behr, J.P. (1995). A versatile vector for gene and oligonucleotide transfer into cells in culture and in vivo: polyethylenimine. Proc Natl Acad Sci U S A *92*, 7297-7301.

Brown-Borg, H.M., Rakoczy, S.G., Wonderlich, J.A., Rojanathammanee, L., Kopchick, J.J., Armstrong, V., and Raasakka, D. (2014). Growth hormone signaling is necessary for lifespan extension by dietary methionine. Aging Cell *13*, 1019-1027.

Chantranupong, L., Scaria, S.M., Saxton, R.A., Gygi, M.P., Shen, K., Wyant, G.A., Wang, T., Harper, J.W., Gygi, S.P., and Sabatini, D.M. (2016). The CASTOR Proteins Are Arginine Sensors for the mTORC1 Pathway. Cell *165*, 153-164.

Chantranupong, L., Wolfson, R.L., Orozco, J.M., Saxton, R.A., Scaria, S.M., Bar-Peled, L., Spooner, E., Isasa, M., Gygi, S.P., and Sabatini, D.M. (2014). The Sestrins interact with GATOR2 to negatively regulate the amino-acid-sensing pathway upstream of mTORC1. Cell Rep *9*, 1-8.

Chen, W.W., Freinkman, E., Wang, T., Birsoy, K., and Sabatini, D.M. (2016). Absolute Quantification of Matrix Metabolites Reveals the Dynamics of Mitochondrial Metabolism. Cell *166*, 1324-1337 e1311.

Dibble, C.C., and Manning, B.D. (2013). Signal integration by mTORC1 coordinates nutrient input with biosynthetic output. Nat Cell Biol *15*, 555-564.

Gossen, M., and Bujard, H. (1992). Tight control of gene expression in mammalian cells by tetracycline-responsive promoters. Proc Natl Acad Sci U S A *89*, 5547-5551.

Hildebrand, A., Remmert, M., Biegert, A., and Soding, J. (2009). Fast and accurate automatic structure prediction with HHpred. Proteins *77 Suppl 9*, 128-132.

Huttlin, E.L., Bruckner, R.J., Paulo, J.A., Cannon, J.R., Ting, L., Baltier, K., Colby, G., Gebreab, F., Gygi, M.P., Parzen, H.*, et al.* (2017). Architecture of the human interactome defines protein communities and disease networks. Nature *545*, 505-509.

Jewell, J.L., Russell, R.C., and Guan, K.L. (2013). Amino acid signalling upstream of mTOR. Nature reviews Molecular cell biology *14*, 133-139.

Jung, J., Genau, H.M., and Behrends, C. (2015). Amino Acid-Dependent mTORC1 Regulation by the Lysosomal Membrane Protein SLC38A9. Mol Cell Biol *35*, 2479-2494.

Kim, D.H., Sarbassov, D.D., Ali, S.M., King, J.E., Latek, R.R., Erdjument-Bromage, H., Tempst, P., and Sabatini, D.M. (2002). mTOR interacts with raptor to form a nutrient-sensitive complex that signals to the cell growth machinery. Cell *110*, 163-175.

Kim, E., Goraksha-Hicks, P., Li, L., Neufeld, T.P., and Guan, K.L. (2008). Regulation of TORC1 by Rag GTPases in nutrient response. Nat Cell Biol *10*, 935-945.

Kozbial, P.Z., and Mushegian, A.R. (2005). Natural history of S-adenosylmethionine-binding proteins. BMC Struct Biol *5*, 19.

Law, J.A., and Jacobsen, S.E. (2010). Establishing, maintaining and modifying DNA methylation patterns in plants and animals. Nat Rev Genet *11*, 204-220.

Locasale, J.W. (2013). Serine, glycine and one-carbon units: cancer metabolism in full circle. Nat Rev Cancer *13*, 572-583.

Mentch, S.J., Mehrmohamadi, M., Huang, L., Liu, X., Gupta, D., Mattocks, D., Gomez Padilla, P., Ables, G., Bamman, M.M., Thalacker-Mercer, A.E.*, et al.* (2015). Histone Methylation Dynamics and Gene Regulation Occur through the Sensing of One-Carbon Metabolism. Cell Metab *22*, 861-873.

Miller, R.A., Buehner, G., Chang, Y., Harper, J.M., Sigler, R., and Smith-Wheelock, M. (2005). Methionine-deficient diet extends mouse lifespan, slows immune and lens aging, alters glucose, T4, IGF-I and insulin levels, and increases hepatocyte MIF levels and stress resistance. Aging Cell *4*, 119-125.

Orentreich, N., Matias, J.R., DeFelice, A., and Zimmerman, J.A. (1993). Low methionine ingestion by rats extends life span. J Nutr *123*, 269-274.

Parmigiani, A., Nourbakhsh, A., Ding, B., Wang, W., Kim, Y.C., Akopiants, K., Guan, K.L., Karin, M., and Budanov, A.V. (2014). Sestrins inhibit mTORC1 kinase activation through the GATOR complex. Cell Rep *9*, 1281-1291.

Peng, M., Yin, N., and Li, M.O. (2017). SZT2 dictates GATOR control of mTORC1 signalling. Nature *543*, 433-437.

Quinlan, C.L., Kaiser, S.E., Bolanos, B., Nowlin, D., Grantner, R., Karlicek-Bryant, S., Feng, J.L., Jenkinson, S., Freeman-Cook, K., Dann, S.G.*, et al.* (2017). Targeting S-adenosylmethionine biosynthesis with a novel allosteric inhibitor of Mat2A. Nat Chem Biol *13*, 785-792.

Rebsamen, M., Pochini, L., Stasyk, T., de Araujo, M.E., Galluccio, M., Kandasamy, R.K., Snijder, B., Fauster, A., Rudashevskaya, E.L., Bruckner, M.*, et al.* (2015). SLC38A9 is a component of the lysosomal amino acid sensing machinery that controls mTORC1. Nature *519*, 477-481.

Sancak, Y., Bar-Peled, L., Zoncu, R., Markhard, A.L., Nada, S., and Sabatini, D.M. (2010). Ragulator-Rag complex targets mTORC1 to the lysosomal surface and is necessary for its activation by amino acids. Cell *141*, 290-303.

Sancak, Y., Peterson, T.R., Shaul, Y.D., Lindquist, R.A., Thoreen, C.C., Bar-Peled, L., and Sabatini, D.M. (2008). The Rag GTPases bind raptor and mediate amino acid signaling to mTORC1. Science *320*, 1496-1501.

Saxton, R.A., Chantranupong, L., Knockenhauer, K.E., Schwartz, T.U., and Sabatini, D.M. (2016a). Mechanism of arginine sensing by CASTOR1 upstream of mTORC1. Nature *536*, 229-233.

Saxton, R.A., Knockenhauer, K.E., Wolfson, R.L., Chantranupong, L., Pacold, M.E., Wang, T., Schwartz, T.U., and Sabatini, D.M. (2016b). Structural basis for leucine sensing by the Sestrin2-mTORC1 pathway. Science *351*, 53-58.

Saxton, R.A., and Sabatini, D.M. (2017). mTOR Signaling in Growth, Metabolism, and Disease. Cell *168*, 960-976.

Sharma, S., Watzinger, P., Kotter, P., and Entian, K.D. (2013). Identification of a novel methyltransferase, Bmt2, responsible for the N-1-methyl-adenosine base modification of 25S rRNA in Saccharomyces cerevisiae. Nucleic Acids Res *41*, 5428-5443.

Sun, L., Sadighi Akha, A.A., Miller, R.A., and Harper, J.M. (2009). Life-span extension in mice by preweaning food restriction and by methionine restriction in middle age. J Gerontol A Biol Sci Med Sci *64*, 711-722.

Sutter, B.M., Wu, X., Laxman, S., and Tu, B.P. (2013). Methionine inhibits autophagy and promotes growth by inducing the SAM-responsive methylation of PP2A. Cell *154*, 403-415.

Tsun, Z.Y., Bar-Peled, L., Chantranupong, L., Zoncu, R., Wang, T., Kim, C., Spooner, E., and Sabatini, D.M. (2013). The folliculin tumor suppressor is a GAP for the RagC/D GTPases that signal amino acid levels to mTORC1. Mol Cell *52*, 495-505.

Wanders, D., Stone, K.P., Forney, L.A., Cortez, C.C., Dille, K.N., Simon, J., Xu, M., Hotard, E.C., Nikonorova, I.A., Pettit, A.P.*, et al.* (2016). Role of GCN2-Independent Signaling Through a Noncanonical

PERK/NRF2 Pathway in the Physiological Responses to Dietary Methionine Restriction. Diabetes *65*, 1499-1510.

Wang, S., Tsun, Z.Y., Wolfson, R.L., Shen, K., Wyant, G.A., Plovanich, M.E., Yuan, E.D., Jones, T.D., Chantranupong, L., Comb, W.*, et al.* (2015a). Metabolism. Lysosomal amino acid transporter SLC38A9 signals arginine sufficiency to mTORC1. Science *347*, 188-194.

Wang, T., Birsoy, K., Hughes, N.W., Krupczak, K.M., Post, Y., Wei, J.J., Lander, E.S., and Sabatini, D.M. (2015b). Identification and characterization of essential genes in the human genome. Science *350*, 1096-1101.

Wang, T., Yu, H., Hughes, N.W., Liu, B., Kendirli, A., Klein, K., Chen, W.W., Lander, E.S., and Sabatini, D.M. (2017). Gene Essentiality Profiling Reveals Gene Networks and Synthetic Lethal Interactions with Oncogenic Ras. Cell *168*, 890-903 e815.

Wolfson, R.L., Chantranupong, L., Saxton, R.A., Shen, K., Scaria, S.M., Cantor, J.R., and Sabatini, D.M. (2016). Sestrin2 is a leucine sensor for the mTORC1 pathway. Science *351*, 43-48.

Wolfson, R.L., Chantranupong, L., Wyant, G.A., Gu, X., Orozco, J.M., Shen, K., Condon, K.J., Petri, S., Kedir, J., Scaria, S.M.*, et al.* (2017). KICSTOR recruits GATOR1 to the lysosome and is necessary for nutrients to regulate mTORC1. Nature *543*, 438-442.

Wyant, G., Abu-Remaileh, M., Wolfson, R., Chen, W., Freinkman, E., Danai, L., Vander Heiden, M., and Sabatini, D. mTORC1 activator SLC38A9 is required to efflux essential amino acids from lysosomes and use protein as a nutrient. Cell *In Press*.

Ye, C., Sutter, B.M., Wang, Y., Kuang, Z., and Tu, B.P. (2017). A Metabolic Function for Phospholipid and Histone Methylation. Mol Cell *66*, 180-193 e188.

Chapter 3

Sestrin-mediated leucine sensing by mTORC1 is essential for detecting and adapting to a low leucine diet in *Drosophila*

Parts of this chapter were first published as:

Xin Gu*, Patrick Jouandin*, Rich Binari, Max L. Valenstein, Michael A. Reid, Marie E. Allen, Pranav V. Lalgudi, Jason W. Locasale, Norbert Perrimon, David M. Sabatini, Sestrin-mediated leucine sensing by mTORC1 is essential for detecting and adapting to a low leucine diet in *Drosophila*, ***Nature***, in revision. (2020)

(*: Contribute equally to the work)
My contributions: (1) Experiments done together by Patrick and me: Figure 1d, Figure 2a,c-h, Figure 4a, Extended data figure 1-6, 10a. (2) Experiments performed by Patrick: Figure 2b, Figure 3g. (3) All other experiments were performed by me, while Patrick mainly maintained and provided the flies with correct developmental stages and genotypes.

Abstract

mTOR complex 1 (mTORC1) regulates cell growth and metabolism in response to multiple nutrients, including the essential amino acid leucine. Recent work in cultured cells established Sestrin as a leucine-binding protein that inhibits mTORC1 signaling during leucine deprivation, but its role in the organismal response to dietary leucine is unknown. Here, we find that *Sestrin* null flies ($Sesn^{-/-}$) fail to inhibit mTORC1 or activate autophagy upon leucine starvation and have impaired development and a shortened lifespan on a low leucine diet. Knock-in flies expressing a leucine-binding deficient Sestrin mutant ($Sesn^{L431E}$) have reduced, leucine-insensitive mTORC1 activity. Interestingly, we found that flies can discriminate between food with or without leucine, and preferentially feed and lay progeny on leucine-containing food. This preference depends on Sestrin and its capacity to bind leucine. Leucine regulates mTORC1 activity in glial cells and a knockdown of *Sesn* in these cells reduces the ability of flies to detect leucine-free food. Thus, nutrient sensing by mTORC1 is not only necessary for flies to adapt to, but also to detect, a diet deficient in an essential nutrient.

Introduction

The mTORC1 (mechanistic target of rapamycin complex 1) protein kinase regulates growth and metabolism in response to diverse signals, including growth factors and nutrients like amino acids (Liu and Sabatini, 2020). Amino acids activate mTORC1 by promoting its translocation to the lysosomal surface, where its essential activator Rheb resides, at least in part (Buerger et al., 2006; Kim et al., 2008; Sancak et al., 2008). The heterodimeric Rag GTPases regulate the lysosomal localization of mTORC1 (Kim et al., 2008; Sancak et al., 2008), which in turn are under the control of several multi-component protein complexes, including GATOR1 and GATOR2 (Bar-Peled et al., 2013). GATOR1 is a GAP (GTPase activating protein) for RagA and RagB and is necessary for amino acid deprivation to inhibit mTORC1 signaling (Shen et al., 2018; Shen et al., 2019). In contrast, GATOR2 is required for amino acids to activate mTORC1 and directly interacts with several of the amino acid sensors so far discovered, indicating that it acts as a nutrient-sensing hub despite its still unknown biochemical function (Bar-Peled et al., 2013).

Amongst the proteogenic amino acids, leucine is the best-established activator of mTORC1 (Dodd and Tee, 2012; Fox et al., 1998; Lynch et al., 2000; Suryawan et al., 2008). Work in cultured mammalian cells has shown that leucine controls mTORC1 by regulating the interaction of GATOR2 with the Sestrin family of proteins (Chantranupong et al., 2014; Kim et al., 2015; Wolfson et al., 2016), which are repressors of mTORC1 signaling (Lee et al., 2010; Ye et al., 2015). Human Sestrin1 and Sestrin2 bind leucine at affinities consistent with the leucine concentration needed to activate mTORC1 and are required for leucine deprivation to inhibit mTORC1 signaling (Wolfson et al., 2016). Moreover, a Sestrin2 mutant that does not bind leucine fails to dissociate from GATOR2 in the presence of leucine, and, in cells expressing this mutant, mTORC1 activity remains low even when the cells are cultured in leucine-replete conditions (Saxton et al., 2016; Wolfson et al., 2016). Despite the evidence that Sestrin is a leucine sensor for the mTORC1 pathway in cultured mammalian cells, the roles of Sestrin-mediated leucine sensing in the physiology of an intact organism remain largely unexplored.

While much of the work on leucine sensing has been in mammalian systems, Sestrin as well as the core nutrient-sensing machinery, including the Rag GTPases, GATOR1, and GATOR2, are conserved in most invertebrates, including the fly *Drosophila melanogaster (Wolfson and Sabatini, 2017)*. Unlike in mammals, flies express only one gene for Sestrin (*Sesn*) (Lee et al., 2010), greatly facilitating the *in vivo* study of leucine sensing by mTORC1. Here, we show that Sestrin and its leucine-binding pocket is required for leucine to regulate mTORC1 in fly tissues *in vivo* and for flies to detect and adapt to leucine-deficient diets.

Results

***Drosophila* Sestrin binds GATOR2 and regulates mTORC1 *in vivo* in response to dietary leucine**

In an equilibrium binding assay, *Drosophila* Sestrin bound leucine with a dissociation constant of ~100 μM (Fig. 1a), an affinity several fold lower than those of human Sestrin1 and 2 (K_ds of ~15-20 μM). This reduced affinity is likely the result of an interesting difference between the leucine binding pockets of human and fly Sestrin. Structural studies show that in human Sestrin2 a tryptophan (W444) forms the floor of the pocket, but in the fly protein the analogous residue is a leucine (L431), a smaller residue that when introduced into Sestrin2 (W444L) is sufficient to reduce its leucine-binding capacity by several fold(Saxton et al., 2016). The low leucine affinity of fly Sestrin is consistent with the observation that fly hemolymph has substantially higher amino acid concentrations than human plasma (Piyankarage et al., 2008; Wolfson and Sabatini, 2017), a difference likely reflected intracellularly. Like the analogous mutant of human Sestrin2 (W444E), fly Sestrin L431E does not bind leucine (Fig. 1b).

To ask if leucine regulates the interaction of fly Sestrin with GATOR2, we stably expressed in *Drosophila* S2R+ cells a Flag-tagged control protein (und, *Drosophila* ortholog of mammalian metap2, methionyl aminopeptidase) or WDR59, one of the five core components of the GATOR2 complex. Sestrin co-immunoprecipitated with GATOR2, but not und, and removal of leucine from the cell media strongly

enhanced the interaction. The addition of leucine, but not isoleucine, valine, or methionine, to the immunoprecipitates was sufficient to release Sestrin from GATOR2 (Fig. 1c). Thus, like the human protein, fly Sestrin binds to GATOR2 in a fashion that is specifically disrupted by leucine.

Figure 1

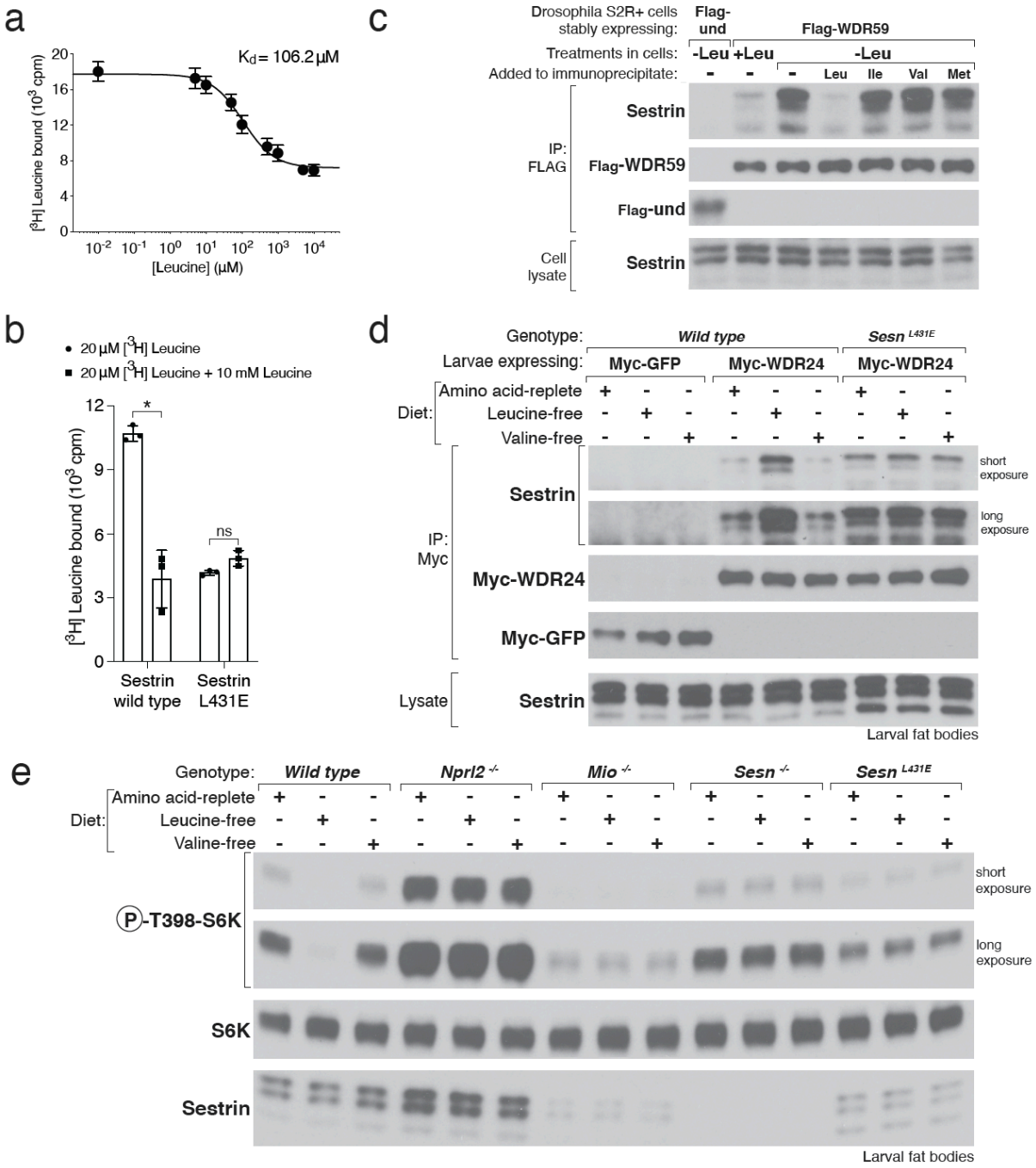

Fig. 1: *Drosophila* Sestrin binds GATOR2 and regulates mTORC1 *in vivo* in response to dietary leucine.
a, In an equilibrium binding assay purified FLAG-Drosophila Sestrin binds leucine with a Kd of ~100 μM. Values are mean ± SD of three technical replicates from a representative experiment.
b, Wild-type Sestrin, but not the L431E mutant, binds leucine. HA-tagged Sestrin proteins were prepared from HEK293T cells expressing the appropriate cDNAs and binding assays performed as in (a).
c, Leucine starvation of *Drosophila* S2R+ cells enhances the interaction of Sestrin with GATOR2. FLAG-immunoprecipitates (IPs) were prepared from S2R+ cell lines stably expressing FLAG-tagged und (negative control) or WDR59 (a GATOR2 component) and starved or not of leucine. IPs and lysates were analyzed by immunoblotting for indicated proteins. Addition to the IPs of 1 mM of leucine, but not other amino acids, disrupted the Sestrin-GATOR2 interaction.
d, Dietary leucine regulates *in vivo* the interaction of Sestrin with GATOR2 in a fashion that depends on the leucine binding site of Sestrin. Immunoprecipitates were prepared from lysates of fat bodies from *Wild-type (OreR)* or $Sesn^{L431E}$ larvae expressing the control protein Myc-GFP or the GATOR2 component Myc-WDR24 in the fat body (*lpp-gal4*). Animals were fed the indicated diets for 4.5 hours prior to sample collection. Amino acid-replete: chemically-defined diet containing all amino acids; leucine- or valine-free: the chemically-defined diet lacking leucine or valine, respectively.
e, *In vivo* Sestrin must be able to bind leucine for dietary leucine to regulate mTORC1 signaling. Immunoblot analyses of Sestrin and phospho-S6K in fat bodies prepared as in (d) from larvae with indicated genotypes. *Nprl2* and *Mio* encode core components of the GATOR1 and GATOR2 complexes, respectively. Dietary composition and feeding period were as in (d).

To extend our work *in vivo*, we generated flies that ectopically express myc-tagged WDR24, another core component of GATOR2 (*lpp>myc-WDR24* flies), in the fat body, and are either wild type at the *Sesn* locus or have a knockin of the L431E mutation that renders Sestrin unable to bind leucine ($Sesn^{L431E}$). For a period of 4.5 hours, we fed third instar larvae a chemically defined diet containing all proteogenic amino acids (amino acid-replete) or the same diet lacking just leucine (leucine-free) or valine (valine-free). Independent of the genotypes, larvae eating the leucine- or valine-fee diets had significant decreases in leucine or valine levels, respectively (Extended Data Fig. 1a, b). In lysates prepared from isolated fat bodies, endogenous Sestrin co-immunoprecipitated with GATOR2, but not a control protein (myc-GFP), and leucine, but not valine, deprivation strongly boosted the interaction. In contrast, Sestrin L431E bound equally well to GATOR2 under all dietary conditions, consistent with the mutant being leucine-insensitive (Fig. 1d). In cultured cells and in fat bodies, we observed that Sestrin has multiple isoforms (Fig. 1c, d), likely the result of differential splicing (Lee et al., 2010).

In wild-type larvae, feeding of the diet free in leucine, but not valine, inhibited mTORC1 in the fat body, as assessed by the phosphorylation of S6K, a canonical mTORC1 substrate. The loss of Sestrin

(*Sesn*$^{-/-}$) did not impact mTORC1 activity in larvae eating the amino acid-replete diet, but completely prevented the inhibition of mTORC1 normally caused by leucine deprivation (Fig. 1e). Sestrin was also required for the leucine-free diet to activate autophagy, a process suppressed by mTORC1, as monitored by the formation of mCherry-Atg8a-positive puncta (Extended Data Fig. 2a). In *Sesn*^{L431E} larvae, mTORC1 activity was low relative to that in wild-type larvae and also unaffected by leucine deprivation, indicating that the leucine-binding mutant of Sestrin acts as a non-repressible inhibitor of mTORC1 (Fig. 1e).

Extended Data Figure 1

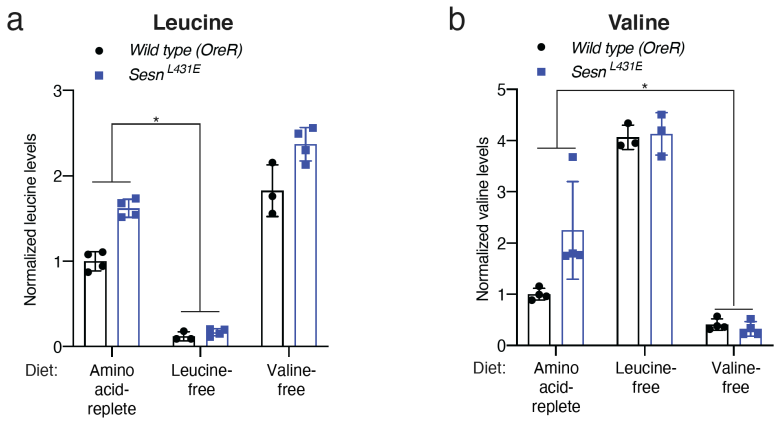

Extended Data Fig. 1: *Drosophila* larvae eating chemically-defined diets lacking individual amino acids have reduced levels of the missing amino acid.
Relative levels of leucine (a) and valine (b) measured by LC-MS/MS in whole larval extracts of *Wild-type (OreR)* or *Sesn*^{L431E} larvae fed the indicated diet for 4.5 hours.

Extended Data Figure 2

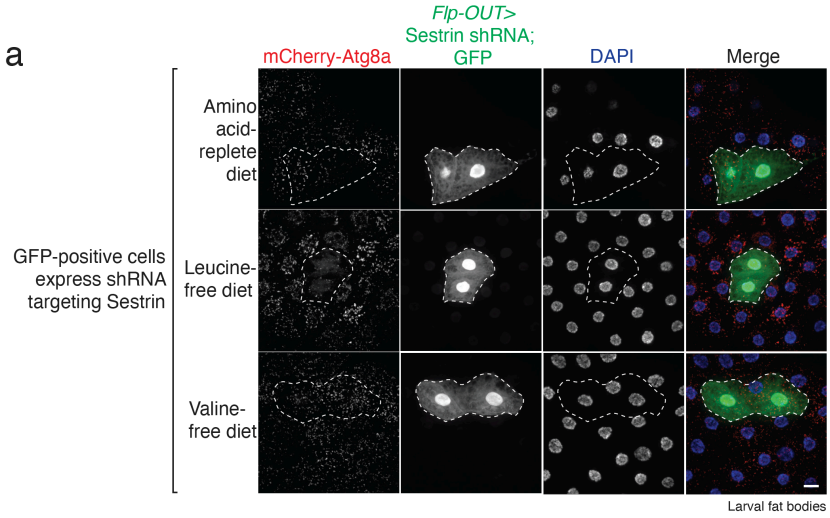

Extended Data Fig. 2: *Sesn* knockdown prevents autophagy induction upon leucine deprivation.
a, Fat body cells in mid-third instar larvae expressing mCherry-Atg8a were fed the indicated diets for 4.5 hours. The *Sesn* shRNA was expressed with a FLP-out system(McGuire et al., 2003) in the outline GFP-positive cells. Scale bar represents 10 µm.

Importantly, when deprived of all food, the *Sesn*$^{-/-}$ larvae inhibited mTORC1 signaling to the same extent as wild-type larvae (Extended Data Fig. 3a), consistent with work in cultured mammalian cells showing that Sestrin has a specific role in transmitting leucine availability to mTORC1 (Kim et al., 2015; Wolfson et al., 2016). Lastly, in larvae lacking a component of GATOR1 (*Nprl2*$^{-/-}$) or GATOR2 (*Mio*$^{-/-}$), the absence of dietary leucine did not impact mTORC1 activity and it remained as hyperactive or suppressed, respectively, as when the larvae were fed the amino acid-replete diet (Fig. 1e). Consistent with mTORC1 promoting *Sesn* transcription as part of a feedback loop (Lee et al., 2010; Park et al., 2017), *Nprl2*$^{-/-}$ and *Mio*$^{-/-}$ flies had increased and decreased Sestrin levels, respectively (Fig. 1e). Collectively, these results show that dietary leucine modulates mTORC1 *in vivo* and that this regulation requires Sestrin and its leucine-binding pocket as well as the GATOR1 and GATOR2 complexes.

Extended Data Figure 3

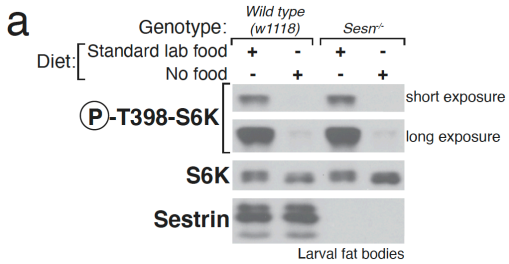

Extended Data Fig. 3: Loss of Sestrin does not affect the inhibition of mTORC1 caused by the deprivation of all food.
a, Immunoblot analyses of phospho-S6K and S6K in adult female flies in the fed state or starved of all food for 1 day.

Sestrin is required for *Drosophila* to adapt to a low leucine diet

We hypothesized that Sestrin-mediated suppression of mTORC1 helps animals adapt to and thus survive a diet low in leucine. We first tried to test this idea by feeding larvae food lacking leucine, but all larvae, independent of genotype, died within 2-3 days of starting the diet, consistent with leucine being

an essential amino acid required for larval growth. When given food containing one tenth of the normal leucine content, ~40% of wild-type larvae survived over a period of 16 days (Fig. 2a). In contrast, only ~10% of *Sesn*$^{-/-}$ larvae did so (Fig. 2a). Moreover, the surviving larvae grew to a much smaller size than their wild-type counterparts (Fig. 2b), a defect rescued by the expression of wild-type Sestrin from the ubiquitous *Tubulin*-Gal4, *Tubulin*-Gal80ts promoter (Fig. 2b). When fed the standard lab diet, *Sesn*$^{-/-}$ and wild-type larvae developed indistinguishably (Extended Data Fig. 4a).

Figure 2

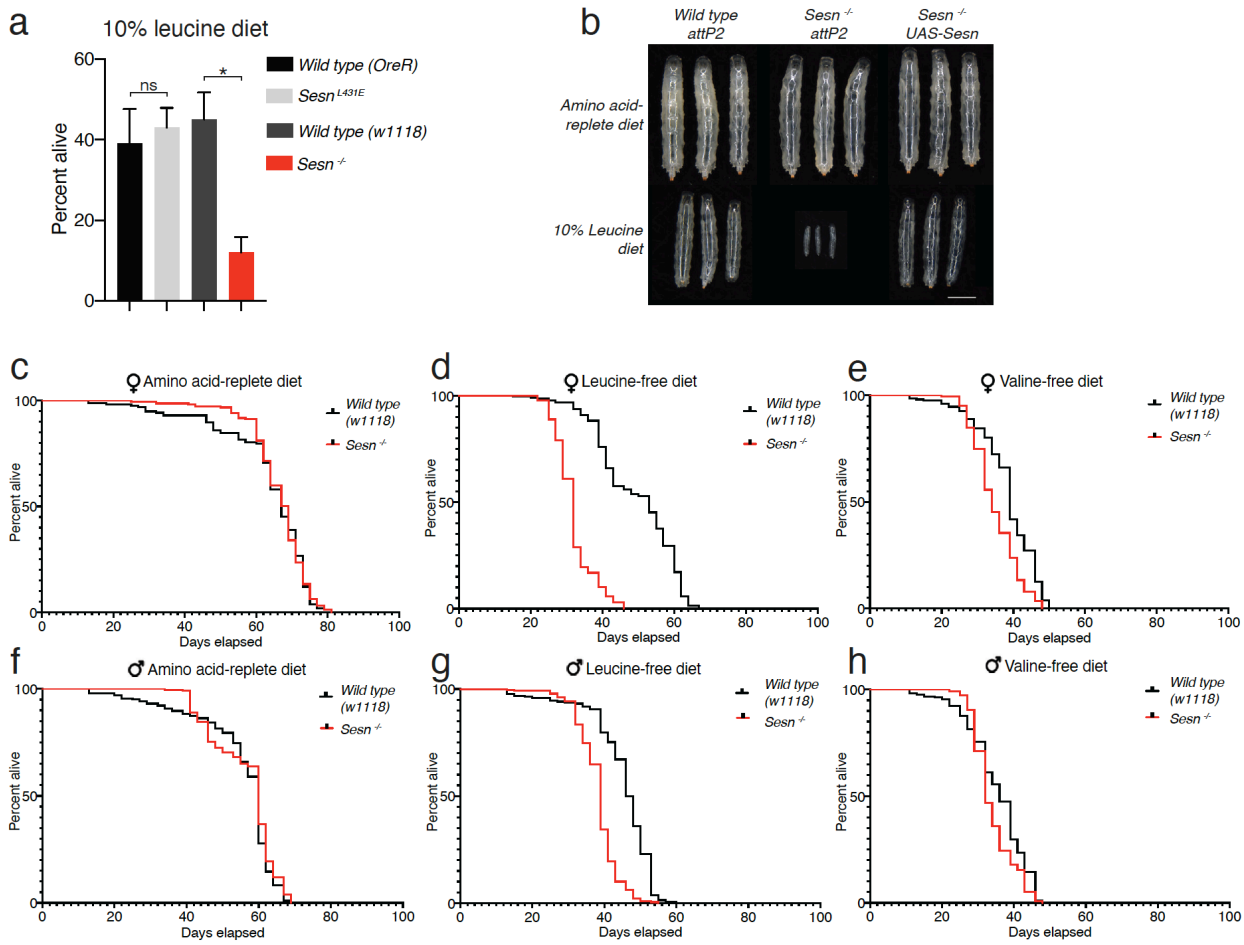

Fig. 2: *Drosophila* require Sestrin to adapt to a low leucine diet.
a, Loss of Sestrin increases mortality during development on a low leucine diet. Percent of larvae surviving following 16 days of development on a chemically-defined diet containing 10% of the leucine in the control diet.

b, On the low leucine diet, the loss of Sestrin impairs larval growth. Age synchronized animals of the indicated genotypes were raised on a reduced (10%) leucine diet. Images were taken on Day 9 of the dietary treatment. Scale bar represents 1 mm.
c-h, Adult *Drosophila* lacking Sestrin (*Sesn*$^{-/-}$) have a shorter lifespan when fed a diet lacking leucine. Age-synchronized adult male or female animals of the indicated genotypes were fed the indicated chemically-defined diets and the number of live flies was measured every 2 or 3 days to generate the curves shown.

Extended Data Figure 4

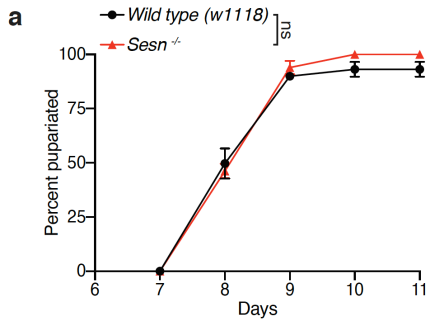

Extended Data Fig. 4: Loss of Sestrin does not the affect development of larva feeding on a complete diet.
a, Time to pupariation for *w*^{1118} *and Sesn* $^{-/-}$ larvae fed the standard yeast-based diet.

Consistent with previous work showing that adult flies can live for weeks on a diet lacking any amino acid source (Wei et al., 2016), wild-type flies also survived for many weeks on a leucine-free diet (Fig. 2c, d, f, g). As with larvae, adult flies also required Sestrin to adapt to leucine scarcity, as *Sesn*$^{-/-}$ male and female animals had greatly shortened lifespans on the leucine-free, but not amino acid-replete, diet (Fig. 2c, d, f, g). On the other hand, *Sesn*$^{-/-}$ flies only had slightly shorter lifespans than wild-type counterparts when eating the valine-free food (Fig. 2e, h), a diet on which the activity of processes controlled by mTORC1, like protein synthesis and autophagy, would be expected to impact survival. When the *Sesn*^{L431E} flies were fed the same chemically defined diets, they survived similarly to the wild type flies (Extended Data Fig. 5a-f). Consistent with the chronic suppression of mTORC1 signaling, *Sesn*^{L431E} larvae reared on the standard lab diet developed more slowly than wild-type ones (Extended Data Fig. 5k).

Extended Data Figure 5

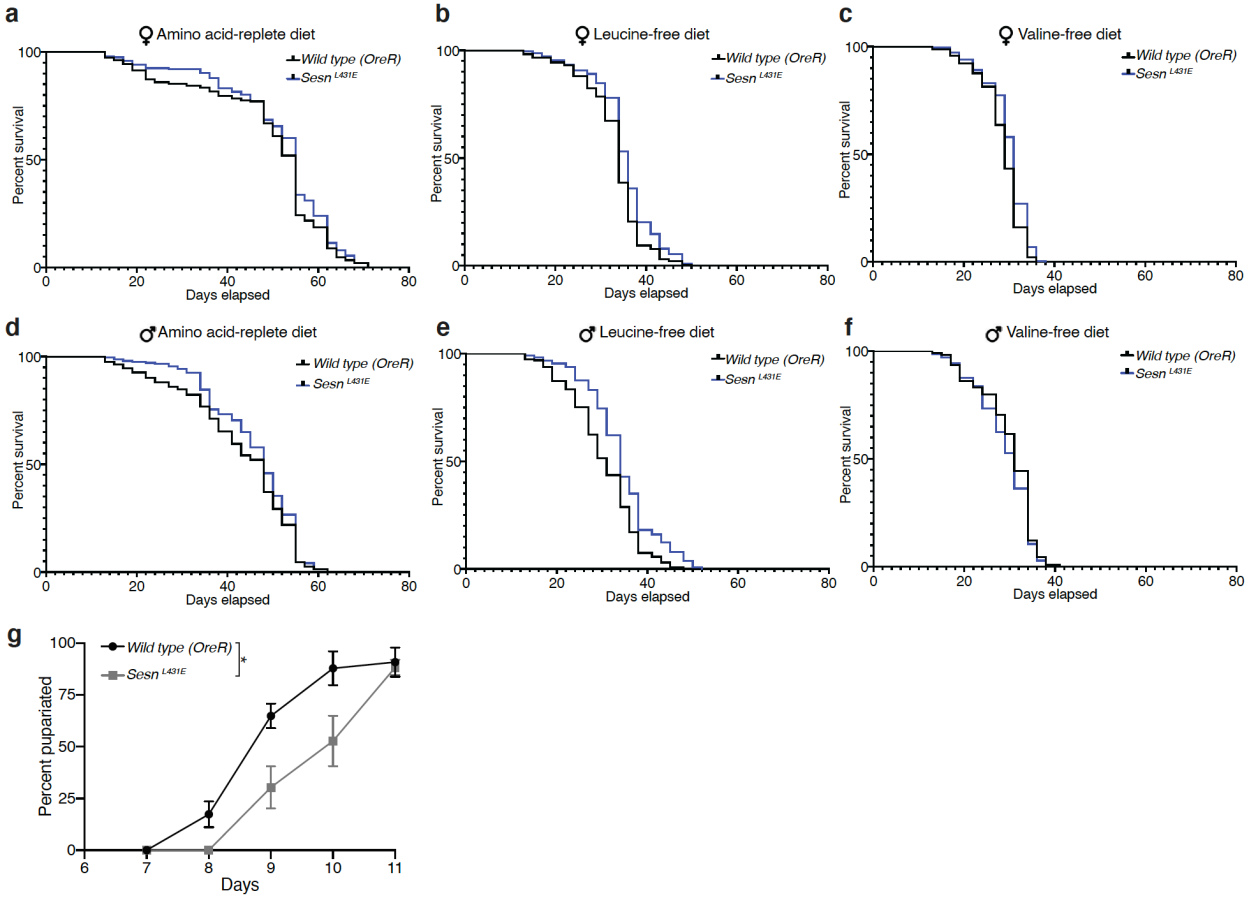

Extended Data Fig. 5: The *Sesn*^{L431E} mutation does not affect adult fly lifespan on the chemically defined diets but does mildly delay larvae development.
a-f, Age-synchronized male or female adult animals of the indicated genotypes were fed the indicated chemically-defined diets and the number of live flies was measured every 2 or 3 days to generate the curves shown.
g. *Sesn*^{L431E} larvae have a delay in developing into pupae on a standard yeast-based diet.

We monitored mTORC1 activity in whole-fly lysates of female and male adult flies that had been fasted overnight and then refed for 90 minutes with the chemically-defined diets used above. The loss of Sestrin prevented the inhibition of mTORC1 caused by the leucine-free diet and this was equally true in male and female flies. Intriguingly, in females, more than in males, the loss of Sestrin boosted mTORC1 activity under all dietary conditions, indicating that beyond controlling the response to leucine starvation, Sestrin also contributes to setting the "tone" of mTORC1 signaling in female flies (Extended Data Fig. 6a, b).

Given that the increase in mTORC1 activity in female *Sesn*$^{-/-}$ flies was detectable in whole-fly lysates, we focused on the ovaries as they account for a significant portion of the mass of female flies. Moreover, diet is known to regulate ovarian function through the GATOR1-GATOR2 complexes (Senger et al., 2011; Wei and Lilly, 2014; Wei et al., 2016; Wei et al., 2014), and *Mio*, the gene for one of the components of GATOR2, was so named because mutations in it result in a missing oocyte phenotype(Iida and Lilly, 2004). We found that mTORC1 activity was strongly increased in the ovaries of *Sesn*$^{-/-}$ flies eating the standard lab diet, and, as in larval fat bodies (Fig. 1e), suppressed in the ovaries of *Sesn*^{L431E} flies (Extended Data Fig. 6c).

When fed the amino acid-replete or valine-free diet, *Sesn*$^{-/-}$ and wild-type flies had ovaries of similar sizes, but the loss of Sestrin greatly accentuated the decrease in ovarian size caused by leucine deprivation (Extended Data Fig. 6d, e), again pointing to a specific role for Sestrin in adapting to leucine scarcity. Consistent with a role for mTOR in controlling the viability of vitellogenic egg chambers during nutritional stress (Pritchett and McCall, 2012; Wei et al., 2016), in the absence of dietary leucine the *Sesn*$^{-/-}$ females had increased egg chamber degeneration compared to wild-type animals, as indicated by the apoptosis marker cleaved Caspase 3 (Extended Data Fig. 6f, g). Additionally, mTOR also controls gonad development, perhaps explaining why the ovaries of the *Sesn*^{L431E} flies were equally small on all the diets (Extended Data Fig. 6d, e) and had similarly high level of degeneration (Extended Data Fig. 6g), consistent with their constitutive low mTORC1 activity (Extended Data Fig. 6c). *Sesn*^{L431E} flies also had reduced fecundity as they laid fewer eggs than wild-type flies (Extended Data Fig. 6h). Eggs from wild-type, *Sesn*^{L431E}, and *Sesn*$^{-/-}$ flies had comparable hatching rates, suggesting that Sestrin does not impact fertility (Extended Data Fig. 6i). Collectively, these data reveal that in larvae and adult flies Sestrin promotes survival on a low leucine diet and has a particularly important role in controlling ovarian size and function.

Extended Data Figure 6

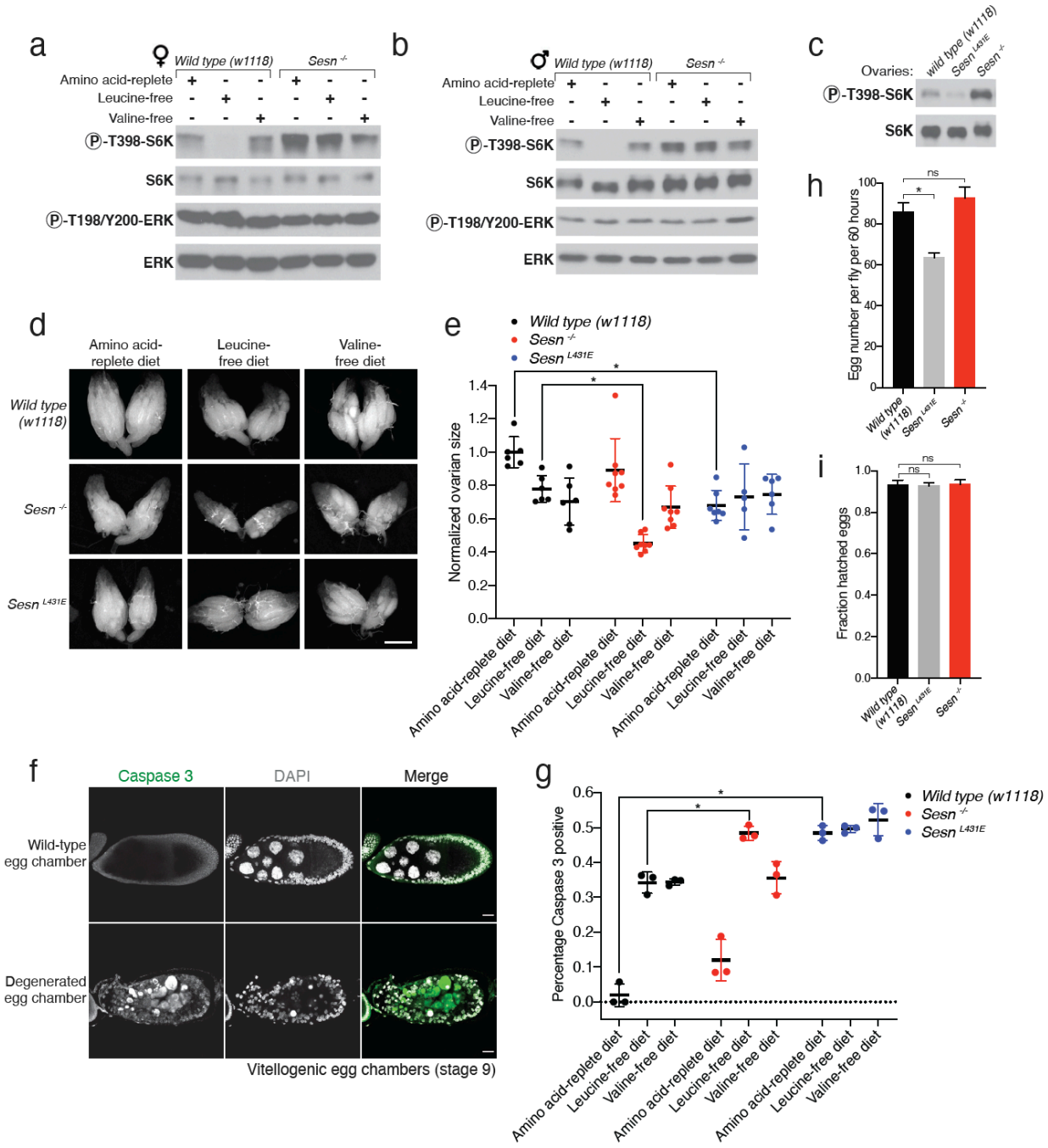

Extended Data Fig. 6: Sestrin-mediated mTORC1 signaling in ovaries.

a, b, Sestrin mediates leucine-sensing by mTORC1 in adult animals. Immunoblot analyses of whole adult animals of the indicated sex and genotype following overnight starvation and 1.5 hours of refeeding with the indicated diets.

c, In flies feeding a standard diet and lacking Sestrin or expressing the leucine-binding deficient Sestrin mutant (L431E), mTORC1 activity is increased or decreased, respectively. Lysates were prepared from isolated ovaries from animals of the indicated genotypes and fed the standard yeast-based diet.

d, e, Loss of Sestrin accelerates the reduction in ovary size caused by leucine starvation. (d) Ovarian size in females of the indicated genotypes fed the indicated diets for 24 hours. Results are quantified in (e). Scale bar represents 500 μm.
f, g, Loss of Sestrin enhances the egg chamber degeneration caused by leucine starvation. (f) Representative images of normal egg chambers and degenerated egg chambers stained for cleaved caspase 3 and with DAPI. The percentage of caspase 3 positive egg chambers in flies fed the indicated diets for 24 hours is quantified in (g). Scale bar represents 20 μm.
h, i, *Sesn*^{L431E} flies have reduced fecundity but not fertility. (h) Number of eggs laid over a period of 60 hours by females of the indicated genotypes maintained on the standard yeast-based diet. (i) Hatching rate of eggs laid in the same conditions as in (h).

Flies prefer to eat leucine-containing food in a fashion that depends on the capacity of Sestrin to bind leucine

Having established that Sestrin is important for flies to adapt to and survive on diets low in leucine, we asked if flies also require Sestrin to detect and thus avoid food that is poor in leucine. To do so we developed an assay to test if adult flies prefer eating leucine-rich over leucine-poor food. The experimental setup consisted of 15 female and 5 male flies in a bottle containing two apple pieces, the first painted with a solution of one or more amino acids and the second with an appropriate control (Fig. 3a). Each also contained a trace amount of a unique DNA oligonucleotide, which served as a barcode for measuring the consumption of each type of food, an approach previously described (Park et al., 2018) and which we validated (Extended Data Fig. 7a, b, c and Methods). We chose apple as the base food because it is carbohydrate-rich and protein-poor (Kumar et al., 2018), allowing us to set up food choices that have different amino acid compositions but the same content of sugars. Apples are reported to contain very little leucine (Feng et al., 2014).

We found that wild-type female flies prefer to eat apple coated with leucine rather than water. This preference emerges after the flies have been eating the food for ~6 hours and increases to 5 to 6-fold by 24 hours, the time point we used in subsequent experiments (Fig. 3b). The preference for leucine is concentration-dependent (Extended Data Fig. 7d) and not every amino acid elicits a preference, as flies do not distinguish between apples coated with valine or water (Extended Data Fig. 7e). And given a choice between equal amount of leucine and valine, flies still prefer leucine, suggesting that the leucine

preference is not simply the result of a nitrogen imbalance (Extended Data Fig. 7e). Moreover, the leucine preference requires differential mTORC1 activity, as when flies were fed the mTORC1 inhibitor rapamycin, they no longer showed a preference (Fig. 3c). Rapamycin treatment also lowered the total amount of food consumed by the flies (Extended Data Fig. 7f), consistent with previous reports (Anisimov et al., 2011; Hebert et al., 2014).

Figure 3

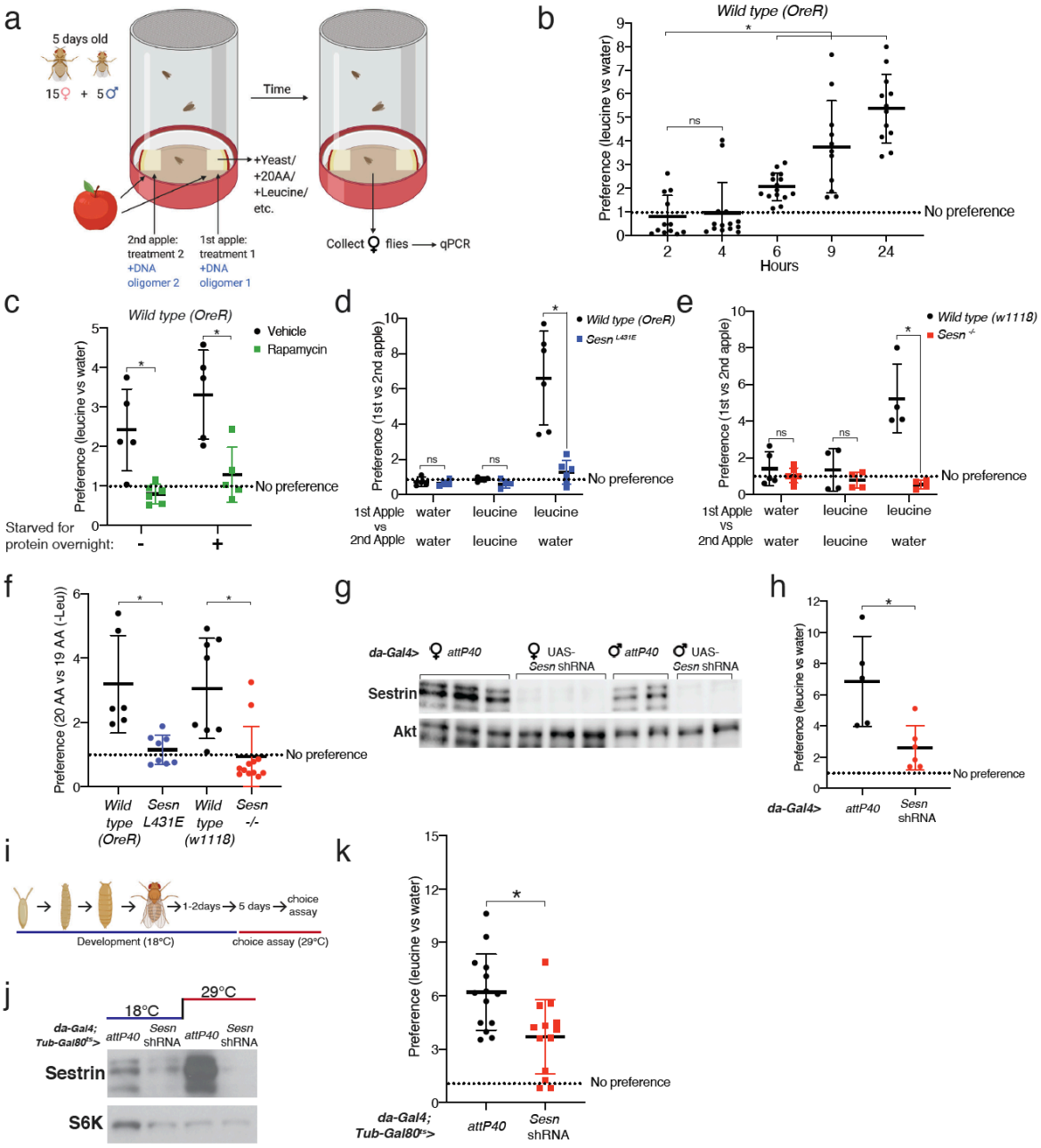

Fig. 3: Flies prefer to eat leucine-containing food in a fashion that depends on the capacity of Sestrin to bind leucine.
a, Schematic of the two-choice food preference assay. Two identical apple pieces were painted with solutions containing different substances and unique DNA oligonucleotides and placed on opposite sides of a container. Animals were allowed to feed *ad libitum* over the course of the assay. The amounts of each oligonucleotide in groups of 5 female flies was quantified by qPCR as a proxy for the amount of food eaten from each apple piece.
b, It takes several hours for wild-type female flies to develop a preference for eating an apple coated with leucine instead of water. At each time point, the amounts of each oligonucleotide were quantified and the fold-difference in intake of each food was calculated and plotted. Age-synchronized adult flies were starved of protein for one day before the assay.
c, Rapamycin impairs flies from developing a preference for the leucine-containing apple. Age-synchronized adult flies were protein-starved or fed standard lab food for one day with or without rapamycin prior to the start of the food preference assay. Rapamycin or vehicle was also added to the apple pieces.
d-f, $Sesn^{L431E}$ and $Sesn^{-/-}$ animals fail to develop a preference for the leucine-containing apple. Female flies of the indicated genotypes were starved overnight prior to use in food preference assays with apples painted with solutions containing the indicated substances.
g, Sestrin levels decrease in females and males following ubiquitous expression of an shRNA targeting its mRNA. Extracts of adult flies were analyzed by immunoblotting for Sestrin or Akt, which serves as a loading control.
h, Ubiquitous knockdown of *Sesn* reduces the preference of adult female flies for leucine-containing apple. The food preference assay was as in (b).
i, Approach used to achieve temporal control of *Sesn* knockdown in (j) and (k).
j, $Gal80^{ts}$-mediated decrease in Sestrin levels in adult, but not developing, female flies. Extracts were prepared from flies at indicated temperatures and analyzed by immunoblotting for Sestrin and S6K, which serves as a loading control. Interestingly, heat shock induces Sestrin protein in flies expressing the *attP40* control shRNA.
k, Knockdown of Sestrin specifically during adulthood is sufficient to decrease the preference of female flies for leucine-containing apples. The food preference assay was as in (b).

Remarkably, neither $Sesn^{-/-}$ nor $Sesn^{L431E}$ females—both of which have leucine-insensitive mTORC1 signaling—had a preference for leucine as they ate similar amounts of leucine-rich and -poor foods (Fig. 3d, e, Extended Data Fig. 7g). The two *Sesn* mutants did differ in the total amount of food each ate. $Sesn^{-/-}$ females ate the same amount of food (leucine-rich or -poor) as wild-type (*w1118*) flies consumed of leucine-rich food (Extended Data Fig. 7h). The opposite was true for $Sesn^{L431E}$ females. These flies ate the same amount of food (leucine-rich or -poor) as wild-type (*OreR*) flies consumed of leucine-poor food (Extended Data Fig. 7i). That $Sesn^{L431E}$ files, which have low mTORC1 signaling, eat less food than wild-type controls is consistent with rapamycin causing a reduction in food consumption (Fig. 3c). We speculate that the two *Sesn* mutants have different innate hunger drives, presumably because

Sesn$^{-/-}$ flies cannot sense the absence of leucine in the water-coated apple and *Sesn*^{L431E} mutants cannot sense the presence of leucine in the leucine-coated apple. Whole body re-expression in the *Sesn*$^{-/-}$ females of Sestrin driven by *Tub*>Gal4 partially restored the leucine preference of the animals (Extended Data Fig. 7j).

Extended Data Figure 7

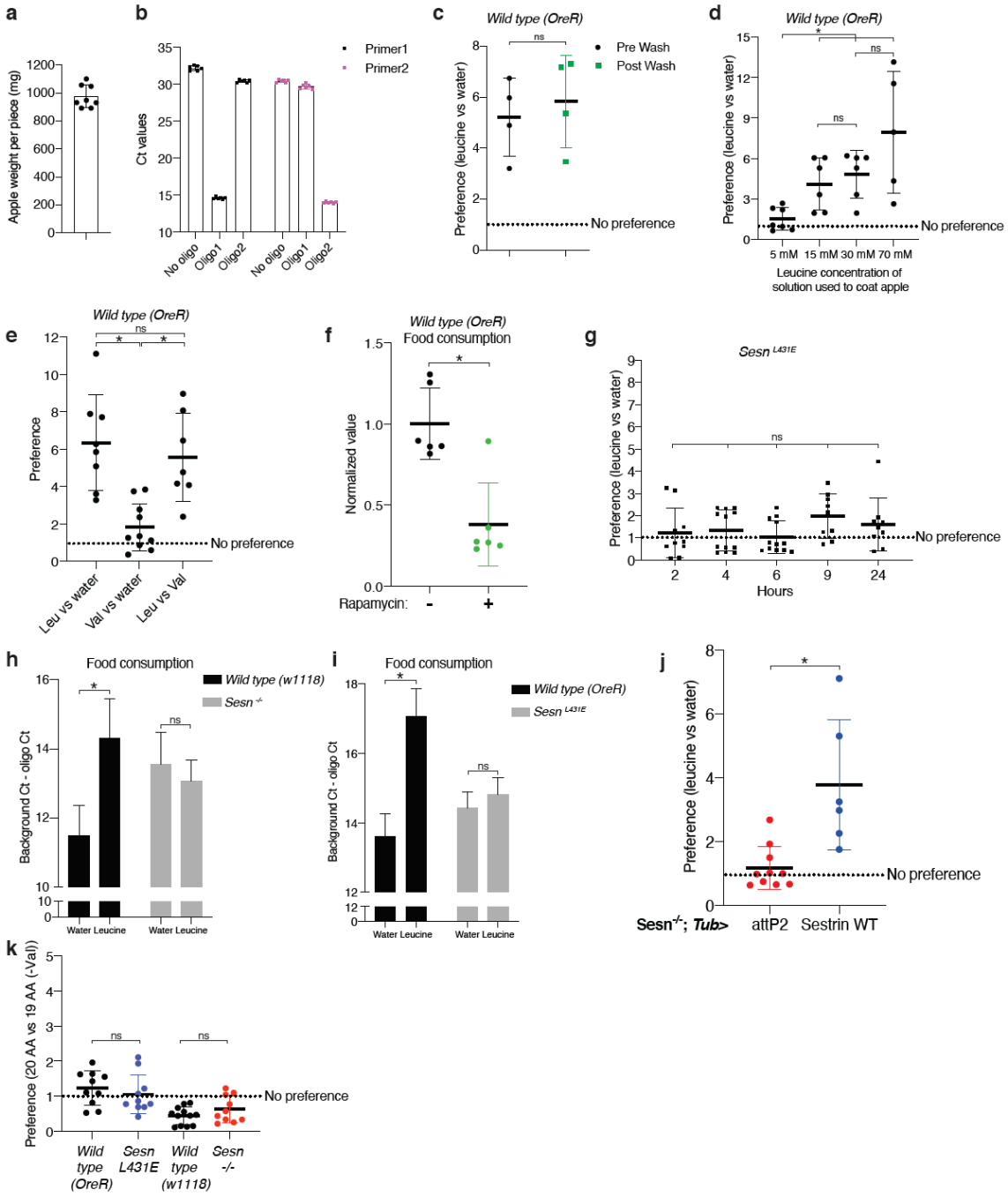

Extended Data Fig. 7: Sestrin mediates the preference for leucine-containing food and influences total food intake.
a-c, Characterization of the methods used in the food two-choice assay. (a) Measurement of the weight of the apple pieces used in the assay. (b) Background qPCR signal determination for each oligonucleotide barcode used in assay. (c) The qPCR signals used to determine the leucine preference of the wild-type flies come primarily from internal DNA oligonucleotides instead of external ones that might contaminate the outside of the body of female flies. qPCR for oligonucleotide barcodes in a leucine versus water choice assay before and after washing animals as described(Park et al., 2018).
d, Preference of the flies for apple pieces painted with the indicated leucine concentrations.
e, Adult female flies do not have a preference for valine- versus water-painted apple pieces.
f, Rapamycin treatment reduces fly food consumption.
g, *Sesn*^{L431E} animals fail to develop a preference for leucine- over water-painted apple.
h, *Sesn*^{L431E} animals have decreased food intake regardless of the leucine content of the food.
i, Sesn $^{-/-}$ animals have increased food intake regardless of the leucine content of the food.
j, Whole-body re-expression of wild-type Sestrin driven by *Tub*>Gal4 is sufficient to partially restore the preference for leucine-containing food of *Sesn* $^{-/-}$ adult female flies.
k, Adult female flies do not develop a preference for valine-containing apple regardless of their genotype.

We also asked if flies can distinguish between foods with a more subtle difference in amino acid composition: apple coated with the 20 proteogenic amino acids versus just 19 of them (i.e., lacking only leucine). Indeed, this was the case and this preference was also absent in the *Sesn*$^{-/-}$ and *Sesn*^{L431E} flies (Fig. 3f). Valine again served as a control: when removed from the 20-amino-acid cocktail, neither wild-type nor *Sesn* mutant flies showed any preference for the valine-containing food (Extended Data Fig. 7k).

To obtain temporal control of Sestrin suppression, we generated a conditional knockdown system utilizing a short hairpin RNA (shRNA) targeting *Sesn*. Ubiquitous expression of the shRNA reduced Sestrin protein levels (Fig. 3g), and, as expected, the preference of the flies for the leucine-containing food (Fig. 3h). Using a temperature sensitive shRNA driver, we suppressed Sestrin only once the flies had reached adulthood (Fig. 3i, j). This too reduced their leucine preference (Fig. 3k), indicating that the acute loss of Sestrin during adulthood is sufficient to impact the leucine preference. Interestingly, the temperature shift to 29°C increased Sestrin levels (Fig. 3j), consistent with previous work showing that multiple stresses induce its transcription (Pasha et al., 2017; Ye et al., 2015). Thus, female flies can

readily detect food lacking leucine even if it contains sugars and other amino acids. Moreover, this ability requires Sestrin and its capacity to bind leucine.

To further analyze the physiological relevance of leucine sensing via the Sestrin-mTORC1 axis, we tested the impact of both leucine and Sestrin on the choice between low and high protein diets: apple coated with a low or high amount of yeast extract, which is a complex food and the major protein source for flies in the lab. Wild type flies had a strong preference for the apple with a higher protein content, which was reduced in the *Sesn*^{L431E} and *Sesn*$^{-/-}$ mutants (Extended Data Fig. 8a, b). The addition of leucine to the protein-poor food reduced the preference of wild type female flies for the protein-rich food, but only minimally impacted those of the *Sesn*^{L431E} or *Sesn*$^{-/-}$ mutants. Altogether, these data suggest that flies use leucine sensing via the Sestrin-mTORC1 axis as a way to detect the food protein content.

Extended Data Figure 8

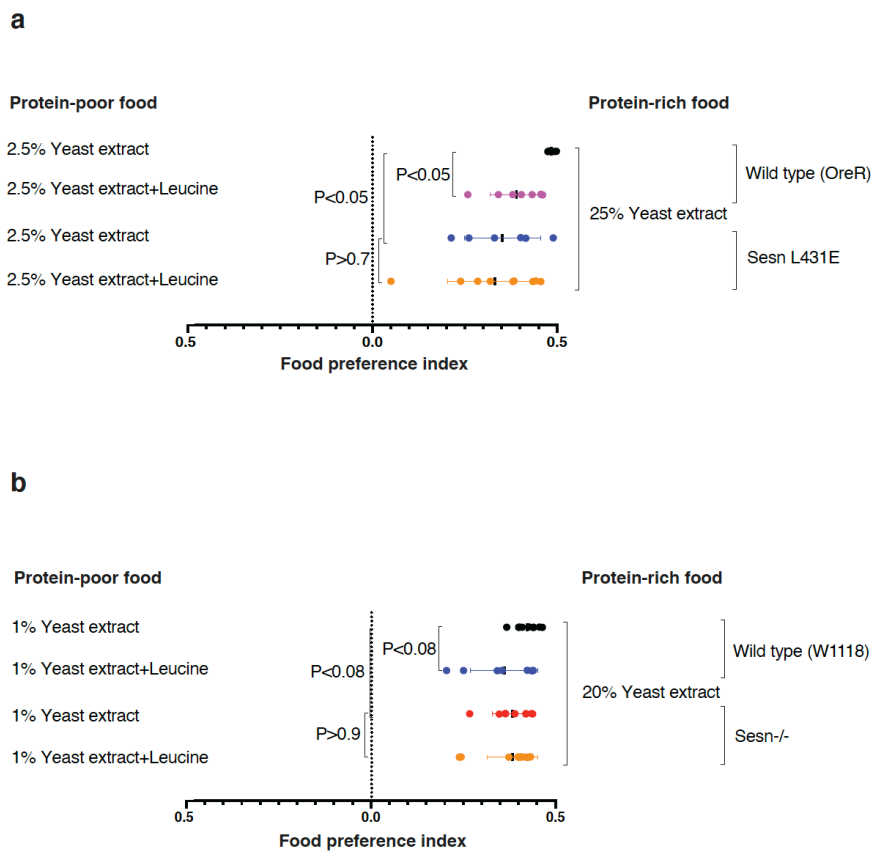

Extended Data Fig. 8: Leucine-sensing via the Sestrin-mTORC1 axis contributes to the detection of the protein content of food.
a, *Wild-type (OreR)* flies prefer food containing a high amount of yeast extract and this preference is reduced by the addition of leucine to food containing a low amount of yeast extract. *Sesn*^{L431E} flies have a reduced preference for the food containing a high amount of the yeast extract and the addition of leucine has minimal impact on the preference. How the food preference index was calculated is described in the methods.
b, As in (a) a choice experiment for *wild-type (W1118)* and *Sesn* $^{-/-}$ flies.

Female flies lay more eggs on leucine-rich than leucine-poor food in a fashion that depends on the leucine-binding capacity of Sestrin

During development of the food choice assay, we noted that female flies prefer to lay eggs on the leucine-coated apples. To explore this further, we put 15 female and 5 male flies in the assay bottle and 24-hours later counted the number of eggs on each piece of apple (Extended Data Fig. 9a). In an initial test, we found that flies laid many more eggs on an apple piece painted with a yeast suspension instead of water, consistent with yeast being a food rich in nutrients and the olfactory cues that attract flies (Baumberger, 1919; Becher et al., 2012; Becher et al., 2018; Steck et al., 2018) (Extended Data Fig. 9b).

Wild-type flies that had been deprived of protein overnight deposited 5 to 6-fold more eggs on an apple piece coated with the 20 proteogenic amino acids instead of water (Extended Data Fig. 9c, d, f). Flies had a similar, albeit smaller (3-fold), preference for leucine-coated apple, and this preference was more profound when the flies had been starved for protein. Importantly, flies did not distinguish between apple pieces painted with the same substance (Extended Data Fig. 9d, f).

Both *Sesn*$^{-/-}$ and *Sesn*^{L431E} mutant flies lacked any preference for laying eggs on the apple coated with leucine and had a severely reduced preference for the apple with the 20 amino acids (Extended Data Fig. 9e, g). Furthermore, the flies preferentially deposited eggs on an apple piece painted with the 20 proteogenic amino acids instead of 19 (i.e., lacking leucine) and this ability was also absent in the *Sesn*$^{-/-}$ and *Sesn*^{L431E} flies (Extended Data Fig. 9h). Thus, consistent with the leucine preference we

observed in the food choice assay, female flies also lay fewer eggs on food lacking leucine and this capacity requires Sestrin and its leucine-binding pocket. This finding might reflect an active site choice for egg deposition or the amount of time that flies spend on each apple due to their preference for eating leucine-containing food.

Extended Data Figure 9

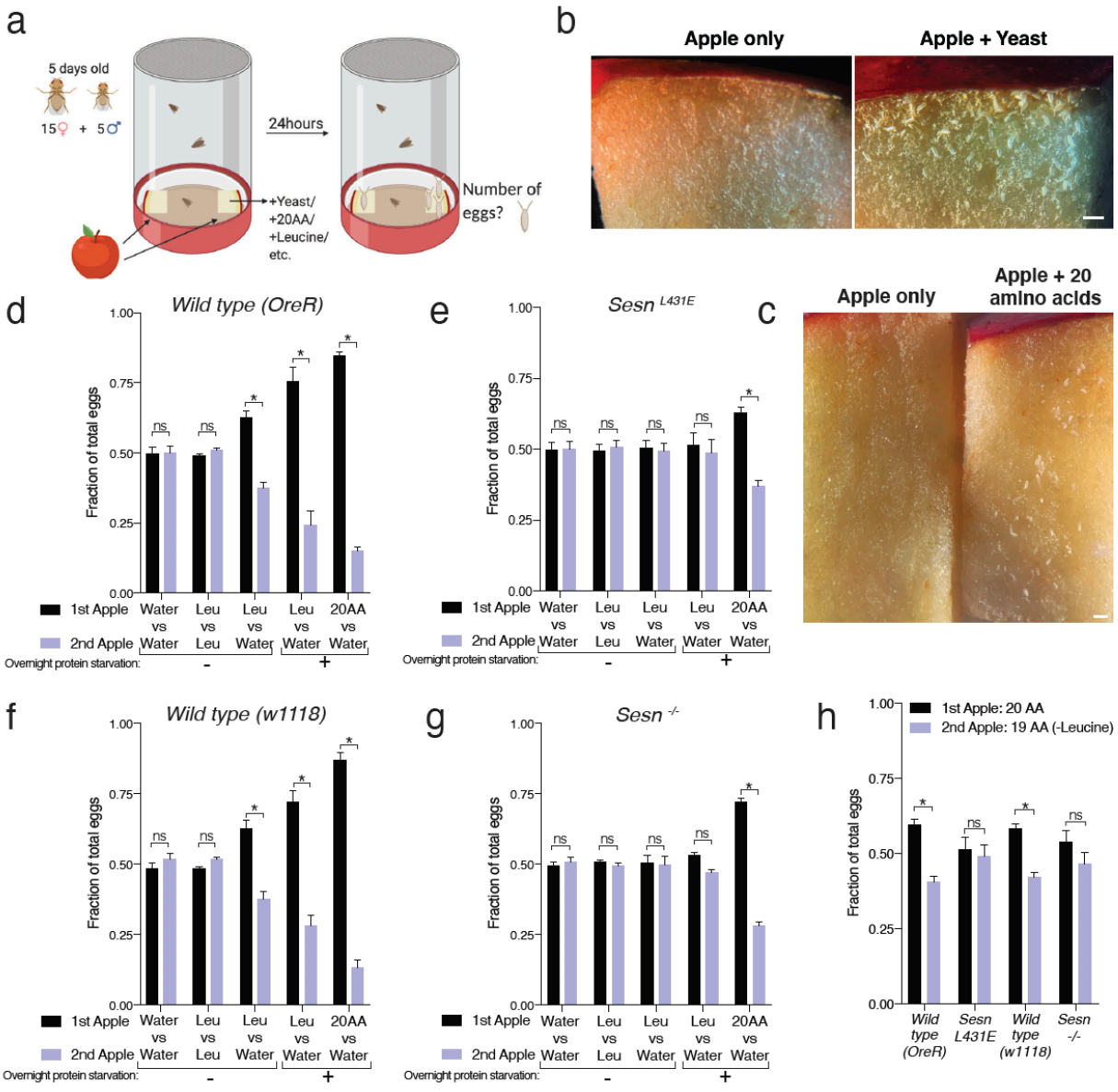

Extended Data Fig. 9: Flies prefer to lay eggs on leucine-containing food in a fashion that requires the leucine-binding capacity of Sestrin.

a, Schematic of the setup used in the egg-laying preference assay. Two identical apple pieces were painted with solutions containing different substances and placed on opposite sides of a container. Animals were allowed to feed *ad libitum* over the course of the assay and the number of eggs deposited on each apple was counted after 24 hours.
b, c, Wild-type flies prefer to lay eggs on yeast- or amino acid-painted apples over water-painted apples. Scale bars represent 1 mm.
d-h, $Sesn^{L431E}$ and $Sesn^{-/-}$ animals do not prefer to lay eggs on the leucine-containing apple.

Sestrin-regulated mTORC1 signaling in glial cells regulates the preference for leucine-containing food

To determine in which tissue(s) Sestrin is required for flies to distinguish between food with or without leucine, we suppressed Sestrin with the *Sesn* shRNA under the control of a variety of cell-type-specific Gal4 drivers. Interestingly, expression of the *Sesn* shRNA just in glial cells (*repo*-Gal4) was sufficient to reduce the preference of flies for the leucine-containing food to a similar extent as when it was expressed throughout the body (*da*-Gal4) (Fig. 4a). In contrast, its expression in many other tissues, including the fat body and muscle, did not impact the leucine preference. It is important to note that the intrinsic capacity of each Gal4 driver line to distinguish between food with or without leucine varied considerably (Extended Data Fig. 10a), likely due to their different genetic backgrounds. Thus, while we are confident that the preference of flies for leucine-containing food requires Sestrin in glial cells, we are cautious in ruling out contributions from other tissues, particularly those examined with driver lines with intrinsically lower leucine preferences, such as the pan (*elav*-Gal4) and dopaminergic and cholinergic (*ddc*-Gal4) neuronal lines (Extended Data Fig. 10a).

Consistent with an important role for glial Sestrin in regulating the leucine preference, expression of wild-type Sestrin just in glial cells in Sestrin null flies partially rescued the defect in detecting leucine-poor food (Extended Data Fig. 10b). In wild-type flies, expression in the glial cells of either wild-type or $Sestrin^{L431E}$ decreased the leucine preference, consistent with the inhibition of mTORC1 caused by Sestrin overexpression (Extended Data Fig. 10b). Indeed, overexpression under the control of *repo*-Gal4 of TSC1 and TSC2—well established inhibitors of mTORC1 signaling—was also sufficient to decrease the leucine preference (Extended Data Fig. 10c).

Figure 4

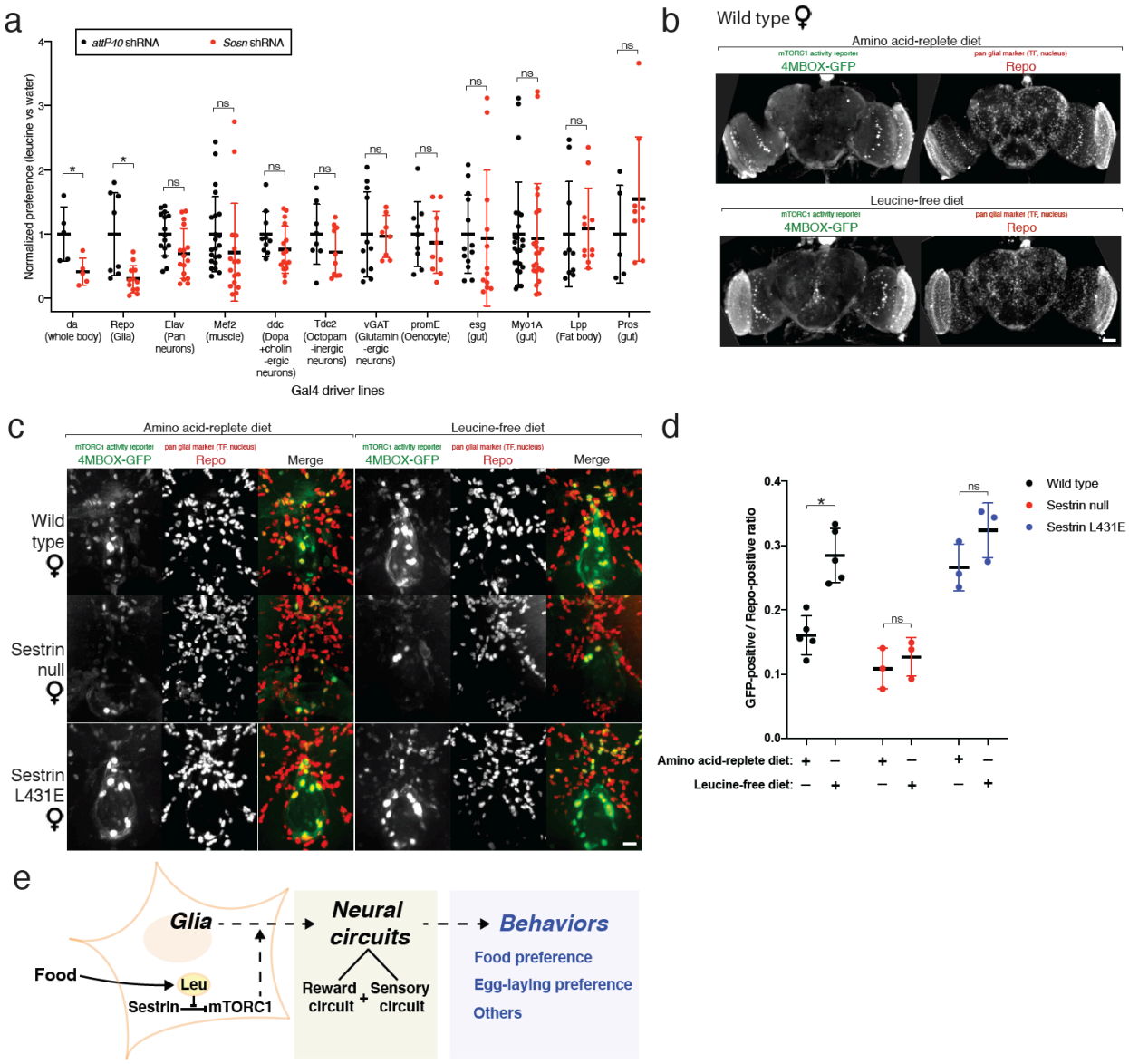

Fig. 4: Sestrin-regulated mTORC1 signaling in glial cells controls the preference of flies for leucine-containing food.

a, Expression of the *Sesn* shRNA in glial cells (*Repo*-Gal4) or across the whole-body (*da*-Gal4), but not using other tissue-specific Gal4 drivers, reduces the preference of flies for the leucine-containing apple. For each Gal4 driver line, data are normalized to the preference of the flies expressing the control shRNA.

b, c, Confocal projection of female brains of the indicated genotypes and containing the 4MBOX-GFP cassette, a reporter for the MITF/TFEB transcription factor that is negatively regulated by mTORC1. Animals were fed the indicated diets for one day and brains were immunostained for GFP and Repo. Images in (b) and (C) were taken with 10X and 40x objectives, respectively. Scale bars in (b) and (c) represent 50 µm and 10 µm, respectively.

d, In wild-type, but not *Sesn*^{L431E} or *Sesn*$^{-/-}$, flies leucine starvation increases the number of GFP-positive peri-esophageal glial cells. Each point represents the ratio of the number of GFP- to Repo-positive cells in the esophageal area of one fly brain. For the wild-type flies, n=5; for both Sestrin mutant flies, n=3. e, A model proposing how the sensing of dietary leucine via the Sestrin-mTORC1 pathway regulates the preference of flies for leucine-containing food.

Analyses of a single-cell RNAseq dataset indicated that Sestrin is expressed in most glial subtypes (Davie et al., 2018) (Extended Data Fig. 10d). Expression of the Sestrin shRNA under the control of Gal4 driver lines that target sub-types of glial cells revealed that none caused as strong a suppression of the leucine preference as with the pan glial driver *repo*-Gal4 (Extended Data Fig. 10e), although *Wrapper*-Gal4 driven Sestrin knockdown led to a partial reduction of the leucine preference. Thus, multiple glial subtypes likely participate in mediating the leucine preference.

Given the importance of glial Sestrin in mediating the leucine-preference, we examined mTORC1 signaling in glial cells in the brains of adult female flies. To do so we used a line expressing a GFP-based reporter for the MITF transcription factor (Zhang et al., 2015), which is the *Drosophila* ortholog of mammalian TFEB (Bouche et al., 2016). mTORC1 suppresses MITF (TFEB) so that upon mTORC1 inhibition MITF activity increases (Bouche et al., 2016) and drives GFP expression. In wild-type flies, starvation for just leucine promoted, as indicated by elevated GFP expression, MITF activity in Repo-positive glial cells, particularly in those surrounding the esophagus (Fig. 4b, c, d, Extended Data Fig. 11). In contrast, in *Sesn*$^{-/-}$ flies, leucine starvation did not increase the number of peri-esophageal GFP-positive glia cells, which were few in number irrespective of the diet (Fig. 4c, d). In *Sesn*^{L431E} flies, there were many peri-esophageal GFP-positive glia cells, and, like in *Sesn*$^{-/-}$ flies, leucine starvation did not increase their numbers (Fig. 4c, d). As expected, starvation for total protein also inhibited mTORC1 in the glial cells close to the esophagus (Extended Data Fig. 10f). Interestingly, quantification of GFP-positive cells in the mushroom body and optic lobe areas showed that, unlike peri-esophageal glial cells, the mTORC1 activity in these cells did not significantly respond to acute dietary treatments (Extended Data Fig. 11). Thus, dietary leucine regulates mTORC1 signaling in a subset of glial cells in a fashion that

depends on Sestrin and its capacity to bind leucine, and this regulation correlates with the ability of flies to distinguish between food that is rich or poor in leucine.

Extended Data Figure 10

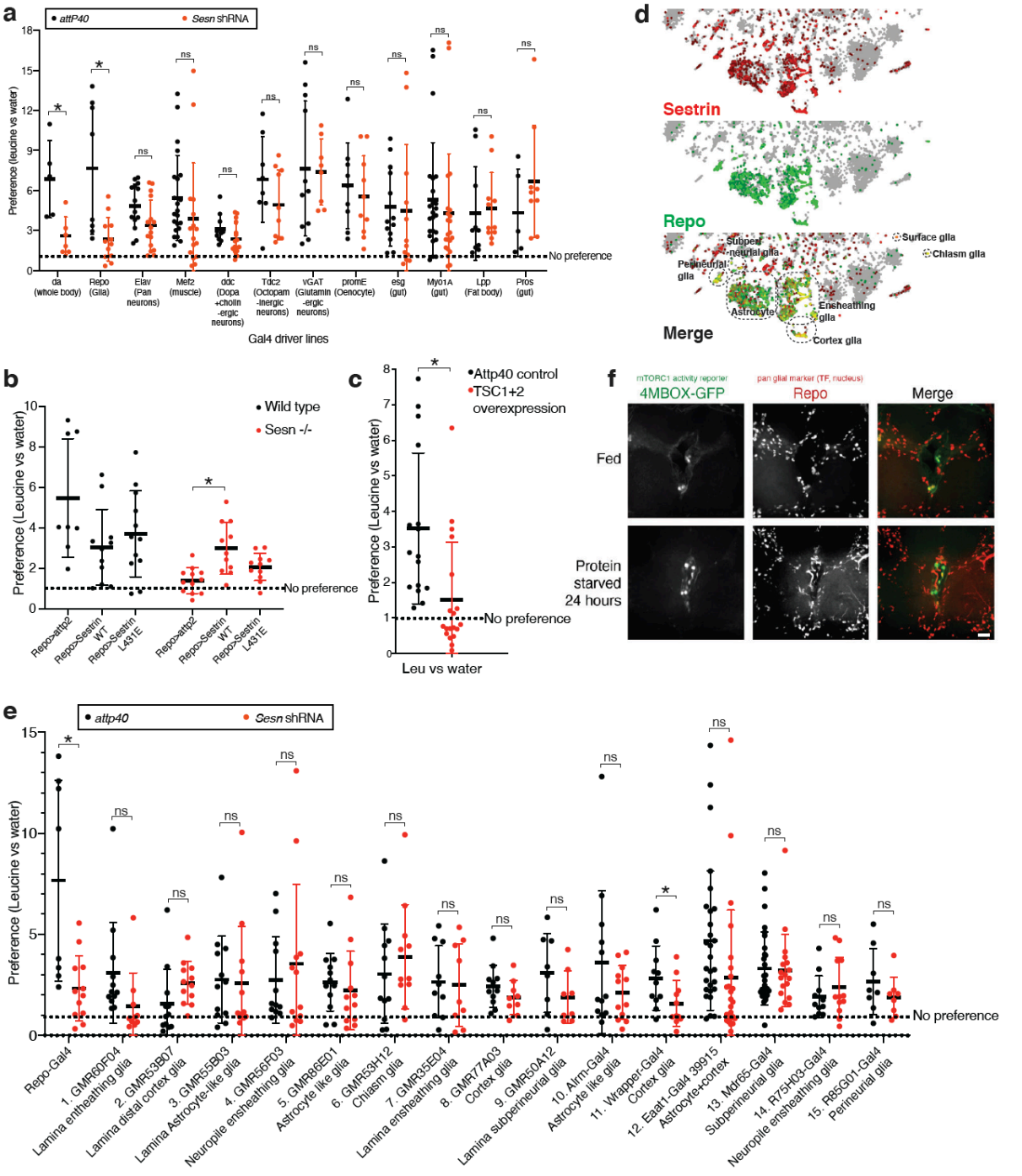

Extended Data Fig. 10: Sestrin-regulated mTORC1 signaling in glial cells controls the preference of flies for leucine-containing food.

a, Same data as in Figure 4a except that the values were not normalized to the values from the flies expressing the control shRNA from each of the indicated drivers.
b, Expression of wild-type Sestrin in *Sesn* $^{-/-}$ flies is sufficient to partially rescue the leucine preference phenotype.
c, Overexpression of TSC1+TSC2 in glial cells using *repo*-Gal4 reduces the preference of flies for leucine containing food.
d, The *Sesn* mRNA (red) is expressed in all classified subtypes of glial cells as indicated by co-expression of a pan glial marker, *Repo* (green). The single cell RNA sequencing dataset is from a previous study(Davie et al., 2018).
e, The knock-down of Sestrin using a pan glial cell driver (*repo*-Gal4) reduces the leucine preference of flies much more significantly than a knockdown using drivers for glial subtypes). The knockdown of Sestrin in cortex glial cells using the *wrapper*-Gal4 driver line significantly decreased the leucine preference of flies.
f, Confocal projection of wild-type female brains expressing 4MBOX-GFP fed the standard yeast-based food or starved of protein for 24 hours. Scale bar represents 10 µm.

Extended Data Figure 11

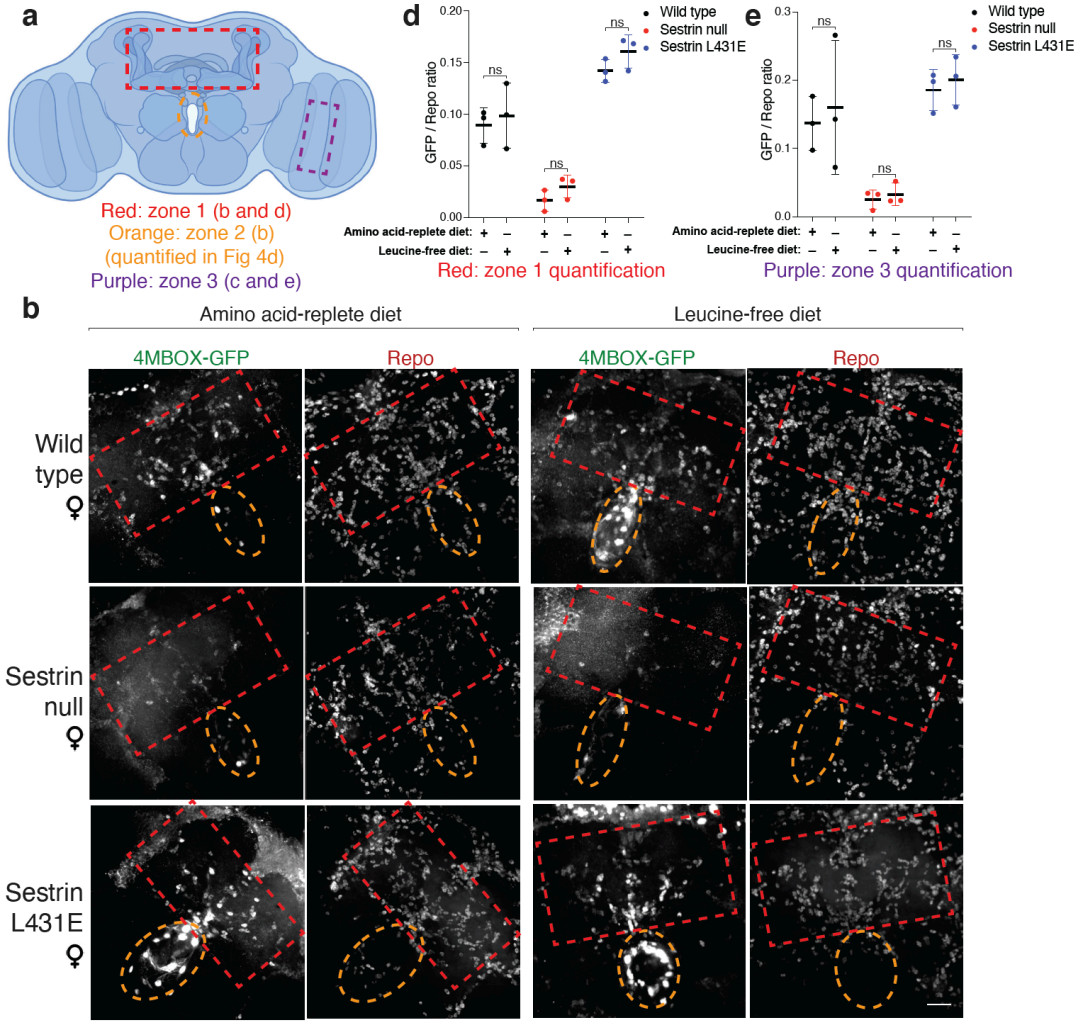

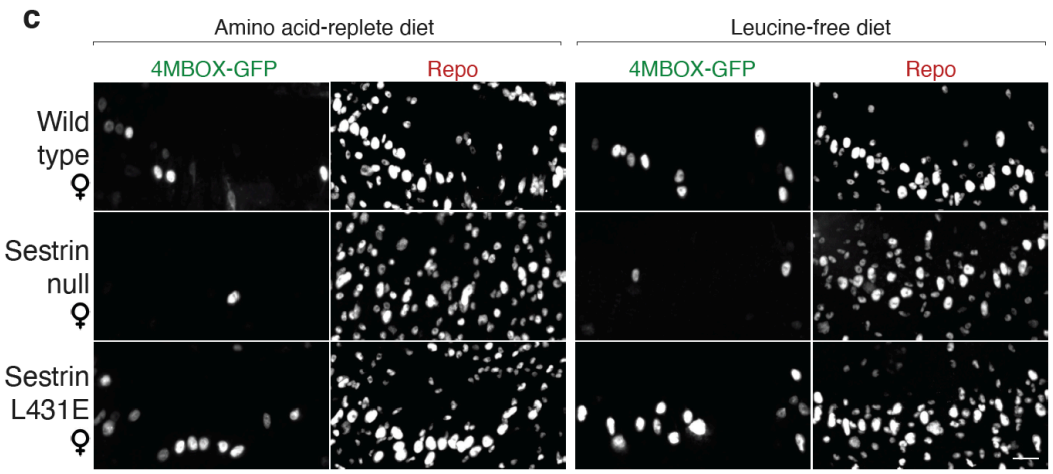

Extended Data Fig. 11: Dietary leucine regulates mTORC1 signaling in glial cells in the peri-esophageal area in a fashion that depends on Sestrin and its capacity to bind leucine.
a, Schematic of the areas imaged and quantified for the ratio of GFP-positive cells to Repo-positive cells. Red rectangle represents zone 1. Orange rectangle represents zone 2. Purple rectangle represents zone 3.
b, Confocal images of zone 1 and zone 2 brain areas from wild-type, *Sesn*$^{-/-}$, *and Sesn*^{L431E} female flies fed with an amino acid-replete or leucine-free diet. Scale bar represents 25 µm.
c, Confocal images of zone 3 brain areas of wild-type, *Sesn*$^{-/-}$, *and Sesn*^{L431E} female flies fed an amino acid-replete or leucine-free diet. Scale bar represents 10 µm.
d, Quantification of the GFP-positive to Repo-positive ratio in zone 1.
e, Quantification of the GFP-positive to Repo-positive ratio in zone 3.

Discussion

We show that *Drosophila melanogaster* requires Sestrin to regulate mTORC1 signaling in response to dietary leucine, survive a leucine-poor diet, and control leucine-sensitive physiology like food choice and ovarian size. Flies with a point mutation that eliminates the leucine-binding capacity of Sestrin (L431E) have suppressed, leucine-insensitive mTORC1 signaling. Moreover, while wild-type flies can live on leucine-free diets for weeks, flies lacking Sestrin die much faster, likely because of a reduced capacity to regulate these processes like autophagy and protein synthesis that are under the control of mTORC1. In all, our results establish Sestrin as a physiologically relevant leucine sensor *in vivo*.

We find that Sestrin and its leucine-binding pocket are required for the preference of adult female flies for consuming, as well as laying eggs on, leucine-rich instead of -poor food even when it

contains sugars and other amino acids. To our knowledge, the ability of flies to reject food that is low in leucine but still retains a complex set of other nutrients has not been previously documented, although such behavior has been reported in mice (Leib and Knight, 2015). When given a starker choice than we provided—a pure sugar, such as sucrose or glucose, versus an individual amino acid—flies prefer to eat a variety of essential amino acids in sex- and developmental stage-dependent fashions (Croset et al., 2016; Kudow et al., 2017; Yang et al., 2018).

There has been a long-standing interest in understanding the mechanisms that enable animals, including flies and rodents (Leib and Knight, 2015; Maurin et al., 2005), to reject diets low in protein. A variety of mechanisms in flies have been implicated, including amino acid transporters (Yang et al., 2018), taste receptors (Croset et al., 2016; Ganguly et al., 2017; Park and Carlson, 2018), GCN2 (Bjordal et al., 2014), serotonin (Vargas et al., 2010) and dopamine signaling (Bjordal et al., 2014; Liu et al., 2017), sex peptide receptor (Ribeiro and Dickson, 2010), microbiome (Henriques et al., 2020), as well as mTOR and S6K (Ribeiro and Dickson, 2010; Vargas et al., 2010). How these mechanisms coordinate together to impact organismal protein detection in the diets remains unclear. It will be interesting to invest further whether each of them conveys the availability of distinct components of protein (i.e., individual amino acids) and whether different cell types predominantly utilize certain mechanisms for the bulk protein detection.

Our work raises several questions for future study. Is there crosstalk between the food preference behavior controlled by glial cells and acute changes in ovarian size caused by nutritional stress? Do female flies actively choose to lay more eggs on the leucine-containing food because it has the nutrients needed for larval growth, or does the apparent preference simply reflect the amount of time they spend on it due to their dietary preference? It takes flies many hours to make this distinction (Fig. 3b), so it seems unlikely that the mutations in Sestrin eliminate the preference for leucine by significantly interfering with the capacity of flies to taste leucine. Rather, we favor the idea that leucine,

via Sestrin-mTORC1, turns on a neuronal reward circuit that drives food consumption (see potential model in Fig. 4e). Consistent with this possibility, *Sesn*$^{-/-}$ flies, in which mTORC1 is constitutively in a leucine-rich-like state, eat more food (irrespective of its leucine content) than *Sesn*^{L431E} mutants, in which mTORC1 is constitutively in a leucine-poor-like state (Extended Data Fig. 7h, i). Previous work has identified a set of dopaminergic neurons that controls protein hunger (Liu et al., 2017) and it will be interesting to ask if Sestrin-mediated leucine-sensitive mTORC1 signaling can impact these cells. In this regard, it is intriguing that the preference for leucine requires the expression of Sestrin in glia as there is increasing evidence that glial cells can be key intermediates between an environmental signal and its modulation of a neuronal circuit (Kottmeier et al., 2020; Ma et al., 2016; Otto et al., 2018). Lastly, it will be interesting to ask why mTORC1 activity in a set of peri-esophageal glial cells is particularly sensitive to Sestrin-dependent regulation by dietary leucine. Does the anatomical location of these glial give them preferred access to nutrients or do they represent a specialized subtype of glia? Answering the latter question will require identifying, if they exist, genetic markers to enable the specific isolation and manipulation of these cells.

Acknowledgements

We thank P. Rosen for critical reading of the manuscript and R. Chivukula and T. Wang for experimental suggestions. We thank all members of the Sabatini and Perrimon Labs for helpful insights and suggestions, as well as J. H. Lee, J. D. Levine, M. A. Lilly, F. Pignoni, A. A. Teleman, the Bloomington Drosophila Stock Center (BDSC), and the Developmental Studies Hybridoma Bank (DSHB) for providing fly stocks and reagents. We thank C. Lewis, B. Chan, and T. Kunchok for performing the LC/MS analysis and L. Parel for help on mutant genotyping. This work was supported by grants from the NIH to D.M.S. (R01 CA103866 and R37 AI47389), N.P. (5P01 CA120964-04 and R01 AR057352), and M.L.V. (F30 CA228229 and T32 GM007753), the Department of Defense (W81XWH-07-0448) to D.M.S., the

Cystinosis Research Foundation to P.J. and N.P., and a fellowship to X.G. from the Koch Institute for Integrative Cancer Research at MIT. N.P. is investigator of the Howard Hughes Medical Institute. D.M.S is an American Cancer Society Research Professor. The data and reagents that support the findings of this study are available from the corresponding authors and the Whitehead Institute (sabadmin@wi.mit.edu) upon reasonable request.

Author Contributions

X.G., P.J., D.M.S., and N.P. developed the research plan and interpreted experimental results. X.G. and P.J. designed and performed all experiments. R.B. helped with ordering and maintaining fly stocks. M.L.V. and P.V.L. helped with experimental design and data analysis. M.A.R., A.E.A. and J.W.L. provided the recipe for the chemically defined food and prepared the first batches of it. X.G. and D.M.S. wrote the manuscript and P.J. and N.P. helped with editing it.

Materials and Methods

Materials

Reagents were obtained from the following sources: HRP-labeled anti-rabbit secondary antibody and the antibodies against Drosophila Phospho-70 S6 Kinase (Thr398) (#9209), Akt (#9272), myc (#2278), and the FLAG (#2368) epitope from Cell Signaling Technology (CST); Anti-Green Fluorescent protein (GFP) antibody from Aves Labs (GFP-1020); 8D12 Anti-Repo antibody from Developmental Studies Hybridoma Bank (DSHB); Alexa 488, 568, and 647-conjugated secondary antibodies and Complete Protease Cocktail from Roche; Schneider's media and Inactivated Fetal Bovine Serum (IFS) from Invitrogen; amino acid-free Schneider's media from US Biologicals; [^{3}H]-leucine from American Radiolabeled Chemicals, Inc.; leucine from Sigma (L8912); rapamycin from LC Laboratories (#R-5000); and Reliance One-Step Multiplex RT-qPCR Supermix from BIO-RAD. Fresh apples (Gala) were from Star Market. The dS6K antibody was a gift from Mary Stewart (North Dakota State University) and the Drosophila Sestrin antibody one from Jun Hee Lee (University of Michigan).

Methods

Tissue culture

Drosophila S2R+ cells were cultured in Schneider's media with 10% IFS at 25°C and 5% CO_2. Suspension HEK293F cells were cultured in FreeStyle 293 expression medium from ThermoFisher (12338018) with a shaking speed of 125 rpm at 37°C and 5% CO_2.

Lysis of cell, tissues, flies and Immunoprecipitations

Cells were rinsed with cold PBS and lysed in lysis buffer (1% Triton, 10 mM β-glycerol phosphate, 10 mM pyrophosphate, 40 mM Hepes pH 7.4, 2.5 mM MgCl2 and 1 tablet of EDTA-free protease inhibitor [Roche] (per 25 ml buffer)). Cell lysates were cleared by centrifugation in a microcentrifuge (15,000 rpm for 10 minutes at 4°C). Cell lysate samples were prepared by addition of 5X sample buffer

(0.242 M Tris, 10% SDS, 25% glycerol, 0.5 M DTT, and bromophenol blue), resolved by 8%-12% SDS-PAGE, and analyzed by immunoblotting.

Dissected tissues and whole flies were crushed physically utilizing a bead beater in 1% Triton lysis buffer (same as above). The resulting lysates were cleared by centrifugation in a microcentrifuge (15,000 rpm for 10 minutes at 4°C) and analyzed as above. For anti-FLAG immunoprecipitations, anti-FLAG M2 affinity gel (Sigma #A2220) was washed with lysis buffer three times and then resuspended to a ratio of 50:50 affinity gel to lysis buffer. 25 µL of a well-mixed slurry was added to cleared lysates and incubated at 4°C in a shaker for 90-120 minutes. For anti-Myc immunoprecipitations, magnetic anti-Myc beads (Pierce) were washed three times with lysis buffer. 30 µL of resuspended beads in lysis buffer was added to cleared lysates and incubated at 4°C in a shaker for 90-120 minutes. Immunoprecipitates were washed three times; once with lysis buffer and twice with lysis buffer with 500 mM NaCl. Immunoprecipitated proteins were denatured by addition of 50 µL of SDS-containing sample buffer (0.121 M Tris, 5% SDS, 12.5% glycerol, 0.25 M DTT, and bromophenol blue) and boiled for 5 minutes. Denatured samples were resolved by 8%-12% SDS-PAGE, and analyzed by immunoblotting.

Leucine-binding assay and K_d calculation

For radiolabelled leucine binding assays using FLAG-tagged *Drosophila* Sestrin, suspension HEK293F cells were seeded at 2.5 million cells/ml, and the pRK5-FLAG-Sestrin cDNA was transfected using polyethylenimine. 72 hours after transfection, cells were rinsed one time in cold PBS and lysed in 1% Triton lysis buffer (1% Triton, 40 mM Hepes pH 7.4, 2.5 mM $MgCl_2$ and 1 tablet of EDTA-free protease inhibitor [Roche] per 25 ml buffer). Following anti-FLAG immunoprecipitation, the beads were washed 4 times with lysis buffer containing 500 mM NaCl and then incubated for one hour on ice in cytosolic buffer (0.1% Triton, 40 mM HEPES pH 7.4, 10 mM NaCl, 150 mM KCl, 2.5 mM $MgCl_2$) with the indicated amount of [^{3}H]-leuine and unlabeled leucine. At the end of one hour, the beads were aspirated dry and

rapidly washed four times with binding wash buffer (0.1% Triton, 40 mM HEPES pH 7.4, 300 mM NaCl, 2.5 mM $MgCl_2$). The beads were aspirated dry again and resuspended in 80 µl of cytosolic buffer. Each sample was mixed well and then 15 µl aliquots were separately quantified using a TriCarb scintillation counter (Perkin Elmer). This process was repeated in pairs for each sample, to ensure similar incubation and wash times for all samples analyzed across different experiments.

The affinity for leucine of *Drosophila* FLAG-Sestrin was determined by first normalizing the bound [^{3}H]-labeled leucine concentrations across three separate binding assays performed with varying amounts of cold leucine. These values were plotted and fit to a hyperbolic equation (Cheng-Prusoff equation) to estimate the IC_{50} value. The K_d value was derived from the IC50 value using the equation:

$K_d = IC_{50} / (1+([^3H]Leucine)/K_d)$.

In vitro GATOR2-Sestrin dissociation assay

Drosophila S2 cells stably expressing Flag-tagged Drosophila WDR59 were leucine-starved for 1 hour or remaining in full media were lysed and subjected to anti-FLAG immunoprecipitations as described above. The GATOR2-Sestrin complexes immobilized on the FLAG beads were washed twice in lysis buffer with 250 mM NaCl, and then incubated for 25 minutes in 0.3 ml of cytosolic buffer (0.1% Triton, 40 mM HEPES pH7.4, 10 mM NaCl, 150 mM KCl, 2.5 mM MgCl2) with the indicated concentrations of leucine or other amino acids in the cold. The beads were then washed three times in the cytosolic buffer. The FLAG-tagged WDR59 and the amount of Sestrin that remained bound to the beads was assayed by SDS-PAGE and immunoblotting.

LC/MS-based metabolomics and quantification of metabolite abundances

LC/MS-based metabolomics were performed and analyzed as previously described (Birsoy et al., 2015; Chen et al., 2016) using 500 nM isotope-labeled internal standards. Briefly, a 80% methanol

extraction buffer with 500 nM isotope-labeled internal standards was used for whole fly metabolite extraction. Samples were briefly vortexed, dried by vacuum centrifugation, and stored at -80°C until analyzed. On the day of analysis, samples were resuspended in 100 µL of LC/MS grade water and insoluble material was cleared by centrifugation at 15,000 rpm. The supernatant was then analyzed as previously described by LC/MS(Birsoy et al., 2015; Chen et al., 2016).

Statistical analyses

Two-tailed t tests were used for comparison between two groups. All comparisons were two-sided, and P values of less than 0.05 were considered to indicate statistical significance.

Fly stocks and maintenance

All flies were reared at 25°C and 60% humidity with a 12 hours on/off light cycle on standard lab food (12.7 g/L deactivated yeast, 7.3 g/L soy flour, 53.5 g/L cornmeal, 0.4 % agar, 4.2 g/L malt, 5.6 % corn syrup, 0.3 % propionic acid, 1% tegosept/ethanol). The following stocks were used: *nprl*^{1} *(Wei et al., 2016)*, *Mio*^{1} (Iida and Lilly, 2004), *Sesn*^{8A11} (Lee et al., 2010), *Lpp-gal4* (gift from S. Eaton and P. Léopold); *PromE-Gal4 (Billeter et al., 2009)*, *yw,hs-Flp; mCherry–Atg8a; Act>CD2>GAL4, UAS–nlsGFP/TM6B* (gift from Eric Baehrecke), *hsFlp; act>CD2>Gal4, UAS nlsGFP* (Karpowicz et al., 2013), *UAS-sfGFP*^{MODC} *(He et al., 2019)*. *Elav-Gal4* (#458), *Repo-Gal4* (#7415), *Mef2-Gal4* (27390), *ddc-gal4* (#7010), *Tdc2-Gal4* (#9313), *vGAT-Gal4* (#58980), *attP40* (#36304), *attP2* (#36303) and *Sesn RNAi* (#64027) were obtained from BDSC. *Da*-Gal4, esg-*Gal4*, *Myo1A-Gal4*, *Pros-Gal4* were constructed (Perrimon lab stocks).

UAS-Sesn, UAS-Sesn-L431E, *UAS-Flag-WDR24* were constructed using the Gateway system. cDNAs were cloned in entry plasmids used for the LR clonase reaction (Invitrogen, 11791-020), with the destination vector pWALIUM10-roe(Ni et al., 2008) or equivalent (Frederik Wirtz-Peitz, unpublished data). The plasmids were then microinjected into embryos for *ϕ31*-mediated recombination at *attP2* or

attP40 landing sites, as per standard procedures to create transgenic flies. *attP40*, *attP2, W^{1118}* and *Or^{R}* were used as controls.

In figure 2b, the larvae of genotype w; Sesn-/-; tubulin-Gal4, tubulin-Gal80ts/UAS-Sesn were raised at a mildly permissive temperature (25°C) to express relatively physiological levels of Sestrin cDNA in Sestrin null larvae.

$Sesn^{L431E}$ knock-in flies were generated with CRISPR/Cas9 technology to achieve di-nucleotide replacement at the endogenous locus. A single strand oligo donor (ssODN) was used, containing the codon change (CTG>GAG) flanked by 20 bp homology arms (Sequence: ACCAAGGACTACGATAGTGTGGAGGTCGAGCTGCAGGACAGTGA). A single sgRNA with a cutting site abutting the nucleotide replacement locus (sequence F/R: GTCGCAAGGACTACGATAGTGTGC/ AAACGCACACTATCGTAGTCCTTG) was cloned in the pCFD3 expression vector as in a previous report(Housden et al., 2014). pCFD3-sgRNA and ssODN were injected into nos-Cas9 embryos and emerging adults crossed to Sco/Cyo. Progenies were screened by sequencing heterozygous animals (5-10 animals/ founder cross) (PCR/Sequencing primers: Forward primer: CGACGACTACGACTATGGCGAA; Reverse primer: GCATGTGTGGGTATGTGTGTGGT). Individual stocks were established, and backcrossed 9 times onto a control *OrR* background (using the same PCR and sequencing primers as above for genotyping).

Synthetic fly food formulation and process

Drosophila diet formulations were derived from previous recipes(Piper et al., 2014; Piper et al., 2017) with the following modifications: (1) the type of Agar (Micropropagation Agar-Type II; Caisson Laboratories #A037), (2) the final percentage of Agar (1%), 3) the amount of sucrose (25 g), and 4) the amino acids that were added to stock solutions before or after autoclaving(Davis et al., 1980) whose order is described below. The amino acid composition of the diet including the concentrations of

leucine, isoleucine, and valine were based on the exome-matched (i.e. the concentrations used for a given amino acid correspond with the prevalence of exons for that amino acid in the Drosophila genome) Drosophila diet formulation developed in a previous study(Piper et al., 2017) that was found to be optimal for growth and fecundity without compromising lifespan. The rationale for which amino acids were part of the autoclaving process was based on solubility considerations(Davis et al., 1980).

The complete procedure, formula, and stock solutions for food production are as follows:

Procedure:

1) Prepare “Part 2” (see below) Mixture and set aside;

2) Prepare “Part 1” (see below) Mixture, adding everything but agar (not everything will go into solution at this point);

3) Add agar to “Part 1” Mixture, stir using stir bar;

4) Autoclave “Part 1” Mixture for 15 minutes;

5) Remove “Part 1” Mixture from autoclave, then combine with “Part 2” Mixture and stir;

6) Quickly pipette food into Drosophila vials (5-10 mL food/vial);

7) Allow food to solidify/cool for roughly an hour, then cover vials (either with cotton plugs or with plastic wrap) and store food at 4°C.

Food is good for about one month at 4°C (will shrink and pull away from sides of vials due to loss of water after this).

Note: After autoclaving, “Part 1” Mixture containing agar can start solidifying (both before and after the two mixtures are combined, but combining the two mixtures will cause food to cool down quite a bit and solidify faster). Quickly combine and pour food while autoclaved mixture is still hot to avoid this. Adding water to the autoclave tray and keeping the “Part 1” Mixture in this hot water until ready to combine and pour helps keep it hot and helps prevent premature solidification.

Formula:

	Category	Ingredient	Amount of stock per liter
Part 1			
	Gelling Agent	Agar-Type II	10 g
	Sugar	Sucrose	25 g
	Metal Ions	CaCl2*6h2o	1 mL
		CuSO4*5h2o	1 mL
		FeSO4*7h2o	1 mL
		MgSO4 (anhydrous)	1 mL
		MnCl2*4h2o	1 mL
		ZnSO4*7h2o	1 mL
	Cholesterol	Cholesterol	15 mL
	Amino Acids	Tyrosine	0.93g
	Amino Acids	Histidine	50 mL
		Isoleucine	50 mL
		Methionine	50 mL
		Phenylalanine	50 mL
		Threonine	50 mL
		Valine	50 mL

Water	Water (milliQ)	158 mL

****AUTOCLAVE 15 minutes**

	Category	Ingredient	Amount of stock per liter
Part 2			
	Base	Buffer	100 ml
	Amino Acids	Arginine	10 mL
		Cysteine	10 mL
		Glutamate	10 mL
		Glycine	10 mL
		Lysine	10 mL
		Proline	10 mL
		Serine	10 mL
	Amino Acids	Alanine	50 mL
		Asparagine	50 mL
		Aspartate	50 mL
		Glutamine	50 mL
		Leucine	50 mL
		Tryptophan	50 mL

Vitamin Solution		21 mL
Folic Acid	Folic Acid	1 mL
Other Nutrients Solution		8 mL
Preservatives	Propionic acid	6 mL
	methyl 4-hydroxybenzoate	15 mL

Stock Solutions:

Amino Acids	**Catalog Number**	**g/50mL**	**Suspend in:**
L-Alanine	Sigma, A7469	1.10	H2O
L-Asparagine	Amresco, 94341	1.03	H2O
L-Aspartic Acid	Alfa Aesar, A13520	1.17	0.5N NaOH
L-Glutamine	Amresco, 0374	1.12	H2O
L-Histidine	Amresco, 1B1164	0.65	H2O
L-Isoleucine	Amresco, E803	1.12	H2O
L-Leucine	Sigma, L8912	2.03	0.2N HCl
L-Methionine	Amresco, E801	0.60	H2O
L-Phenylalanine	Sigma, P5482	1.01	H2O
L-Threonine	Sigma, T8441	1.11	H2O
L-Tryptophan	Amresco, E800	0.32	H2O
L-Valine	Amresco, 1B1102	1.20	H2O
L-Arginine HCl	Amresco, 0877	8.16	H2O

L-Cysteine	Sigma, 30089	1.71	1N HCl
L-Glutamic acid	Alfa Aesar, A12919	7.59	H2O
L-Glycine	Alfa Aesar, A13816	3.84	H2O
L-Lysine HCl	Amresco, 0437	6.83	H2O
L-Proline	Sigma, P5607	4.89	H2O
L-Serine	Sigma, S4311	6.89	H2O
L-Tyrosine	Sigma, T8566	**add Tyr powder	
Vitamin solution	**Catalog Number**	**g/50mL**	**Suspend in:**
Biotin	Sigma, B4501	0.001	H2O
Ca pantothenate	Sigma, 21210	0.039	H2O
Nicotinic acid	Sigma, N4126	0.030	H2O
Pyridoxine HCl	Sigma, P9755	0.006	H2O
Riboflavin	Sigma, R4500	0.003	H2O
Thiamine (aneurin)	Sigma, T4625	0.005	H2O
Folic acid solution	**Catalog Number**	**g/50mL**	**Suspend in:**
Folic acid	Sigma F8758	0.0250	0.004N NaOH
Other Nutrients solution	**Catalog Number**	**g/50mL**	**Suspend in:**
Choline chloride	MP Biomedicals, 194639	0.3125	H2O
Inosine	Sigma, I4125	0.4065	H2O
Myo-Inositol	Sigma, I7508	0.0315	H2O
Uridine	Sigma, U3003	0.3750	H2O

Methyl 4-hydroxybenzoate solution	**Catalog Number**	**g/50mL**	**Suspend in:**
Methyl 4-hydroxybenzoate	Sigma, H3647	5.0	95% EtOH
Buffer	**Catalog Number**	**50mL stock**	
Glacial Acetic Acid	Millipore, AX0074	1.5 mL	
KH2PO4	JT Baker, 3246	1.5 g	
NaHCO3	Sigma, S8875	0.5 g	
Water		Up to 50mL	
Metal Ions	**Catalog Number**	**g/50mL**	**Suspend in:**
CaCl2*6h2o	Sigma, 21108	12.5	H2O
CuSO4*5h2o	Sigma, C7631	0.125	H2O
FeSO4*7h2o	Sigma, F7002	1.25	H2O (store -20C)
MgSO4 (anhydrous)	Sigma, M7506	12.5	H2O
MnCl2*4h2o	Sigma, M3634	0.05	H2O
ZnSO4*7h2o	Sigma, Z0251	1.25	H2O
Cholesterol solution	**Catalog Number**	**g/50mL**	**Suspend in:**
Cholesterol	Sigma, C8253	1	EtOH

Catalog Numbers for other reagents:

Sucrose: Sigma, S7903

Agar: Caisson, A037

Propionic acid: Sigma, P5561

Stocks can be stored at 4°C for several months unless otherwise specified.

Generation of clones expressing *Sesn* shRNA

Clones were generated by crossing yw,hs-flp; mCherry–Atg8a; Act>CD2>GAL4, UAS–nlsGFP/TM6B with the indicated UAS lines. Progeny of the relevant genotype was reared at 25°C and spontaneous clones were generated in the fat body due to the leakiness of the heat-shock flipase (hs-flp).

Food preference assay

The of idea of using a DNA oligomer to follow food consumption and its sequence were from a previous report(Park et al., 2018).

DNA Oligomer 1:

5’ACCTACACGCTGCGCAACCGAGTCATGCCAATATAAGCAGATTAGCATTACTTTGAGCAACGTATCGGCGATCAGTTCGCCAGCAGTTGTAATGAGCCCC-3’

Forward qPCR Primer 1 – 5’ – GCAACCGAGTCATGCCAATA – 3’

Reverse qPCR Primer 1 – 5’ – TTACAACTGCTGGCGAACTG – 3’

DNA Oligomer 2: 5’GGGCAGCAGGATAACTCGAATGTCTTAGTGCTAGAGGCTTGGGGCGTGTAAGTGTATCGAAGAAGTTCGTGTTAAACGCTTTGGAATGACTGTAATGTAG-3’

Forward qPCR Primer 2 – 5’ – CAGCAGGATAACTCGAATGTCTTA – 3’

Reverse qPCR Primer 2 – 5’ – CAGTCATTCCAAAGCGTTTAACA – 3’

Genomic *Cyp1* qPCR primers:

Cyp1 Forward qPCR primer – 5’ – ACCAACCACAACGGCACTG – 3’

Cyp1 Reverse qPCR primer – 3’ – TGCTTCAGCTCGAAGTTCTCATC – 5’

The DNA oligomers and their corresponding qPCR primers are purchased from Integrated DNA Technologies (IDT) with 4 nmole per tube and diluted in nuclease-free water to final stocks with a DNA concentration of 3.5 μg/μl.

Spray and clean the surface of fresh Gala apples using 70% ethanol. Fresh Gala apple pieces (~1 g) that contain both a piece of peel and pulp were cut on a clean field using a knife, and both the knife and field were precleaned by 70% ethanol. Two apple pieces with similar shape and weight were placed in the opposite corners of a 6 oz (177 ml; 57L x 57W x 103H (in mm)) clean Drosophila bottle. 100 μL solutions that contained one DNA oligomer (final concentration is 3.5 ng/μL) and substances (i.e., sterile water, amino acid solutions, etc.) were placed evenly on top of the apple pieces and allowed to soak in for 1.5-2 hours. Age-synchronized adult flies (15 females and 5 males) were flipped into these assay bottles and allowed to feed on the apples for the indicated times in the time course experiments (Fig 3B and Supplemental Fig 7G) and for 24 hours in the other food preference experiments.

CO_2-anesthetized flies were collected using a tweezer. From each bottle, two tubes of female flies were collected with five flies per tube. Five flies were homogenized for each qPCR sample. Homogenization was performed using a beads beater in the cold after adding 250 μL of squishing buffer (10 mM Tris-HCl pH 8.2, 1 mM EDTA, 1 mM NaCl) and 0.5 μL of 20 mg/ml proteinase K (Thermofisher Scientific # AM2546). The whole fly lysates were digested at 37 °C for 30-40 minutes after homogenization followed by proteinase K inactivation at 95 °C for 5 minutes. The samples were centrifuged for 10 minutes at 15,000 rpm at room temperature and 2 μL of the supernatant was loaded to each qPCR reaction in a 96-well qPCR plate. We used the SYBR green qPCR master mix from BIO-RAD and a CFX96 Touch Real-Time PCR Detection System with a Tm=60°C and 40 cycles per run.

Genomic *Cyp1* qPCR Ct values were used to control for extraction efficiency. For every batch of samples, an average of *Cyp1* qPCR Ct values was taken and all samples beyond -/+ 0.5 away from the average were discarded. Standard curves for each DNA oligomer 1 and 2 were generated, and the

amount of DNA oligomer from each tube of flies was calculated by fitting their Ct values to the standard curves. And the preference index was generated by dividing the calculated DNA oligomer 1 amount by the calculated DNA oligomer 2 amount.

To remove external oligomer that may stick to the outside of the flies, we used a four-step protocol described previously(Park et al., 2018): (1) a ten-minute wash with 10% Contrex AP Powdered labware detergent (Cat #5204, Decon Laboratories, Inc.); (2) a five-minute wash in ddH2O; (3) a two-minute wash in 30% bleach; and (4) a five-minute wash in ddH2O. All washes are performed in a 1500 uL microfuge tube with continuous rocking at room temperature.

For Fig 3c, we fed the flies with food containing either 25µM Rapamycin or 25µM ethanol for 2 days prior either protein starvation overnight or not (including 25µM Rapamycin or 25µM ethanol). Then for the final choice assay, 25µM of Rapamycin or 25µM ethanol was added to both apple pieces in the container.

Egg laying preference assay

The set-up for the egg laying preference assay was identical as the food preference assay. Instead of collecting female flies for qPCR analyses, the two apple pieces were removed from the bottle and examined under a dissection scope. The number of eggs on each apple piece was counted.

Developmental timing

Three-day-old crosses were used for 3-4 hour periods of egg collection on standard lab food. Newly hatched L1 larvae were collected 24 hours later for synchronized growth using the indicated diets at a density of 30 animals/vial. The time to develop was monitored by counting the number of animals that underwent pupariation, every two hours in fed conditions, or once/twice a day in starved conditions. The time at which half the animals had undergone pupariation is reported.

Life span experiments

To generate age-synchronized adult flies, larvae were raised on lab food at low density, transferred to fresh food upon emerging as adults and mated for 48h. Animals were anaesthetized with low levels of CO_2 and sorted at a density of 25 flies/vial. Each condition examined used 8-10 vials of flies. Flies were transferred to fresh vials three times per week at which point deaths were also scored.

Immunofluorescence assays

Fat bodies from 96 hours AEL (after egg laying) larvae were dissected in phosphate-buffered saline (PBS) at room temperature, fixed 25-30 min in 4% formaldehyde, washed twice for 10 min in PBS 0.3% Triton (PBST), blocked 30 min (PBST, 5% BSA, 2% FBS, 0.02% NaN3), incubated with primary antibodies in the blocking buffer overnight, and washed 4 times for 15 min. Secondary antibodies diluted 1:500 in PBST were added for 1 hour and tissues washed 4 times before mounting in Vectashield (Vector Laboratories) containing DAPI. Brains from 5-10 days old adult female flies were dissected and processed as in a previous study(Wu and Luo, 2006).

Images for Fig 2B and Supplemental Fig 5D were acquired on Zeiss Axio Zoom V16. Images for Fig 4B, 4C, Supplemental Fig 2A, and Supplemental Fig 9C were acquired on a Zeiss AxioVert200M microscope with a 63X or 40X oil immersion objective or 10X objective and a Yokogawa CSU-22 spinning disk confocal head with a Borealis modification (Spectral Applied Research/Andor) and a Hamamatsu ORCA-ER CCD camera. The MetaMorph software package (Molecular Devices) was used to control the hardware and image acquisition. The excitation lasers used to capture the images were 405 nm, 488 nm, and 561 nm.

References

Anisimov, V.N., Zabezhinski, M.A., Popovich, I.G., Piskunova, T.S., Semenchenko, A.V., Tyndyk, M.L., Yurova, M.N., Rosenfeld, S.V., and Blagosklonny, M.V. (2011). Rapamycin increases lifespan and inhibits spontaneous tumorigenesis in inbred female mice. Cell Cycle *10*, 4230-4236.

Bar-Peled, L., Chantranupong, L., Cherniack, A.D., Chen, W.W., Ottina, K.A., Grabiner, B.C., Spear, E.D., Carter, S.L., Meyerson, M., and Sabatini, D.M. (2013). A Tumor suppressor complex with GAP activity for the Rag GTPases that signal amino acid sufficiency to mTORC1. Science *340*, 1100-1106.

Baumberger, J.P. (1919). A nutritional study of insects, with special reference to microorganisms and their substrata. J Exp Zool *28*, 1-81.

Becher, P.G., Flick, G., Rozpedowska, E., Schmidt, A., Hagman, A., Lebreton, S., Larsson, M.C., Hansson, B.S., Piskur, J., Witzgall, P*., et al.* (2012). Yeast, not fruit volatiles mediate Drosophila melanogaster attraction, oviposition and development. Funct Ecol *26*, 822-828.

Becher, P.G., Hagman, A., Verschut, V., Chakraborty, A., Rozpedowska, E., Lebreton, S., Bengtsson, M., Flick, G., Witzgall, P., and Piskur, J. (2018). Chemical signaling and insect attraction is a conserved trait in yeasts. Ecol Evol *8*, 2962-2974.

Billeter, J.C., Atallah, J., Krupp, J.J., Millar, J.G., and Levine, J.D. (2009). Specialized cells tag sexual and species identity in Drosophila melanogaster. Nature *461*, 987-991.

Birsoy, K., Wang, T., Chen, W.W., Freinkman, E., Abu-Remaileh, M., and Sabatini, D.M. (2015). An Essential Role of the Mitochondrial Electron Transport Chain in Cell Proliferation Is to Enable Aspartate Synthesis. Cell *162*, 540-551.

Bjordal, M., Arquier, N., Kniazeff, J., Pin, J.P., and Leopold, P. (2014). Sensing of amino acids in a dopaminergic circuitry promotes rejection of an incomplete diet in Drosophila. Cell *156*, 510-521.

Bouche, V., Espinosa, A.P., Leone, L., Sardiello, M., Ballabio, A., and Botas, J. (2016). Drosophila Mitf regulates the V-ATPase and the lysosomal-autophagic pathway. Autophagy *12*, 484-498.

Buerger, C., DeVries, B., and Stambolic, V. (2006). Localization of Rheb to the endomembrane is critical for its signaling function. Biochem Biophys Res Commun *344*, 869-880.

Chantranupong, L., Wolfson, R.L., Orozco, J.M., Saxton, R.A., Scaria, S.M., Bar-Peled, L., Spooner, E., Isasa, M., Gygi, S.P., and Sabatini, D.M. (2014). The Sestrins interact with GATOR2 to negatively regulate the amino-acid-sensing pathway upstream of mTORC1. Cell Rep *9*, 1-8.

Chen, W.W., Freinkman, E., Wang, T., Birsoy, K., and Sabatini, D.M. (2016). Absolute Quantification of Matrix Metabolites Reveals the Dynamics of Mitochondrial Metabolism. Cell *166*, 1324-1337 e1311.

Croset, V., Schleyer, M., Arguello, J.R., Gerber, B., and Benton, R. (2016). A molecular and neuronal basis for amino acid sensing in the Drosophila larva. Sci Rep *6*, 34871.

Davie, K., Janssens, J., Koldere, D., De Waegeneer, M., Pech, U., Kreft, L., Aibar, S., Makhzami, S., Christiaens, V., Bravo Gonzalez-Blas, C*., et al.* (2018). A Single-Cell Transcriptome Atlas of the Aging Drosophila Brain. Cell *174*, 982-998 e920.

Davis, R.W., Botstein, D., Roth, J.R., and Cold Spring Harbor Laboratory. (1980). Advanced bacterial genetics (Cold Spring Harbor, N.Y.: Cold Spring Harbor Laboratory).

Dodd, K.M., and Tee, A.R. (2012). Leucine and mTORC1: a complex relationship. Am J Physiol Endocrinol Metab *302*, E1329-1342.

Feng, F., Li, M., Ma, F., and Cheng, L. (2014). Effects of location within the tree canopy on carbohydrates, organic acids, amino acids and phenolic compounds in the fruit peel and flesh from three apple (Malus x domestica) cultivars. Hortic Res *1*, 14019.

Fox, H.L., Pham, P.T., Kimball, S.R., Jefferson, L.S., and Lynch, C.J. (1998). Amino acid effects on translational repressor 4E-BP1 are mediated primarily by L-leucine in isolated adipocytes. Am J Physiol *275*, C1232-1238.

Ganguly, A., Pang, L., Duong, V.K., Lee, A., Schoniger, H., Varady, E., and Dahanukar, A. (2017). A Molecular and Cellular Context-Dependent Role for Ir76b in Detection of Amino Acid Taste. Cell Rep *18*, 737-750.

He, L., Binari, R., Huang, J., Falo-Sanjuan, J., and Perrimon, N. (2019). In vivo study of gene expression with an enhanced dual-color fluorescent transcriptional timer. Elife *8*.

Hebert, M., Licursi, M., Jensen, B., Baker, A., Milway, S., Malsbury, C., Grant, V.L., Adamec, R., Hirasawa, M., and Blundell, J. (2014). Single rapamycin administration induces prolonged downward shift in defended body weight in rats. PLoS One *9*, e93691.

Henriques, S.F., Dhakan, D.B., Serra, L., Francisco, A.P., Carvalho-Santos, Z., Baltazar, C., Elias, A.P., Anjos, M., Zhang, T., Maddocks, O.D.K*., et al.* (2020). Metabolic cross-feeding in imbalanced diets allows gut microbes to improve reproduction and alter host behaviour. Nat Commun *11*, 4236.

Housden, B.E., Lin, S., and Perrimon, N. (2014). Cas9-based genome editing in Drosophila. Methods Enzymol *546*, 415-439.

Iida, T., and Lilly, M.A. (2004). missing oocyte encodes a highly conserved nuclear protein required for the maintenance of the meiotic cycle and oocyte identity in Drosophila. Development *131*, 1029-1039.

Karpowicz, P., Zhang, Y., Hogenesch, J.B., Emery, P., and Perrimon, N. (2013). The circadian clock gates the intestinal stem cell regenerative state. Cell Rep *3*, 996-1004.

Kim, E., Goraksha-Hicks, P., Li, L., Neufeld, T.P., and Guan, K.L. (2008). Regulation of TORC1 by Rag GTPases in nutrient response. Nat Cell Biol *10*, 935-945.

Kim, J.S., Ro, S.H., Kim, M., Park, H.W., Semple, I.A., Park, H., Cho, U.S., Wang, W., Guan, K.L., Karin, M*., et al.* (2015). Sestrin2 inhibits mTORC1 through modulation of GATOR complexes. Sci Rep *5*, 9502.

Kottmeier, R., Bittern, J., Schoofs, A., Scheiwe, F., Matzat, T., Pankratz, M., and Klambt, C. (2020). Wrapping glia regulates neuronal signaling speed and precision in the peripheral nervous system of Drosophila. Nat Commun *11*, 4491.

Kudow, N., Miura, D., Schleyer, M., Toshima, N., Gerber, B., and Tanimura, T. (2017). Preference for and learning of amino acids in larval Drosophila. Biol Open *6*, 365-369.

Kumar, P., Sethi, S., Sharma, R.R., Singh, S., Saha, S., Sharma, V.K., Verma, M.K., and Sharma, S.K. (2018). Nutritional characterization of apple as a function of genotype. J Food Sci Technol *55*, 2729-2738.

Lee, J.H., Budanov, A.V., Park, E.J., Birse, R., Kim, T.E., Perkins, G.A., Ocorr, K., Ellisman, M.H., Bodmer, R., Bier, E*., et al.* (2010). Sestrin as a feedback inhibitor of TOR that prevents age-related pathologies. Science *327*, 1223-1228.

Leib, D.E., and Knight, Z.A. (2015). Re-examination of Dietary Amino Acid Sensing Reveals a GCN2-Independent Mechanism. Cell Rep *13*, 1081-1089.

Liu, G.Y., and Sabatini, D.M. (2020). mTOR at the nexus of nutrition, growth, ageing and disease. Nat Rev Mol Cell Biol *21*, 183-203.

Liu, Q., Tabuchi, M., Liu, S., Kodama, L., Horiuchi, W., Daniels, J., Chiu, L., Baldoni, D., and Wu, M.N. (2017). Branch-specific plasticity of a bifunctional dopamine circuit encodes protein hunger. Science *356*, 534-539.

Lynch, C.J., Fox, H.L., Vary, T.C., Jefferson, L.S., and Kimball, S.R. (2000). Regulation of amino acid-sensitive TOR signaling by leucine analogues in adipocytes. J Cell Biochem *77*, 234-251.

Ma, Z., Stork, T., Bergles, D.E., and Freeman, M.R. (2016). Neuromodulators signal through astrocytes to alter neural circuit activity and behaviour. Nature *539*, 428-432.

Maurin, A.C., Jousse, C., Averous, J., Parry, L., Bruhat, A., Cherasse, Y., Zeng, H., Zhang, Y., Harding, H.P., Ron, D*., et al.* (2005). The GCN2 kinase biases feeding behavior to maintain amino acid homeostasis in omnivores. Cell Metab *1*, 273-277.

McGuire, S.E., Le, P.T., Osborn, A.J., Matsumoto, K., and Davis, R.L. (2003). Spatiotemporal rescue of memory dysfunction in Drosophila. Science *302*, 1765-1768.

Ni, J.Q., Markstein, M., Binari, R., Pfeiffer, B., Liu, L.P., Villalta, C., Booker, M., Perkins, L., and Perrimon, N. (2008). Vector and parameters for targeted transgenic RNA interference in Drosophila melanogaster. Nat Methods *5*, 49-51.

Otto, N., Marelja, Z., Schoofs, A., Kranenburg, H., Bittern, J., Yildirim, K., Berh, D., Bethke, M., Thomas, S., Rode, S*., et al.* (2018). The sulfite oxidase Shopper controls neuronal activity by regulating glutamate homeostasis in Drosophila ensheathing glia. Nat Commun *9*, 3514.

Park, A., Tran, T., and Atkinson, N.S. (2018). Monitoring food preference in Drosophila by oligonucleotide tagging. Proc Natl Acad Sci U S A *115*, 9020-9025.

Park, J., and Carlson, J.R. (2018). Physiological responses of the Drosophila labellum to amino acids. J Neurogenet *32*, 27-36.

Park, Y., Reyna-Neyra, A., Philippe, L., and Thoreen, C.C. (2017). mTORC1 Balances Cellular Amino Acid Supply with Demand for Protein Synthesis through Post-transcriptional Control of ATF4. Cell Rep *19*, 1083-1090.

Pasha, M., Eid, A.H., Eid, A.A., Gorin, Y., and Munusamy, S. (2017). Sestrin2 as a Novel Biomarker and Therapeutic Target for Various Diseases. Oxid Med Cell Longev *2017*, 3296294.

Piper, M.D., Blanc, E., Leitao-Goncalves, R., Yang, M., He, X., Linford, N.J., Hoddinott, M.P., Hopfen, C., Soultoukis, G.A., Niemeyer, C.*, et al.* (2014). A holidic medium for Drosophila melanogaster. Nat Methods *11*, 100-105.

Piper, M.D.W., Soultoukis, G.A., Blanc, E., Mesaros, A., Herbert, S.L., Juricic, P., He, X., Atanassov, I., Salmonowicz, H., Yang, M.*, et al.* (2017). Matching Dietary Amino Acid Balance to the In Silico-Translated Exome Optimizes Growth and Reproduction without Cost to Lifespan. Cell Metab *25*, 1206.

Piyankarage, S.C., Augustin, H., Grosjean, Y., Featherstone, D.E., and Shippy, S.A. (2008). Hemolymph amino acid analysis of individual Drosophila larvae. Anal Chem *80*, 1201-1207.

Pritchett, T.L., and McCall, K. (2012). Role of the insulin/Tor signaling network in starvation-induced programmed cell death in Drosophila oogenesis. Cell Death Differ *19*, 1069-1079.

Ribeiro, C., and Dickson, B.J. (2010). Sex peptide receptor and neuronal TOR/S6K signaling modulate nutrient balancing in Drosophila. Curr Biol *20*, 1000-1005.

Sancak, Y., Peterson, T.R., Shaul, Y.D., Lindquist, R.A., Thoreen, C.C., Bar-Peled, L., and Sabatini, D.M. (2008). The Rag GTPases bind raptor and mediate amino acid signaling to mTORC1. Science *320*, 1496-1501.

Saxton, R.A., Knockenhauer, K.E., Wolfson, R.L., Chantranupong, L., Pacold, M.E., Wang, T., Schwartz, T.U., and Sabatini, D.M. (2016). Structural basis for leucine sensing by the Sestrin2-mTORC1 pathway. Science *351*, 53-58.

Senger, S., Csokmay, J., Akbar, T., Jones, T.I., Sengupta, P., and Lilly, M.A. (2011). The nucleoporin Seh1 forms a complex with Mio and serves an essential tissue-specific function in Drosophila oogenesis. Development *138*, 2133-2142.

Shen, K., Huang, R.K., Brignole, E.J., Condon, K.J., Valenstein, M.L., Chantranupong, L., Bomaliyamu, A., Choe, A., Hong, C., Yu, Z.*, et al.* (2018). Architecture of the human GATOR1 and GATOR1-Rag GTPases complexes. Nature *556*, 64-69.

Shen, K., Valenstein, M.L., Gu, X., and Sabatini, D.M. (2019). Arg-78 of Nprl2 catalyzes GATOR1-stimulated GTP hydrolysis by the Rag GTPases. J Biol Chem *294*, 2970-2975.

Steck, K., Walker, S.J., Itskov, P.M., Baltaza, C., Moreira, J.M., and Ribeiro, C. (2018). Internal amino acid state modulates yeast taste neurons to support protein homeostasis in Drosophila. Elife *7*.

Suryawan, A., Jeyapalan, A.S., Orellana, R.A., Wilson, F.A., Nguyen, H.V., and Davis, T.A. (2008). Leucine stimulates protein synthesis in skeletal muscle of neonatal pigs by enhancing mTORC1 activation. Am J Physiol Endocrinol Metab *295*, E868-875.

Vargas, M.A., Luo, N., Yamaguchi, A., and Kapahi, P. (2010). A role for S6 kinase and serotonin in postmating dietary switch and balance of nutrients in D. melanogaster. Curr Biol *20*, 1006-1011.

Wei, Y., and Lilly, M.A. (2014). The TORC1 inhibitors Nprl2 and Nprl3 mediate an adaptive response to amino-acid starvation in Drosophila. Cell Death Differ *21*, 1460-1468.

Wei, Y., Reveal, B., Cai, W., and Lilly, M.A. (2016). The GATOR1 Complex Regulates Metabolic Homeostasis and the Response to Nutrient Stress in Drosophila melanogaster. G3 (Bethesda) *6*, 3859-3867.

Wei, Y., Reveal, B., Reich, J., Laursen, W.J., Senger, S., Akbar, T., Iida-Jones, T., Cai, W., Jarnik, M., and Lilly, M.A. (2014). TORC1 regulators Iml1/GATOR1 and GATOR2 control meiotic entry and oocyte development in Drosophila. Proc Natl Acad Sci U S A *111*, E5670-5677.

Wolfson, R.L., Chantranupong, L., Saxton, R.A., Shen, K., Scaria, S.M., Cantor, J.R., and Sabatini, D.M. (2016). Sestrin2 is a leucine sensor for the mTORC1 pathway. Science *351*, 43-48.

Wolfson, R.L., and Sabatini, D.M. (2017). The Dawn of the Age of Amino Acid Sensors for the mTORC1 Pathway. Cell Metab *26*, 301-309.

Wu, J.S., and Luo, L. (2006). A protocol for dissecting Drosophila melanogaster brains for live imaging or immunostaining. Nat Protoc *1*, 2110-2115.

Yang, Z., Huang, R., Fu, X., Wang, G., Qi, W., Mao, D., Shi, Z., Shen, W.L., and Wang, L. (2018). A post-ingestive amino acid sensor promotes food consumption in Drosophila. Cell Res *28*, 1013-1025.

Ye, J., Palm, W., Peng, M., King, B., Lindsten, T., Li, M.O., Koumenis, C., and Thompson, C.B. (2015). GCN2 sustains mTORC1 suppression upon amino acid deprivation by inducing Sestrin2. Genes Dev *29*, 2331-2336.

Zhang, T., Zhou, Q., Ogmundsdottir, M.H., Moller, K., Siddaway, R., Larue, L., Hsing, M., Kong, S.W., Goding, C.R., Palsson, A*., et al.* (2015). Mitf is a master regulator of the v-ATPase, forming a control module for cellular homeostasis with v-ATPase and TORC1. J Cell Sci *128*, 2938-2950.

Chapter 4

Summary and future directions

SECTION 1. Summary

In Chapter 2 and Chapter 3, the results presented have revealed the identification of a novel sensor SAMTOR that expands the mTORC1 pathway and the exploration of *in vivo* roles of nutrient sensing that sheds light on how mTORC1 senses dietary nutrients to regulate organismal physiology and behaviors. We successfully identified and validated that SAMTOR interacts with GATOR1-KICSTOR complex in a S-adenosylmethionine dependent manner to inhibits mTORC1 using a combination of approaches like biochemistry, cell biology and genetics (Gu et al., 2017). Furthermore, our explorations of the physiological functions of the cytosolic sensor Sestrin in fruit flies have provided insights related to the key roles of the mTORC1 pathway in organismal nutrient sensing and behavioral regulation. In all, these presented findings marked an important advance of understanding of the mTORC1 pathway, particularly the upstream regulations.

In this chapter, I outline the future directions and potentially interesting questions on the topics of SAMTOR mechanism to work as a SAM sensor and the cellular foundations of the amino acid preference behavior in fruit flies.

SECTION 2. S-adenosylmethionine sensing by SAMTOR

A. Reveal the mechanistic basis for SAMTOR-dependent GATOR1 activity

Aberrant mTORC1 activity is linked to numerous diseases, including epilepsy (Liu and Sabatini, 2020). Recently, mutations in the interacting GATOR1, KICSTOR, and SAMTOR (unpublished) protein complexes have been identified in a range of focal epilepsy syndromes (Baldassari et al., 2019; Basel-Vanagaite et al., 2013; Iodice et al., 2019; Nakamura et al., 2018; Tsuchida et al., 2018). My work in chapter 2 revealed that, at low SAM levels, SAMTOR binds the GATOR1-KICSTOR complex and inhibits

mTORC1 through a mechanism that depends on GATOR1 GTPase activating protein (GAP) activity on RagA/B (Gu et al., 2017). However, the mechanism by which SAMTOR controls GATOR1 GAP activity remains elusive. A thorough biochemical and structural understanding of the GATOR1-KICSTOR-SAMTOR ternary complex may therefore allow us to reveal both how these complexes control mTORC1 signaling and how epilepsy mutations dysregulate their functions.

One hypothesis is that SAMTOR association causes structural changes in GATOR1 that augment GTP hydrolysis of RagA/B. Future efforts are needed to purify the GATOR1-KICSTOR-SAMTOR ternary complex. We have developed a preliminary protocol for the expression and purification of biochemically useful quantities of GATOR1, KICSTOR, and SAMTOR. Furthermore, the assembly of the stable GATOR1-KICSTOR and GATOR1-KICSTOR-SAMTOR protein complexes is needed for future structural and biochemical work.

Going forward, determination of the structure of the GATOR1-KICSTOR-SAMTOR complex using cryo-electron microscopy will potentially elucidate an interesting mechanism of how SAMTOR association alters the GATOR1-KICSTOR complex. Of particular interest will be the local structure near the active site of GATOR1, the interfaces among GATOR1, KICSTOR, and SAMTOR, and regions commonly mutated in epilepsies. It will also be therapeutically valuable to identify exposed surfaces potentially amenable targeting by small molecules designed to stabilize the GATOR1-KICSTOR-SAMTOR complex. We anticipate that such molecules would negatively regulate mTORC1 and counteract hypofunctional mutations in GATOR1 or KICSTOR.

In combination, it will be informative to biochemically characterize the regulation of GATOR1 GAP activity by SAMTOR using a variety of cell-based and *in vitro* assays. Specifically, one should add back mutations predicted from the structure that affect the interfaces among GATOR1-KICSTOR-SAMTOR to knockout cells for corresponding proteins stably, then evaluate the mTORC1 activity in these cells to assess the cellular consequences of these mutations. In parallel, it will be helpful to mix the

assembled protein complexes *in vitro* with purified Rag GTPases loaded with radiolabeled GTP to determine the rates of GATOR1-stimulated GTP hydrolysis over a range of concentrations to assess the effects of KICSTOR and SAMTOR on kinetic parameters. A similar kinetic analysis should be performed with epilepsy-associated alleles of GATOR1-KICSTOR-SAMTOR, anticipating they will lead to reduced GATOR1 catalytic activity.

However, the SAMTOR association might not cause a dramatic structural change in GATOR1 that directly impact the GTP hydrolysis rate from RagA/B. Other possibilities include the regulation of GATOR1-KICSTOR localization on the lysosomal surface by SAMTOR or the influence on other proteins that interact with GATOR-KICSTOR, such as Rag GTPases and GATOR2 complex. Revealing the mechanistic basis of SAMTOR is a fantastic mechanistic question that is worth further exploration to facilitate our molecular understanding of the mechanism of S-adenosylmethionine sensing by the mTORC1 pathway.

B. Determine SAMTOR structure using X-ray crystallography

Human SAMTOR is a 46kDa protein, a reasonable size for structural determination by X-ray crystallography. We have made several attempts to obtain SAMTOR structure by performing crystallization of:

(1) Full-length human SAMTOR and its truncations purified from bacteria;

(2) Full-length human SAMTOR purified from mammalian expression cells (Expi 293 cells);

(3) Full-length SAMTOR from rat, horse, or *Drosophila melanogaster* purified from bacteria and mammalian cells.

Despite all these efforts, we have met a series of problems related to these constructs and purification systems, which are:

(1) Our protein yield is too low;

(2) Purified SAMTOR crashes out easily, indicating high instability;

(3) Small crystals can be found for particular buffer conditions, it was challenging to optimize to grow the small crystals large enough, sufficient for obtaining solvable X-ray diffraction.

Thus, the structure of SAMTOR remains elusive and holds a significant missing piece for our understanding of SAM sensing via SAMTOR upstream of mTORC1.

C. Elucidate the potential role of SAMTOR in regulating one-carbon metabolism

In healthy cells, mTORC1 is a critical regulator of cellular growth, partially by modulating one-carbon metabolism (Rosenzweig et al., 2018). Through various upstream sensors, mTORC1 can detect nutrient availability and activate the production of one-carbon units to support cellular growth and proliferation (Rosenzweig et al., 2018; Saxton and Sabatini, 2017). Conversely, the one-carbon pool serves as a significant supplier for *de novo* nucleotide synthesis, and the availability of nucleotides in the cell forms a feedback loop to regulate mTORC1 activity (Hoxhaj et al., 2017; Valvezan et al., 2017). Unsurprisingly, both mTORC1 and one-carbon metabolism are massively hyperactivated in various types of cancers (Rosenzweig et al., 2018; Saxton and Sabatini, 2017; Yang and Vousden, 2016), yet we know very little about their direct cross talk. In chapter 2, SAMTOR was identified as a sensor of cellular levels of S-adenosylmethionine (SAM), an essential element in one-carbon metabolism. The binding of SAM to SAMTOR acts as a switch that releases repression of mTORC1 signaling and stimulates cellular growth (Gu et al., 2017).

In our latest unpublished work, we discovered that SAMTOR binds to cytosolic serine hydroxy-methyltransferase (SHMT1), an essential enzyme in one-carbon metabolism that utilizes pyridoxal 5'-phosphate (PLP) as a cofactor and charges the universal acceptor of one-carbon units, tetrahydrofolate

(THF), with a methyl group (one carbon unit) (Florio et al., 2011). Interestingly, unlike the interaction between SAMTOR and its partners in the mTORC1 pathway (GATOR1 complex (Nprl3) and KICSTOR complex (SZT2)), the SAMTOR-SHMT1 interaction is strengthened by starvation of methionine in cells. However, it is not regulated by SAM or its downstream metabolite SAH *in vitro*, indicating a different mechanism at play.

We hypothesize that SAMTOR association might affect the enzymatic activity of SHMT1, in turn regulating the one-carbon metabolism. It will be interesting to explore the functions of the interaction between SAMTOR and SHMT1 in other organisms to understand the evolutionary trajectory of this interaction. SHMT1 is conserved from bacteria to humans, while the sequence orthologs of SAMTOR can be found in all vertebrates and some invertebrates like *Drosophila melanogaster*. It will be interesting to test in other organisms whether SAMTOR and SHMT1 also form a complex that is regulated similarly as in mammalian cells.

Furthermore, revealing the biochemical and cellular consequences of the SAMTOR-SHMT1 complex formation will enable a deeper understanding of this interaction. One should perform enzymatic assays, cell signaling experiments, and metabolic content analysis to elucidate how the SAMTOR-SHMT1 interaction affects cells. Additionally, it will be useful to trace the upstream metabolite of SHMT1 (i.e., serine) in wild-type and SAMTOR knockout cells (*in vitro*) to reveal the potential regulation of SAMTOR to SHMT1. Meanwhile, we have successfully generated and validated mice that lack SAMTOR expression, which will enable the metabolic tracing experiments in mice (*in vivo*). Conversely, assessing the SAM sensing capacity of SAMTOR in wild type and SHMT1 knockout cells will help evaluate the influence from SHMT1 on SAMTOR.

Preliminary data indicated that we can express and purify both SAMTOR and SHMT1 from mammalian suspension cells and assemble them to form a stable complex *in vitro*. The yield and purity of the complex are more than sufficient for further structural analysis. Thus, it will be worth trying to

determine the structure of SAMTOR-SHMT1 co-complex with cryo-electron microscopy (cryo-EM). The resulting structure will allow us to gain an atomic-level insight into the cross-talk mechanism and enable mutagenesis studies to test its cellular function with surgical precision.

Instead of SAMTOR regulating SHMT1, SHMT1 might impact the function of SAMTOR. For example, we have observed that SAMTOR expression level is reduced in SHMT1 knockout cells. Therefore, in parallel, we will investigate whether and how SHMT1 regulates the stability and the mTORC1 inhibitory ability of SAMTOR.

D. Explore whether SAMTOR functions as an active methyltransferase

Based on what has been published, most proteins that contain a SAM binding domain serve as active enzymes (Jain et al., 2016). It will be of great interest to test whether SAMTOR, under certain circumstances, also serves as an active methyltransferase. Although in chapter 2, we already established that the inhibitory function of SAMTOR toward mTORC1 when SAM is absent does not require functional SAM binding domain, it remains possible that when SAM is present, SAMTOR dissociates from GATOR1-KICSTOR, leaving a methylation mark on one of the components. Consistently, the mTORC1 activity fails to increase acutely upon SAM added back to SAM deprived cells, which is different from leucine or arginine restimulation, even though SAMTOR already dissociates from GATOR1-KICSTOR acutely. Further *in vitro* methylation assay is required to test whether SAMTOR might act as a methyltransferase to either GATOR1-KICSTOR complex or SHMT1 protein. Excitingly, if SAMTOR indeed is an active enzyme, it will be so far the only mammalian sensor that contains an active enzymatic activity and this post-translation modification mediated via SAMTOR will represent an interesting regulation in the mTORC1 pathway.

SECTION 3. Elucidate the mechanism of nutrient-regulated feeding behaviors

A. Identify and characterize the amino acid regulated glial cell types

To thrive in a complex environment, organisms must sense the nutritional content of food sources and accordingly modulate feeding behaviors. My graduate work in chapter 3 revealed that *Drosophila* requires the mTORC1 pathway leucine sensor Sestrin to adapt to diets low in leucine or to discriminate between diets containing or missing leucine. Furthermore, we showed that dietary leucine dynamically regulates mTORC1 signaling in fly glia in a Sestrin-dependent manner and that proper mTORC1 activity in these cells is important for leucine preference development. However, as the precise glial cell types which sense leucine remain unknown, the mechanistic basis for these behavioral phenomena remains unclear. It depends on the identification and characterization of these specialized cells.

Our findings are consistent with the hypothesis that the mTORC1 activity of specific glial cells is dynamically regulated by dietary variability, and they have specific gene expression features that can be clustered. Theoretically, these glial cells should present changes in transcriptomic, proteomic, or metabolomic levels under different diets.

There are several targeted approaches one can take for the identification of the relevant glial cell type(s). Approach 1: Design a series of fluorescent probes targeting known glial markers for different glial types and Sestrin, then perform *in situ* hybridization using these probes for dissected fly brains that contain a mTORC1 activity fluorescent reporter. This approach will enable us to identify cells that both express Sestrin and exhibit inhibited mTORC1 activity under rapamycin or protein starvation and screen for which glial probe(s) also show positive signals in those cells. Approach 2: Perform a Sestrin knockdown screen using different Gal4 driver lines that target specific subtypes of glial cells. We expect

that when we knock down Sestrin in relevant glial cells, the flies will present a reduced leucine preference, phenocopying pan-glial Sestrin knockdown.

Furthermore, it will be informative to explore the changes of the transcriptome, proteome and metabolome in the relevant glial cells under various dietary treatments. Generating a series of flies harboring fluorescent protein expression specific to particular glial cells will allow flow cytometric sorting of these specialized populations. Using these reagents, one should collect glial cell subtypes upon fed, rapamycin-treated, protein-starved, and leucine-starved conditions to perform transcriptomic, proteomic, and metabolomic analysis. Paired analysis in Sestrin mutant strains will allow delineation of those signaling changes which are Sestrin-dependent.

On the other hand, instead of a particular glial cell population defined with specific gene expression signature, possibly these nutrient sensitive glial cells are primarily determined by their location in the brain. The closer they locate to the blood-brain-barrier, the faster presumably they will experience the nutrient level fluctuations in the hemolymph. Therefore, if transcriptomic analysis gives little clue, the localization of these glial cells in the brain will be very informative. Taken further, more detailed analysis and determination of the localization of the glial cells of interest in fly brains will be needed.

B. Identify neuronal populations involved in the regulation of amino acid preference

Identifying nutrient-sensing glial cells raises an important question: how do the mTORC1 activity changes in these glial cells control neuronal circuits and alter feeding behavior? Answering this question requires the identification of neuronal populations involved in developing the amino acid preference. Previous studies reported that a set of dopaminergic reward circuit neurons control preference toward protein-rich food (Liu et al., 2017). It will be of great interest to test whether the activity of these

neurons or others, is required to develop the amino acid preference that we identified as dependent on glial mTORC1 activity.

First of all, it should be determined whether the activity of the dopaminergic reward circuit neurons is necessary for glial-sensed amino acid preference. Assessing the influence on the amino acid preference by experimentally inhibiting dopaminergic neuron activity acutely during adulthood will require crossing the Gal4 driver lines specifically targeting dopaminergic neurons with fly lines that ubiquitously express UAS-Kir2.1, an inward-rectifying potassium channel that hyperpolarizes and inhibits neuronal firing. By tuning the expression level of Gal80ts, a temperature-sensitive Gal4 antagonizing protein, we can thereby achieve acute inhibition of the reward circuit in adult flies, then evaluate whether the amino acid preference of these animals is reduced compared to wild type flies.

Going forward, visualization of the activity changes of these dopaminergic neurons under different dietary treatments will significantly facilitate the understanding of the neuronal basis of amino acid sensing. In collaboration with the laboratory of Carlos Ribeiro, we will take advantage of the highly sensitive genetically encoded calcium indicator GCaMP to measure neuronal activity of the *Drosophila* reward circuit specifically. Performing two-photon imaging of head-fixed live flies fed with various amino acid solutions to assay the activity changes in dopaminergic neurons directly will provide detailed live information towards the neuronal basis.

However, if these reported dopaminergic neurons fail to regulate the amino acid preference, more examination of other neuronal cell types, such as octopaminergic neurons, which have been linked previously with hunger-driven foraging behaviors (Zhang et al., 2013), will be needed. Additionally, it will be useful to utilize insect immediate early genes, such as Hr38 (Fujita et al., 2013) (similar to mammalian c-Fos) to acutely map the comprehensive neuronal activity pattern upon amino acid starvation/reactivation, facilitating the possibility of using RNA-seq to reveal the relevant neuronal identity.

C. Investigate the relationship between mTORC1 activity in optic lobe glia and its association with egg-laying circadian rhythm

The roles of nutrient-sensitive signaling in coordinating circadian rhythm remain unknown. We recently found that Sestrin deficient females flies display abnormal temporal egg-laying patterns, suggesting Sestrin may regulate the circadian rhythm. Additionally, we observed that mTORC1 activity in optic lobe glia depends on Sestrin genotype but not on the diet: cells in Sestrin L431E (hypermorph) mutant flies inhibit mTORC1 activity even under fed conditions, whereas those from Sestrin null flies have constitutively hyperactive mTORC1 activity. These observations strongly indicate the baseline activity of mTORC1 in these optic lobe glial cells depends on Sestrin. Furthermore, it has been reported that several pacemaker neurons located precisely in the inner edge of the optic lobe receive input from the optic lobe and regulate circadian behaviors (Helfrich-Forster et al., 1998).

It is fascinating to hypothesize that the mTORC1 activity in optic lobe glial cells might serve as potential a key modulator towards pacemaker neurons and underlie Sestrin-related circadian rhythm abnormalities.

The exploration of this hypothesis can only be facilitated by identification and characterization of the glial cell type(s) in the optic lobe that is highly sensitive to Sestrin manipulations. A similar strategy as SECTION 3A can be used to identify the relevant glial cell type(s) and look for potential specific markers to label these cells genetically. The multi-omic approach described above will be informative to gain a deeper understanding of these glial cells in the optic lobe. The most interesting differences one should seek for should be the ones that are Sestrin-dependent.

In parallel, since the identity of the pacemaker neurons has been intensely studied, it will be of great interest to explore the activity of the pacemaker neurons in wild-type and Sestrin mutant fly

brains. The calcium indicator mentioned above can be utilized to record the activity of these neurons and evaluate whether the neuronal activity is dependent on functional Sestrin in the optic lobe glial cells.

To further establish the link between the optic lobe glial cells and circadian rhythm behaviors, it will be needed to knock down Sestrin acutely in the optic lobe glial cells using the genetic tool established before, then assess the changes of the pacemaker neuron activity as well as the egg-laying circadian rhythm. It will be interesting to characterize the role of Sestrin by restoring wild-type Sestrin expression specifically in the optic lobe glial cells of Sestrin null flies. These experiments will allow the demonstration of both necessity and sufficiency of functional Sestrin and mTORC1 activity in optic lobe glial cells for circadian rhythm behaviors.

It is possible that the mTORC1 dysregulation in the optic lobe glial cells does not cause the egg-laying circadian rhythm abnormality. Instead, it can lead to other phenotypes that have not been observed yet, such as vision alteration. To investigate the cause of the egg-laying circadian rhythm abnormality, one should start from the neuronal activity of pacemaker neurons in wild-type and Sestrin mutant flies and explore whether the Sestrin impact can be cell-autonomous.

SECTION 4. Several comments on the future of the mTORC1 field

The mTOR pathway functions as a critical nutrient antenna that conveys the availability of important nutrients like amino acids to regulate numerous aspects of metabolism at the cellular and organismal level. In the past two decades, many new insights have been discovered to boost our understanding of both the upstream and downstream regulations of mTORC1. Extensive physiological and pharmacological research has been performed in various model organisms to demonstrate the importance of mTORC1 and how misregulated mTORC1 activity contributes to disease.

I think that the future of the mTORC1 field (focus on the nutrient sensing branch) will primarily focus on four areas:

(1) Identification of more upstream nutrient sensors, such as for glucose or its metabolites, in specific cell types or different organisms. Unpublished work from the Sabatini lab has already shown that species specific sensors upstream of mTORC1 exist. However, a systematic search is urgently needed, as it will be an extremely valuable dataset to help gain evolution perspectives of the mTORC1 pathway;

(2) Exploration more of the physiological functions of mTORC1 based on current extensive knowledge on its upstream regulation in human cells. Studies that initiate from genes, to proteins or metabolites, to relevant cell types, to physiological alterations, eventually to behavioral changes are the ones that complete a loop. I think one needs to reach this systematic level to even be remotely close to understand how a particular gene functions in an organismal level. Performing this analysis for the whole pathway components will require many years of work. Then connecting all these individual lines of studies together to shed light on the pathway's organismal roles will take even more time, but I think it will be very useful;

(3) Biochemical analysis and reconstitution of mTORC1 upstream regulatory protein complexes *in vitro* to dissect mechanistically how several mega Dalton complexes co-exist and coordinate together to regulate a single kinase complex. A pure reconstituted system will enable single-molecule tracing and kinetic analysis with surgical precision, which will significantly facilitate molecular understanding of how the complex regulation upstream of mTORC1 happens;

(4) Pharmacological targeting of mTOR in a more specific and context-dependent manner. Although there are rapalogs that inhibit the catalytic functions of mTOR, there are many drawbacks, such as strong toxicities due to lack to tissue specificity and the co-inhibition of mTORC2 (Stefanovska et al., 2020; Yu et al., 2010). So how to develop therapeutic compounds that only target mTORC1 or mTORC2 will be of great interest. Especially, mTORC1 specific inhibitors might have usage in diabetes and lifespan extension. Targeting the upstream components of mTORC1 might solve these issues due to the more restricted expression pattern *in vivo* and the biochemical nature of these proteins (many of them have built-in small molecule binding pockets).

References

Baldassari, S., Picard, F., Verbeek, N.E., van Kempen, M., Brilstra, E.H., Lesca, G., Conti, V., Guerrini, R., Bisulli, F., Licchetta, L*., et al.* (2019). The landscape of epilepsy-related GATOR1 variants. Genet Med *21*, 398-408.

Basel-Vanagaite, L., Hershkovitz, T., Heyman, E., Raspall-Chaure, M., Kakar, N., Smirin-Yosef, P., Vila-Pueyo, M., Kornreich, L., Thiele, H., Bode, H*., et al.* (2013). Biallelic SZT2 mutations cause infantile encephalopathy with epilepsy and dysmorphic corpus callosum. Am J Hum Genet *93*, 524-529.

Florio, R., di Salvo, M.L., Vivoli, M., and Contestabile, R. (2011). Serine hydroxymethyltransferase: a model enzyme for mechanistic, structural, and evolutionary studies. Biochim Biophys Acta *1814*, 1489-1496.

Fujita, N., Nagata, Y., Nishiuchi, T., Sato, M., Iwami, M., and Kiya, T. (2013). Visualization of neural activity in insect brains using a conserved immediate early gene, Hr38. Curr Biol *23*, 2063-2070.

Gu, X., Orozco, J.M., Saxton, R.A., Condon, K.J., Liu, G.Y., Krawczyk, P.A., Scaria, S.M., Harper, J.W., Gygi, S.P., and Sabatini, D.M. (2017). SAMTOR is an S-adenosylmethionine sensor for the mTORC1 pathway. Science *358*, 813-818.

Helfrich-Forster, C., Stengl, M., and Homberg, U. (1998). Organization of the circadian system in insects. Chronobiol Int *15*, 567-594.

Hoxhaj, G., Hughes-Hallett, J., Timson, R.C., Ilagan, E., Yuan, M., Asara, J.M., Ben-Sahra, I., and Manning, B.D. (2017). The mTORC1 Signaling Network Senses Changes in Cellular Purine Nucleotide Levels. Cell Rep *21*, 1331-1346.

Iodice, A., Spagnoli, C., Frattini, D., Salerno, G.G., Rizzi, S., and Fusco, C. (2019). Biallelic SZT2 mutation with early onset of focal status epilepticus: Useful diagnostic clues other than epilepsy, intellectual disability and macrocephaly. Seizure *69*, 296-297.

Jain, K., Warmack, R.A., Debler, E.W., Hadjikyriacou, A., Stavropoulos, P., and Clarke, S.G. (2016). Protein Arginine Methyltransferase Product Specificity Is Mediated by Distinct Active-site Architectures. J Biol Chem *291*, 18299-18308.

Liu, G.Y., and Sabatini, D.M. (2020). mTOR at the nexus of nutrition, growth, ageing and disease. Nat Rev Mol Cell Biol *21*, 183-203.

Liu, Q., Tabuchi, M., Liu, S., Kodama, L., Horiuchi, W., Daniels, J., Chiu, L., Baldoni, D., and Wu, M.N. (2017). Branch-specific plasticity of a bifunctional dopamine circuit encodes protein hunger. Science *356*, 534-539.

Nakamura, Y., Togawa, Y., Okuno, Y., Muramatsu, H., Nakabayashi, K., Kuroki, Y., Ieda, D., Hori, I., Negishi, Y., Togawa, T.*, et al.* (2018). Biallelic mutations in SZT2 cause a discernible clinical entity with epilepsy, developmental delay, macrocephaly and a dysmorphic corpus callosum. Brain Dev *40*, 134-139.

Rosenzweig, A., Blenis, J., and Gomes, A.P. (2018). Beyond the Warburg Effect: How Do Cancer Cells Regulate One-Carbon Metabolism? Front Cell Dev Biol *6*, 90.

Saxton, R.A., and Sabatini, D.M. (2017). mTOR Signaling in Growth, Metabolism, and Disease. Cell *169*, 361-371.

Stefanovska, B., Vicier, C.E., Dayris, T., Ogryzko, V., Scott, V., Bouakka, I., Delaloge, S., Rocca, A., Le Saux, O., Tredan, O.*, et al.* (2020). Rapalog-Mediated Repression of Tribbles Pseudokinase 3 Regulates Pre-mRNA Splicing. Cancer Res *80*, 2190-2203.

Tsuchida, N., Nakashima, M., Miyauchi, A., Yoshitomi, S., Kimizu, T., Ganesan, V., Teik, K.W., Ch'ng, G.S., Kato, M., Mizuguchi, T.*, et al.* (2018). Novel biallelic SZT2 mutations in 3 cases of early-onset epileptic encephalopathy. Clin Genet *93*, 266-274.

Valvezan, A.J., Turner, M., Belaid, A., Lam, H.C., Miller, S.K., McNamara, M.C., Baglini, C., Housden, B.E., Perrimon, N., Kwiatkowski, D.J.*, et al.* (2017). mTORC1 Couples Nucleotide Synthesis to Nucleotide Demand Resulting in a Targetable Metabolic Vulnerability. Cancer Cell *32*, 624-638 e625.

Yang, M., and Vousden, K.H. (2016). Serine and one-carbon metabolism in cancer. Nat Rev Cancer *16*, 650-662.

Yu, K., Shi, C., Toral-Barza, L., Lucas, J., Shor, B., Kim, J.E., Zhang, W.G., Mahoney, R., Gaydos, C., Tardio, L.*, et al.* (2010). Beyond rapalog therapy: preclinical pharmacology and antitumor

activity of WYE-125132, an ATP-competitive and specific inhibitor of mTORC1 and mTORC2. Cancer Res *70*, 621-631.

Zhang, T., Branch, A., and Shen, P. (2013). Octopamine-mediated circuit mechanism underlying controlled appetite for palatable food in Drosophila. Proc Natl Acad Sci U S A *110*, 15431-15436.